# EXPERIMENTAL AND NUMERICAL STUDIES OF MODEL PILE BEHAVIOUR IN SAND

A Thesis

by

MD. SAIFUL ALAM SIDDIQUEE

Submitted to the Department of Civil Engineering, Bangladesh University of Engineering and Technology, Dhaka in partial fulfilment of the requirements for the degree

of

MASTER OF SCIENCE IN CIVIL ENGINEERING

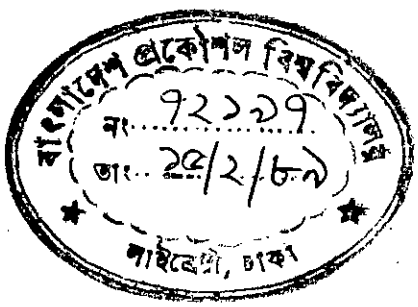


NOVEMBER, 1988

BANGLADESH UNIVERSITY OF ENGINEERING AND TECHNOLOGY, DHAKA

# EXPERIMENTAL AND NUMERICAL STUDIES OF MODEL PILE BEHAVIOUR IN SAND



A thesis

by

MD. SAIFUL ALAM SIDDIQUEE

Approved as to style and content by:

A.M.M. Sf. Mal
(Dr. A. M. M. Safiullah) — Chairman
Professor of Civil Engineering,
BUET, Dhaka.

Abdul Muqtadir
(Dr. A. Muqtadir) — Co-Chairman
Assistant Professor,
Dept. of Civil Engineering,
BUET, Dhaka.

Dr.Md. Alee Murtuza — Member
Professor and Head,
Dept. of Civil Engineering
BUET, Dhaka.

(Dr. M. Zoynul Abedin) — Member
Associate Professor,
Dept. of Civil Engineering
BUET, Dhaka.

(Dr. A.J. Khan) — Member (External)
Director, PMACS Ltd.
Road No.2, House No. 34,
Dhanmondi, Dhaka.

November, 1988

## ABSTRACT

Load transfer mechanism of piles has been studied in this research, Model piles of various diameters have been installed in uniformly bedded sand deposits and were tested in compression for two different sand densities and under various installation conditions.

Vertical load carried by the pile shaft were measured at various depths by electric strain gauges. This enabled the total load carried by the pile to be separated into skin frictional resistance and end bearing. The results were analysed in order to establish relations between skin friction at different pile depths for different placement conditions and pile diameters. An empirical model of skin friction is proposed which incorporate reduction in stress due to sand arching.

Coefficient of lateral earth pressures have been calculated for both densities of sand used in the experiment and for the type of installation method followed. Variations in the coefficient of earth pressure have been explained in terms of installation conditions.

Bearing capacity factor, $N_q$ for the model piles has been determined and compared with values suggested by various authors. Effect of installation on the bearing capacity factor at different placement conditions are also reported.

Finally, finite element analysis of the pile model test was carried out assuming linear elastic behaviour of soil and the results were compared with those obtained from experiment. The results showed good correlation between FEM computed and experimental values.

## ACKNOWLEDGEMENT

The author expresses his profound gratitude to his supervisor, Dr. A.M.M. Safiullah, Professor of Civil Engineering, Bangladesh University of Engineering and Technology, Dhaka, for his valuable suggestions, untiring effort and erudite guidance throughout the research programme.

The author is grateful to his co-supervisor, Dr. A. Muqtadir, Assistant Professor, Civil Engineering Department, Bangladesh University of Engineering and Technology, for his valuable advice and persistant inspiration.

Sincere gratitude is expressed to Dr. Alee Murtuza, Professor and Head of the Department of Civil Engineering, Bangladesh University of Engineering and Technology, Dhaka, for his valuable co-operation.

The help rendered by Mr. A. Jalil, Lecturer, Civil Engineering Department, Bangladesh University of Engineering and Technology, Dhaka, at various stages of the work is gratefully acknowledged.

The author expresses his thanks to Mr. Habibur Rahman, of Geotechnical Engineering Laboratory, for his sincere help in carrying out the experiment. The author also extends his thanks to Mr. M.A. Malek, Mr. A. Hamid and Mr. Shahiduddin for their help in typing the scripts and preparing the sketches.

# TABLE OF CONTENT

# NOTATION

$A_p$ = area of pile point;

$A_s$ = area of pile shaft;

B = pile diameter (or, for noncircular piles, the diameter of a circle with the same area as the pile cross section);

c = cohesion of soil;

D = depth of pile penetration;

d = diameter of pile segment;

$D_b$ = pile diameter at the base;

$D_r$ = relative density of sand;

D/B = relative depth;

E = Young's modulus of elasticity;

$E_p$ = modulus of elasticity of pile ;

$E_s$ = modulus of elasticity of soil;

F = factor of safety;

$f_s$ = ultimate unit side resistance;

$f_{sa}$ = predicted skin friction;

$f_{st}$ = theoretical($K_0$) skin friction;

$G_s$ = shear modulus of soil;

$I_p$ = displacement influence factor;

$I_r$ = rigidity index;

$I_{rr}$ = reduced rigidity index;

K = lateral earth pressure coefficient;

$K_a$ = coefficient of active earth pressure;

$K_p$ = coefficient of passive earth pressure;

$K_o$ = coefficient of earth pressure at rest;

$L_b/B$ = average depth ratio of point or tip;

$L_c$ = critical depth of pile below which point bearing becomes constant;

N = SPT value;

$N_\gamma$, $N_q$, $N_c$ = bearing capacity factors ;

OCR = over consolidation ratio;

P,q = effective overburden pressure;

$P_o$ = effective vertical overburden pressure at pile point level;

$P_T$ = the point resistance;

$Q_p$ = ultimate load carried by the pile point;

$Q_s$ = ultimate load carried by pile shaft;

$Q_T$ = total axial load on pile;

$Q_u$ = ultimate total axial load on pile;

$Q_o$ = computed load for the pile;

$q_o$ = ultimate unit point resistance;

$q_c$ = cone point resistance;

$R_b$ = empirical reduction factor for the ultimate unit point resistance;

$S_\gamma$, $S_c$, $S_q$ = shape factors;

S = shear strength;

$X_v$ = a coefficient for skin friction determination;

$X_m$ = a factor for skin friction determination;

$y_o$ = pile top displacement;

$y_T$ = a small tip movement;

$\gamma_s$ = effective unit weight of soil;

$\delta$ = angle of friction between pile and soil;

$\phi$ = peak friction angle of soil based on effective stresses;

$\phi_{res}$ = residual friction angle of soil, based on effective stresses.

$\sigma$ = normal stress;

$\varepsilon_v$ = volumetric strain;

$\alpha$ = adhesion factor;

$\lambda$ = a coefficient proposed by Vijayvergiya(1972);

$\beta$ = a factor which correlates skin friction to effective stress parameters;

$\psi$ = an angle used in the determination of bearing capacity factor;

$\nu_s$ = poisson's ratio for soil;

$\nu_p$ = poisson's ratio for pile;

$\varepsilon_p$ = strain in the pile material;

$\tau_a$ = load transfer or, adhesion;

$\rho_{col}$ = computed column deformation;

$\rho$ = observed settlement;

# CHAPTER 1

## INTRODUCTION


### 1.1 General

Piles are the oldest foundation element used over the centuries to build foundation on soils. The purpose of any foundation is to transmit loads or forces to the ground without excessive settlement. A piled foundation is used where it is necessary to carry the load to an underlying stratum through a layer of weak or compressible material or through water.

Essentially a pile is an elongated or columnar body installed in the ground for the purpose of transmitting load to a firm strata. When a pile carries most of its axial load by the soil reaction of the bottom or tip it is called a tip bearing pile. Wheréas, if it carries most of its axial load by mobilizing skin friction from the surrounding soil, the pile is called a friction pile.

The design of a pile foundation rests upon three equally important basic considerations: first a knowledge of the geology of the site is required, secondly the type of pile and its installation procedures to be followed and thirdly the study of pile capacity based on its transfer mechanism is to be

considered.

The present research is related to the third consideration i.e. the transfer mechanism and pile-capacity. Pile capacity depends on the load transfer mechanism of a pile. So the process of load transfer mechanism in order to evaluate pile load capacity has been investigated here. In the subsequent articles the scope and the main area of this research are briefly outlined.

## 1.2 Load Transfer Mechanism of Piles

Load transfer mechanism is the most intriguing question in the design principles of piled foundation. Capacity of a pile largely depends on the load transfer patterns of the pile. Pile may transfer its load through skin friction and/or tip bearing. Contribution of skin friction/tip bearing to axial pile capacity is controlled by many interacting parameters.

Normally load-transfer pattern of a pile at a site is investigated by constructing a load-transfer curve which shows the dissipation of total load along with pile depth.

Load transfer pattern however depends on many factor such as depth of pile, pile diameter and pile installation procedure. Load transfer pattern also varies with loading condition and displacement mobilization.

## 1.3 The Area of Research

A pile element transfers its load by skin friction and tip bearing. Although there is an established practice for design of piles for load transfer, the details of the transfer mechanism is not clearly understood. This research is, therefore, aimed at the study of load transfer mechanism in piles.

Tests were carried out with model piles on uniform sand beds for various pile geometry, placement condition and soil density. In this study material properties of soil and model piles were experimentally determined. A fully three-dimensional finite element analysis was also performed and the finite element results were compared with the experimental findings.

# CHAPTER 2

## LITERATURE REVIEW

### 2.1 Introduction

As load transfer mechanism comprises skin friction and and bearing, these have formed the major portion of this review. Other phenomena which influence the load transfer mechanism are also reviewed. Outstanding design principles are discussed. A chronological development of analytical methods for estimating pile load capacity is also presented in this chapter.

### 2.2 Load-transfer Mechanism

The following static formula is commonly used to determine the ultimate axial bearing capacity of a pile.

$$Q_u = Q_p + Q_s = q_0 . A_p + f_s . A_s \qquad (2.1)$$

in which $Q_u$ = Ultimate axial bearing capacity

$q_0$ = ultimate unit point resistance

$f_s$ = ultimate unit side resistance

$A_p$ = area of pile point

and $A_s$ = area of pile shaft.

The equation is schematically shown in Fig. 2.1. The above equation is the outcome of limit state design. This does not explain clearly the different stress components in a working pile. Therefore, to evaluate the stress components working in a pile, the load transfer mechanism of the pile should be properly understood. Main components of load transfer mechanism are

1. Side stress or, unit side frictional resistance.
2. Point stress or, unit point resistance.

The load acting on a pile is resisted by those two stresses. Initially load is transferred by skin friction or unit side resistance.

### 2.2.1 Skin friction

The theoretical determination of side or shaft resistance for piles in sands has received little attention of the researchers. Only Meyerhof(1959) and Nordlund(1963) considered this portion of bearing capacity of piles with adequate attention.

The interaction between the soil and the pile is very complex and poorly understood. The determination of the ultimate unit side resistance, $f_s$, is based on the laws of mechanics considering friction between two different surfaces. Figure 2.2 shows the system of stresses considered. The magnitude of fs is commonly determined using

$$f_s = K.P.\tan(\delta) \qquad (2.2)$$

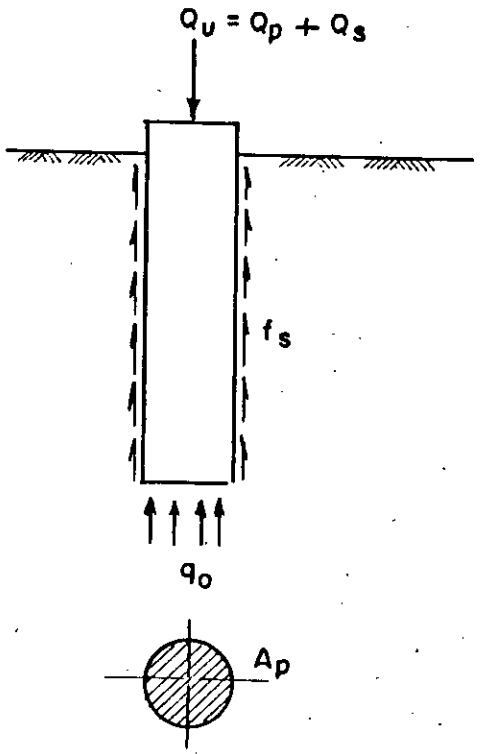


Fig. 2.1 Schemetic Representation of Equation 2.1

in which $K_s$ is the lateral earth pressure coefficient ; $P_o$ is the average effective overburden pressure along the segment of pile being considered; and $\tan(\delta)$ coefficient of friction between pile and soil.

Potyondy (1961) determined in the laboratory the coefficients of friction between various construction materials and cohesionless soils using direct shear tests.In addition to the determination of the coefficient of friction $\tan(\delta)$, between the soil and the pile material, the angle of friction of the sand, $\phi$ , was also determined. Consequently, it was possible to develop a relationship between $\phi$ and $\delta$.

Vesic (1977) proposed a different approach for the determination of $\tan(\delta)$. The sand located at the interface between the soil and the pile is considered to be at a state of ultimate failure for determination of side resistance. Consequently the angle of friction between the pile and the soil, $\delta$ is independent of the initial soil density and pile material. Therefore it can be considered equal to the residual friction angle of the sand $\phi_{res}$. The difference between the values determined by Potyondy (1961) and those suggested by Vesic (1977) did not seem to be significant.

Meyerhof(1959) and Nordlund(1963) dealt theoretically with the problem of the determination of the lateral earth pressure coefficient, K. Assumption made in both studies was

that the pile displaces the sand in a horizontal direction, without any vertical deformation. This displacement induced compaction in the surrounding soil which is maximum at the pile-soil interface. Since the wall pushes against the sand and the horizontal movement is large (equal to the pile radius), it is theoretically possible for the magnitude of the lateral earth pressure coefficient, K, to be as high as the passive earth pressure coefficient.

A list of typical values of lateral earth pressure coefficients for pile foundations, compiled by Kezdi (1975) on the basis of many author's findings are presented in Table 2.1 It should be noted that with the exception of Ireland(Kezdi,1975) who presented a range of values, only a single value was suggested by each author and no consideration was given to parameter defining the soil-pile system such as pile penetration, effect of driving or method of placement.

### 2.2.2 End bearing

The theoretical determination of the point load ($Q_p$) in Fig. 2.1 has received extensive attention through the years. According to Vesic (1967) the theoretical approach to solve this problem was started by Prandtl(1920) and Reissner(1924). They initiated with the assumptions that soil is elasto-plastic material and the failure is punching failure.

TABLE 2.1 Typical Values of Earth Pressure Coefficients (Coyle and Castello, 1981)

| Author | Basis of relationship | Soil type | Values of K |
|---|---|---|---|
| Brinch Hansen | theory | sand | $\cos^2 \phi$ |
| Lundgren (1960) | pile test | sand | 0.8 |
| Henry | theory | sand | $K_p$ |
| Ireland (1957) | pulling tests | sand | 1.75 to 3 |
| Meyerhof (1951) | analysis of field data | loose sand<br>dense sand | 0.5<br>1.0 |
| Mansur-Kaufman (1958) | analysis of field data | silt<br>silt | 0.3(Comp.)<br>0.6(Ten.) |
| Lambe-Whitman (1969) | guess | | 2 |
| Kezdi (1958) | theory | granular | $K_p$ |

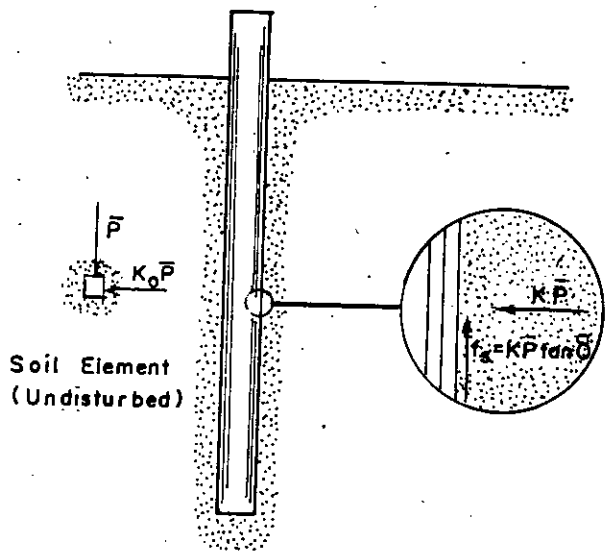


Fig.2.2 Side Resistance Along Pile (Coyle etal 1981)

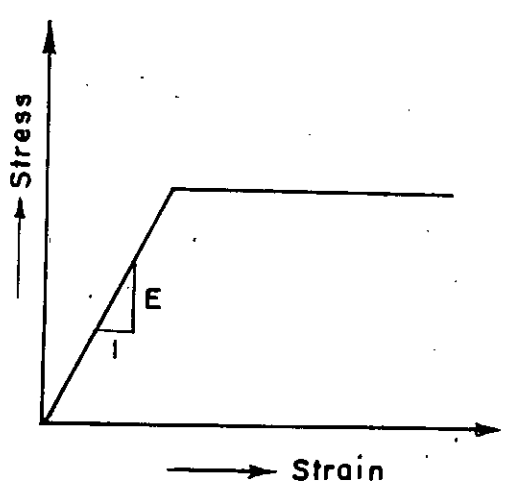


Fig. 2.3(a) Stress - Strain Diagram for Elasto Plastic Material.

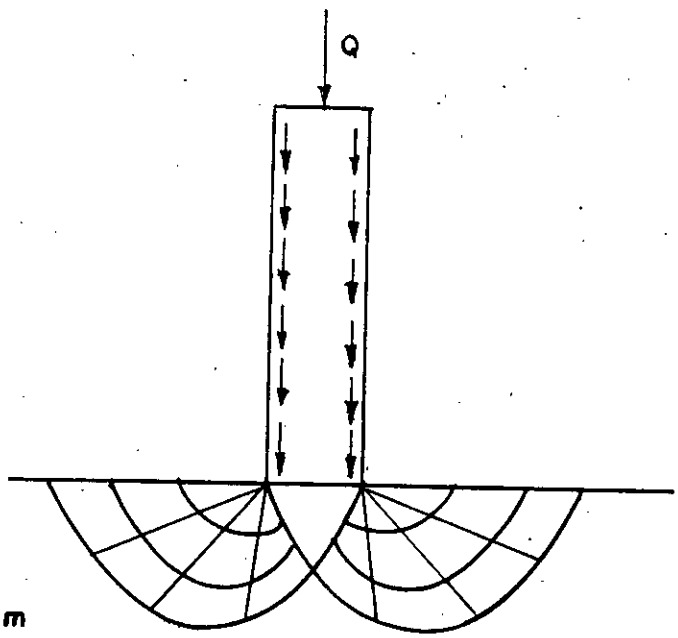


Fig. 2.3(b) Punching Failure Pattern.

Fig. 2.3(a) shows the elasto-plastic behaviour of soil. Fig. 2.3(b) shows how punching failure develops. Main characteristics of a punching failure is that there will be no well defined shear zones at the sides of the footing and no heave will occurs. Terzaghi(1943) extended the classical work on punching failure done by Prandtl and Reissner.

Following the same basic approach (elasto-plastic soil model), several different solutions were subsequently presented with different assumption concerning the failure pattern. Meyerhof(1953) presented new analyses considering the failure pattern shown in Fig. 2.4.

He proposed rigid-plastic soil model (shown in Fig. 2.5) which means that there are no strains at any point until the failure condition is fulfilled. On the otherhand Bishop, Collingridge and O'sullivan (1948) and Vesic (1977) considered the soil to be compressible which was more realistic and shown in Fig. 2.6.

A different approach was taken by Vesic(1972) and he considered the soil failure induced by the pile point as a special case of the expansion of a cavity inside a solid mass.

Fig. 2.7 illustrates the cavity expansion theory. Soil mass is assumed homogeneous and under an isotropic effective stress, there exists a spherical cavity of radius Ri (dashed

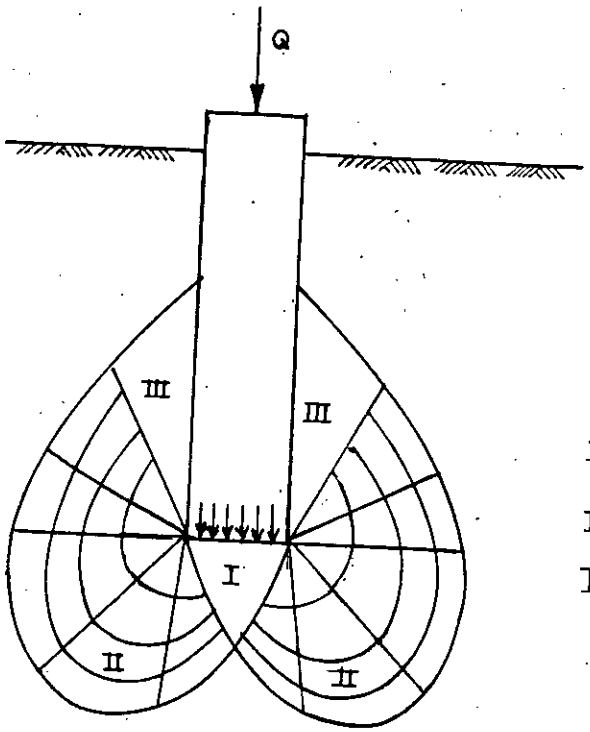


I = Elastic Zone

II = Plastic Zone

III = Elastic Zone

Fig. 2.4 Terzaghi's (1943) Failure Pattern.

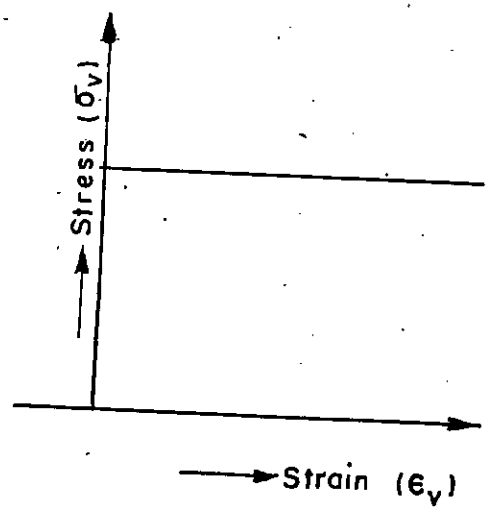


Fig. 2.5 Stress - Strain Curve for Plastic Material.

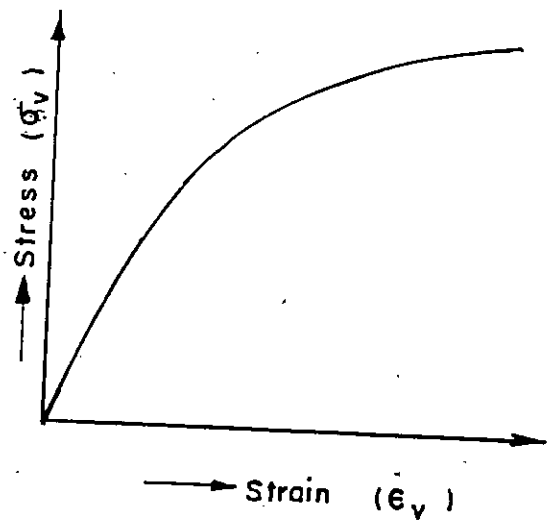


Fig. 2.6 Stress - Strain Curve for for Compressive Material.

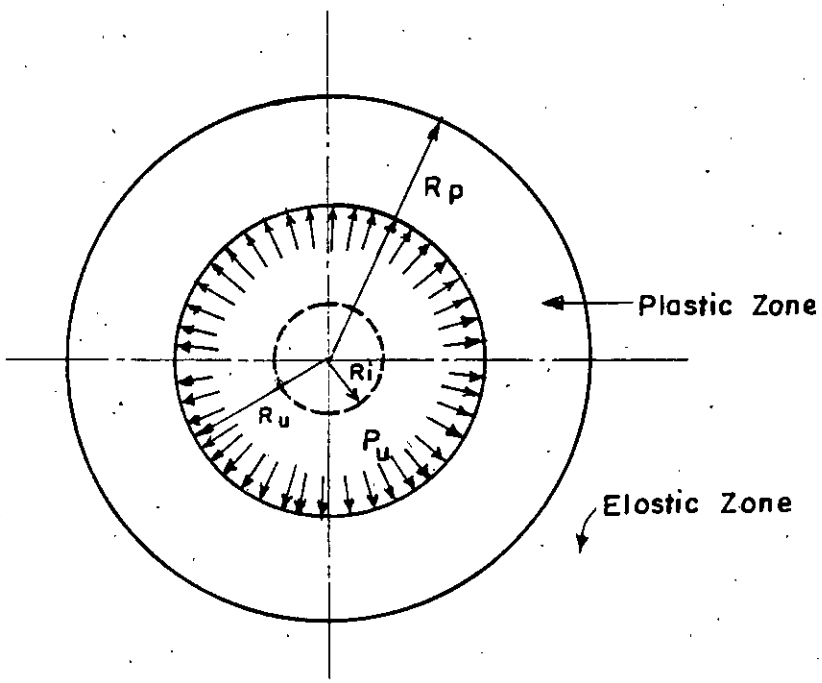


Fig. 2.7 Expansion of a Spherical Cavity

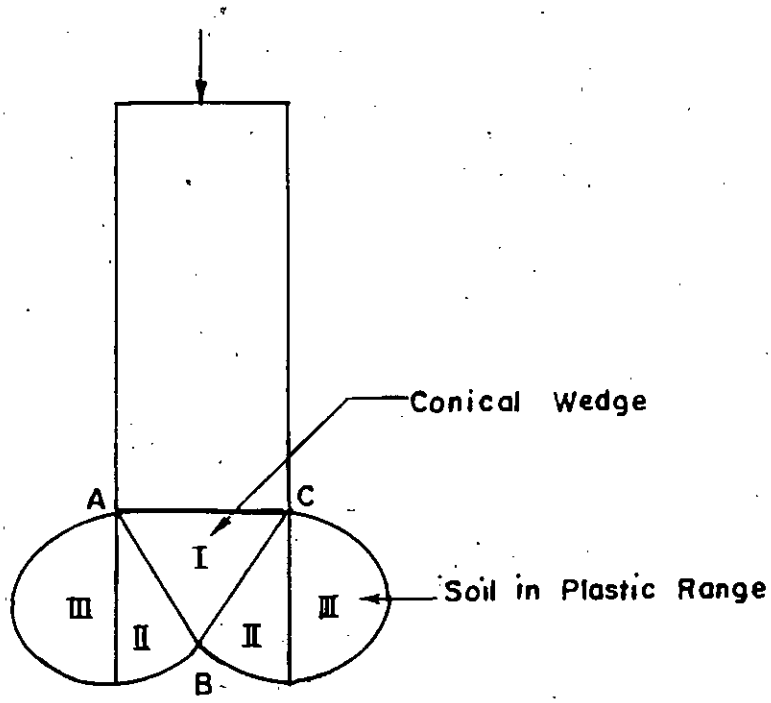


Fig. 2.8 Vesic Model of Pile Behaviour.

line) within the soil mass. Soil behaviour in the elastic range can be described by a modulus of deformation, E and poisson's ratio, $\nu_s$. In the plastic range, it can be described by the Mohr - coulomb shear strength parameters, $c - \phi$ . At a particular internal pressure $P_u$, the cavity has a radius $R_u$ and the limit of the annulus in the plastic range is defined by $R_p$.

Cavity expansion concepts was again applied to pile foundation by Vesic (1977). He compared the failure patterns of end bearing piles in model tests and of the field with the failure patterns developed by cavity expansion theory in an aim to predict the end bearing capacity by using cavity expansion concepts. Fig. 2.8 indicates a highly compressed conical wedge I of soil. This wedge forces its way through loose sand without forming slip surfaces. The pile advances by compression along zones II and I and by expansion along the boundary AB. It is then assumed that the average normal stress along AB is equal to the pressure needed to expand the cavity in the infinite soil mass around it.

In all theoretical solutions the ultimate unit point resistance, $q_o$ is usually expressed in the form (Coyle and Castello, 1981) :

$$q_o = \gamma_s b N_\gamma . S_\gamma + C N_c . S_c + P_o N_q . S_q \qquad (2.3)$$

in which $\gamma_s$ is the effective unit weight of the soil at the

pile point; b is the least foundation dimension; $P_o$ is the effective overburden pressure at the pile point level; C is the cohesion of the soil; $S_\gamma$, $S_c$, $S_q$ are shape factors and $N_\gamma$, $N_c$, $N_q$ are bearing capacity factors usually depending upon the soil friction angle, and the assumed pattern or mechanism of failure. In engineering practice Equation 2.3 is usually made simplified. In the first place, since the study is restricted to sands (cohesionless soils), the second term of the equation can be eliminated. Secondly, when comparing the two remaining terms, it seems that the first term is relatively small and can be neglected. The final simplification concerns the form of the remaining term. Since most piles have circular or square cross sections and the shape factor is the same, it is reasonable to use the only bearing capacity factor, Nq, that incorporates this constant shape factor. Therefore, the commonly used form of Equation 2.3 becomes

$$q_o = P_o N_q \qquad (2.4)$$

In most of the theories the basic parameters, in addition to the pile geometry, are the friction angle, $\phi$ which is used to determine the bearing capacity factor, $N_q$, and the effective confining pressure of the soil.

All of the bearing capacity theories require the evaluation of $N_q$ for the use in Equation (2.4) should be considered. A summary of the ranges of values of $N_q$ according to the different theories is presented in Table 2.2. It is evident

TABLE 2.2 - Bearing Capacity Factors for Deep Foundation (Vesic, 1972, 1977)

| Theories | Approximate $N_q$ Values for Various Friction Angles, $\phi$, in degrees | | | | |
|---|---|---|---|---|---|
| | 25 | 30 | 35 | 40 | 45 |
| De Beer (1945) | 59 | 155 | 380 | 1150 | 4000 |
| Meyerhof (1953): Driven piles | 38 | 89 | 255 | 880 | 4000 |
| Caquot-Kerisel (1956) | 26 | 55 | 140 | 350 | 050 |
| Brinch Hansen (1961) | 23 | 46 | 115 | 350 | 1650 |
| Skempton-Yassin-Gibson(1953) | 46 | 66 | 110 | 220 | 570 |
| Brinch Hansen (1951) | 32 | 54 | 97 | 190 | 400 |
| Berezantsev (1961) | 16 | 33 | 75 | 186 | ---- |
| Vesic (1963) | 15 | 28 | 58 | 130 | 315 |
| Vesic (1972):*$I_r$ = 60 | 36 | 46 | 57 | 70 | 84 |
| $I_r$ = 200 | 60 | 79 | 103 | 131 | 164 |
| Terzaghi (1943): General shear | 12.7 | 22.5 | 41.4 | 81.3 | 173.3 |
| : Local shear | 5.6 | 8.3 | 12.6 | 20.5 | 35.1 |

*$I_r$ = Rigidity Index

that there are major deviation from one theory to another, leading to the conclusion that the true failure mechanism is not generally well understood. Vesic(1977) stated: " Computation of the ultimate load is quite difficult and a general solution is not yet available". and added " In view of the many uncertainties involved in analysis of pile foundations, it has become customary, and in many cases mandatory to perform a certain number of full-scale pile load tests at site of more important projects".

## 2.3 Experimental Works on Bearing Capacity and Skin Friction

It has been shown that the variation of predicted values of Bearing capacity factor, $N_q$ and lateral earth pressure coefficient, K is so wide that the choice of one theory over another is a difficult exercise in engineering judgment. The need for better understanding of failure mechanisms and development of an acceptable theory has resulted in a number of experimental investigations.

Mayer and L'Herminier (1953) reported a work done by others and recognized three distinct patterns for sand failure according to depth of penetration. These patterns are for a general shear failure for very shallow foundations, a localized shear failure for deep foundations, and a Meyerhof type failure (a failure, where plastic flow occurs in upward direction, is shown in Fig. 2.4) for intermediate penetrations. These failure

patterns, with soil being displaced upwards and away from the pile, indicated a tendency to form a gap between the pile shaft and the soil. Consequently, the active case of lateral earth pressure could develop.

Meyerhof(1959) indicated that, in cohesionless soils, the effect of pile driving is general compaction resulting from permanent rearrangement and some crushing of the soil particles. In addition, the driving of pile in the soil mass alters its state of stress. Subsequently, Broms(1966) reported that in cohesionless soil, pile driving alters its original state of stress and the soil mass undergo general compaction.

Measurements made by Szechy (1961), using laboratory model tests indicated that the idea of general sand compaction is not valid. Szechy found that-- "the highly compressed concentration areas are surrounded with areas of stress-relief below the pile toe as well as around the the pile shaft." Robinsky and Morrison(1964) with more sophisticated measurements made on loose and medium dense sands in the laboratory, confirmed the findings of Szechy (1961). According to Robinsky and Morrison the overall process of sand compaction results in a seemingly erratic accumulation of high and low density areas. A thin sleeve of loose sand is created around the pile wall, which is encircled by a cylinder of dense sand. This cylinder,(Fig. 2.9) by arching, prevents the development of full lateral earth pressure on the pile. Also, Robinsky and Morrison(1964) reported an

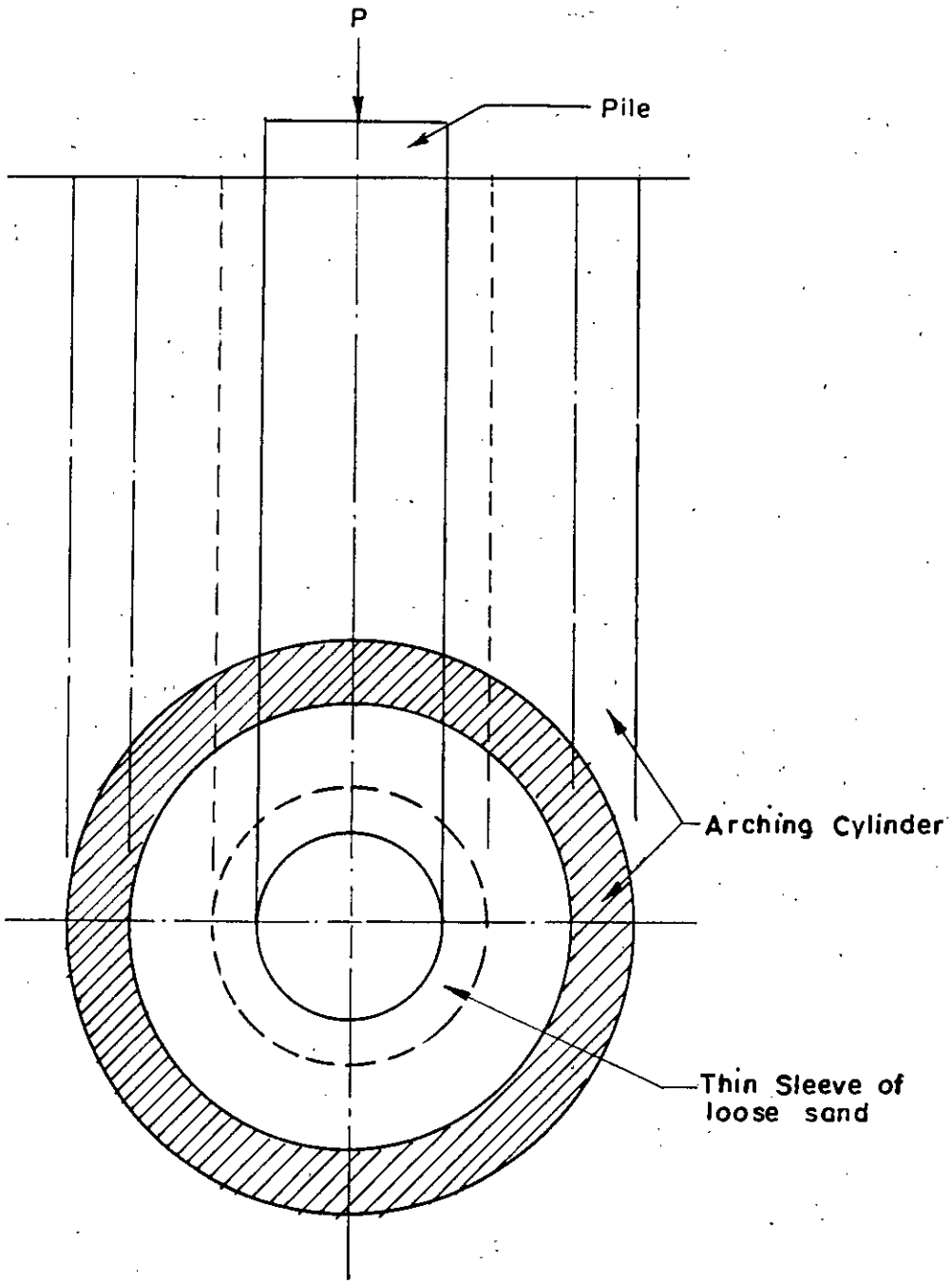


Fig. 2.9 Horizontal Arching in Dense Sand.

additional experimentation which indicated that with pile penetration the "arches" around areas of loosened sand could be built up and broken down,inducing continuous changes in mobilized side resistance.

Kerisel(1961) published a noteworthy paper concerning laboratory experiments in sand. It was observed that different size piles in the same sand attained a maximum value of unit load resistance (both point and side) which remained constant with increasing penetration. The depth, where the constant value was attained varied with the pile diameter.

Vesic(1970) confirmed, with field tests, the tendency for unit resistances (both side and point) to increase with depth to some limiting value. Vesic noted that even though the rate of increase sharply decreases at some depth called "critical depth", there was an additional increase with further penetration. This "critical" depth was defined as being between 10 pile diameters for loose sands and 20 for denser sands.

Biarez and Gresillan(1972) reported a laboratory experiment performed at Grenoble, France. Pile models of various diameters were penetrated into metallic rollers (a bidimensional problem), into glass spheres of same diameter, surcharges applied by means of air pressure (with membranes covering the sand). Once again limiting unit resistance (both side and point) were obtained.

## 2.4. Design Considerations

In pile design load carrying capacity of a pile is the main problem to be solved. Load carrying capacity of a pile is attributed to two component of resistances offered by a pile i.e. (1) skin friction and (2) point bearing.

Point or tip bearing of a pile can be computed by variety of ways depending on the estimation of the bearing capacity factors. Meyerhof (1951, 1976) proposed the following relation:

if $L/B < L_c/B$ and $\phi > 0$ (cohesionless soil)

$$P_{pu} = A_p \, q \, N_q \qquad (2.5)$$

if $L/B > L_c/B$ (bearing stress cannot exceed a limiting value as below)

$$P_{pu} = A_p \, q \, N_q < A_p(50N_q) \tan(\phi) \qquad (2.6)$$

where

$P_{pu}$ = Tip bearing

$L$ = Embedded length of the pile

$A_p$ = Tip area of pile

$q$ = Effective vertical stress at pile point.

$N_q$ = bearing capacity factor (can be obtained from Fig. 2.10)

$L_c$ = critical depth of pile below which point bearing

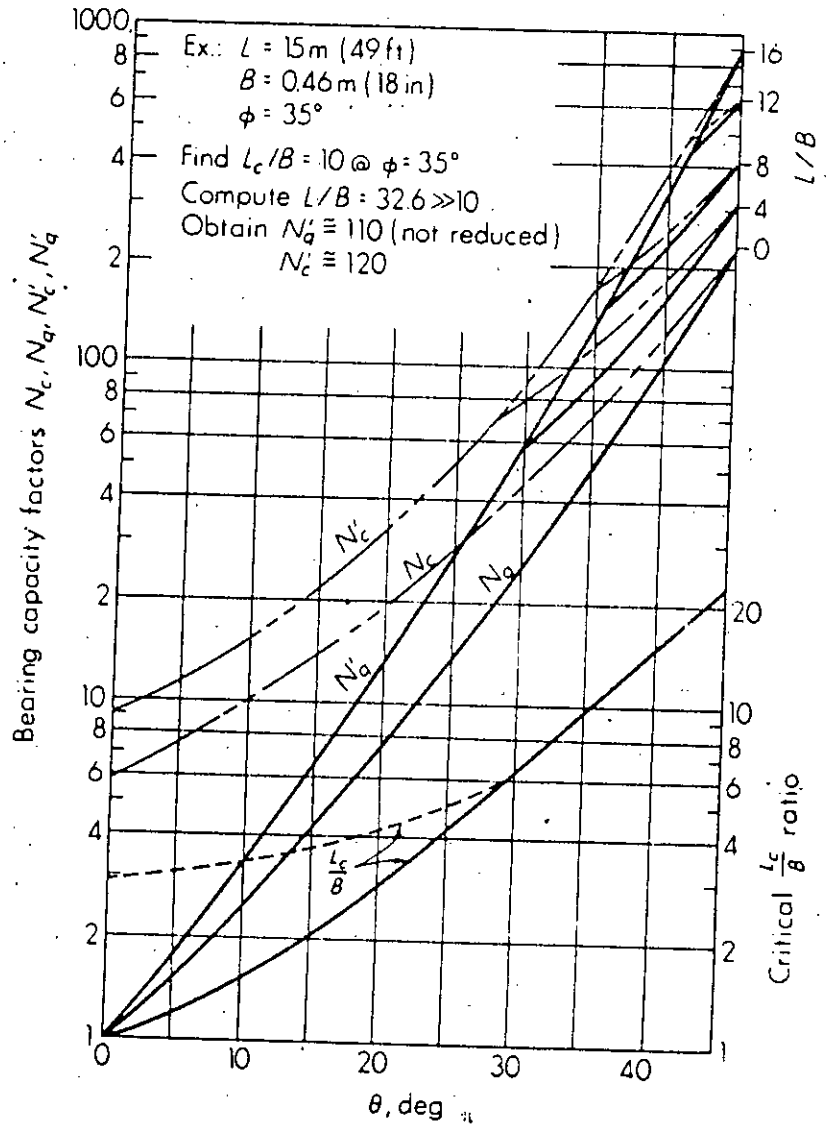


**Figure** 2.10 Bearing-capacity factors for deep foundations. [*After Meyerhof (1976).*]

becomes constant.

B = Diameter or, width of pile.

Vesic (1975) proposed a new formula for the determination of bearing capacity factor $N_q$ depending on the cavity expansion theory.

$$N_q = \frac{3}{3-\sin(\phi)} \{\exp[(\pi/2-\phi)\tan(\phi)]\tan^2(45+\phi/2) \times I_{rr}^{\frac{4\sin(\phi)}{3(1-\sin(\phi))}} \quad (2.7)$$

The reduced rigidity index $I_{rr}$ in this equation can be computed as $I_{rr} = I_r/(1+ I_r)$

Again, the rigidity index, $I_r$ can be computed using the shear modulus $G_s$ and shear strength, s of the soil as

$$I_r = G_s/(c+q\tan(\phi)) = G_s/s$$

He further proposed that the bearing capacity term for cohesion can be computed similar to spread footings as

$$N_c = (N_q - 1)\cot(\phi) \quad (2.8)$$

According to Janbu(1976) $N_q$ can be computed as follows:

$$N_q = (\tan(\phi) + \sqrt{1+\tan^2(\phi)})^2 \exp(2\psi \times \tan(\phi)) \quad (2.9)$$

where $\psi$ is the angle shown in Fig. 2.11 and varies from

60° in soft compressible soil to 105° in dense soils. Analyzing large value of Standard Penetration Test (ASTM D1586) data Meyerhof (1956, 1976) proposed that,

$$P_{pu} = A_p\ (38N)\ L_b/B < 380N\ (A_p) \qquad (2.10)$$

where

$P_{pu}$ = Point resistance

N = statistical average of Standard Penetration Test (ASTM D1586) blow numbers in a zone of about 8B above to 3B below the pile point.

$L_b/B$ = average depth ratio of point or tip.

For cone penetration data Meyerhof further proposed,

$$P_{pu} = A_p\ q_c\ (\text{units of } q_c) \qquad (2.11)$$

where $q_c$ is the statistical average of the cone point resistance.

In 1971 Tomlinson propounded the $\alpha$ (alpha) method to predict skin friction of a pile. He proposed,

$$f_s = c + qK \tan(\delta) \qquad (2.12)$$

where $\alpha$ = coefficient from chart.(Fig: 2.12)

c = average cohesion for the soil stratum of interest.

q = effective vertical stress.

K = coefficient of lateral earth pressure ranging from $k_o$ to about 1.75

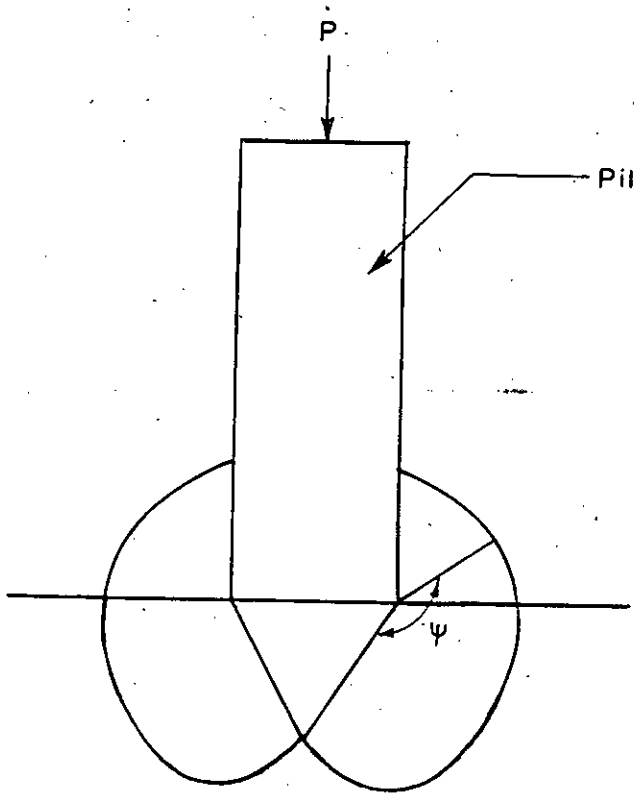


Fig 2.11 Position of the Angle ψ.

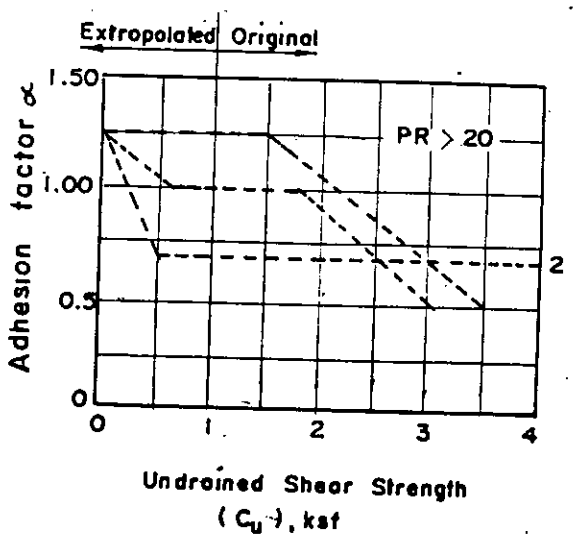


Fig. 2.12 Relationship between soil and adhesion factor
(After Tomlinson 1971)

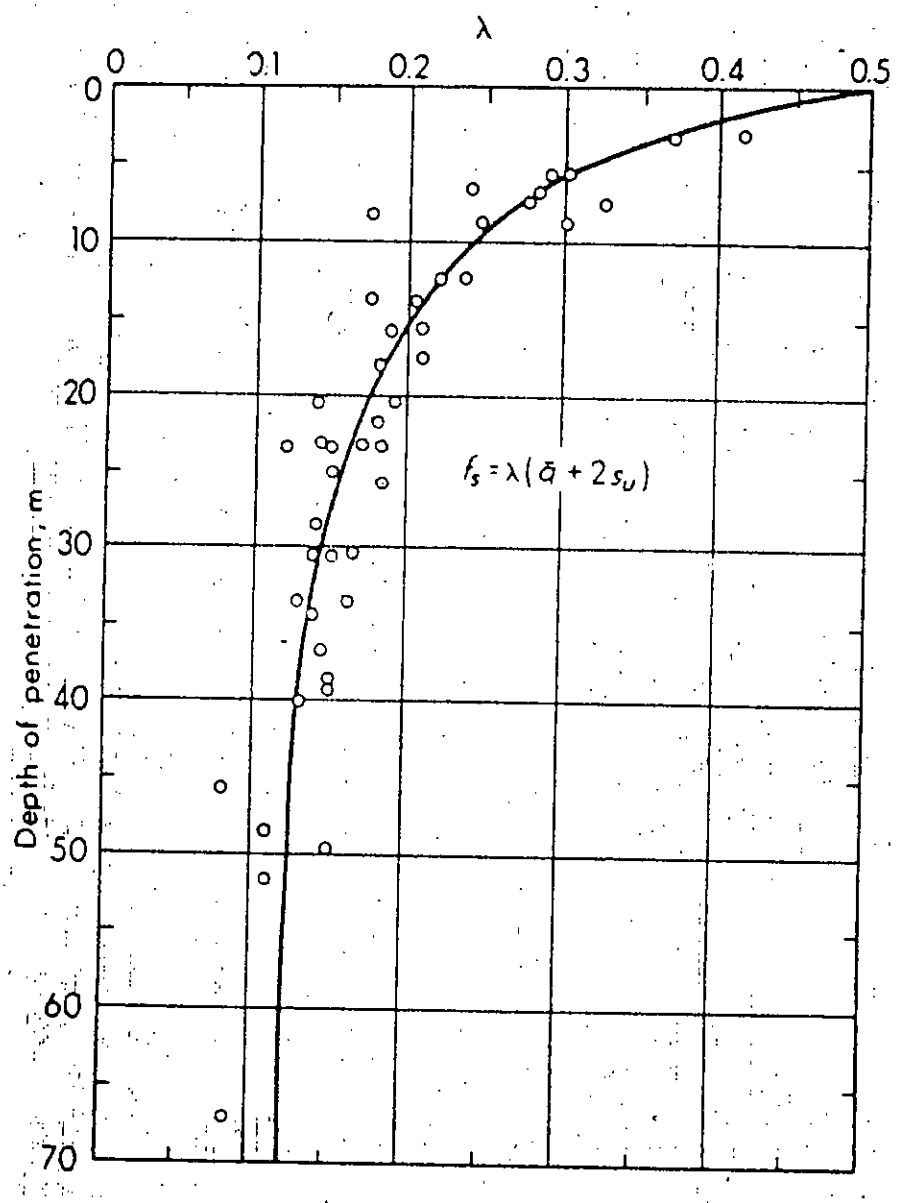


Fig. 2.13 Coefficients depending on Pile Penetration (Vijayvergiya and Focht (1972)).

$\delta$ = effective friction angle between soil and pile material.

$K_o$ for piles is most commonly computed as $K_o = (1-\sin(\phi))\ OCR$.

Vijayvergiya and Focht in 1972 proposed a new formulation called $\lambda$ method.

$$fs = \lambda\ (q + 2\ Su) \qquad (2.13)$$

where

$\lambda$ = Coefficient to be taken from Fig. 2.13

Su = average shear strength for the soil stratum of interest

Then having reanalyzed existing data and equipped with more recent tests, proposed a better correlation of skin friction to effective stress parameters called Beta($\beta$) method.

$$f_s = Kq \tan(\delta) \qquad (2.14)$$
$$= \beta q \quad [\beta = k \tan(\delta)]$$

In 1970 Vesic related skin friction to relative density of sand for a pile empirically

$$f_s = X_v(10)^{1.540r} \qquad (2.15)$$

where $f_s$ = Skin friction in KPa

$X_v$ = 8 for larger volume displacement pile

= 2.5 for bored, open ended pile.

$D_r$ = Relative density.

For SPT data Meyerhof (1965, 1976) suggested that

$$f_s = Xm\ N. \qquad (2.16)$$

where $f_s$ = Skin friction in KPa

$X_m$ = 2.0 for piles with large volume displacement

= 1.0 for piles with small volume displacement.

N = statistical average of standard penetration below count.

For Cone penetration data Meyerhof (1956) and Thornburn and MacVicar (1971) suggested

$$f_s = 0.005\ q_c \qquad (2.17)$$

where fs = Skin friction in KPa

$q_c$ = Cone penetration resistance, KPa.

When Cone penetrometer is used and side friction $q_{cs}$ is measured, therefore Vicar (1971) suggested

$f_s = q_{cs}$ (small volume displacement pile) (2.18)

$f_s$ = 1.5 to 2.0 $q_{cs}$ (large volume displacement piles)

Conventional methods of calculation of the ultimate load capacity of piles in sand (Broms, 1966; Nordlund, 1963) assume

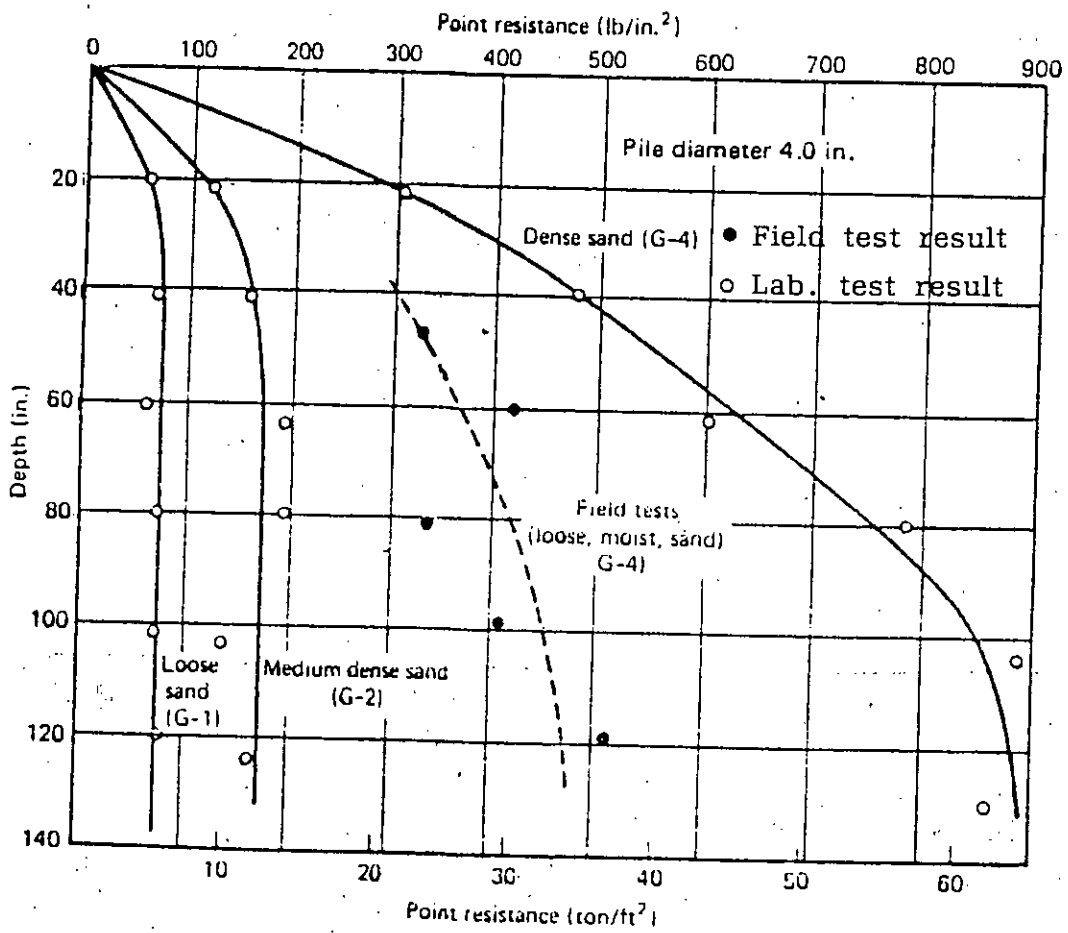


Fig. 2.14 Variation of Point Resistance with Pile Length (Vesic,1967).

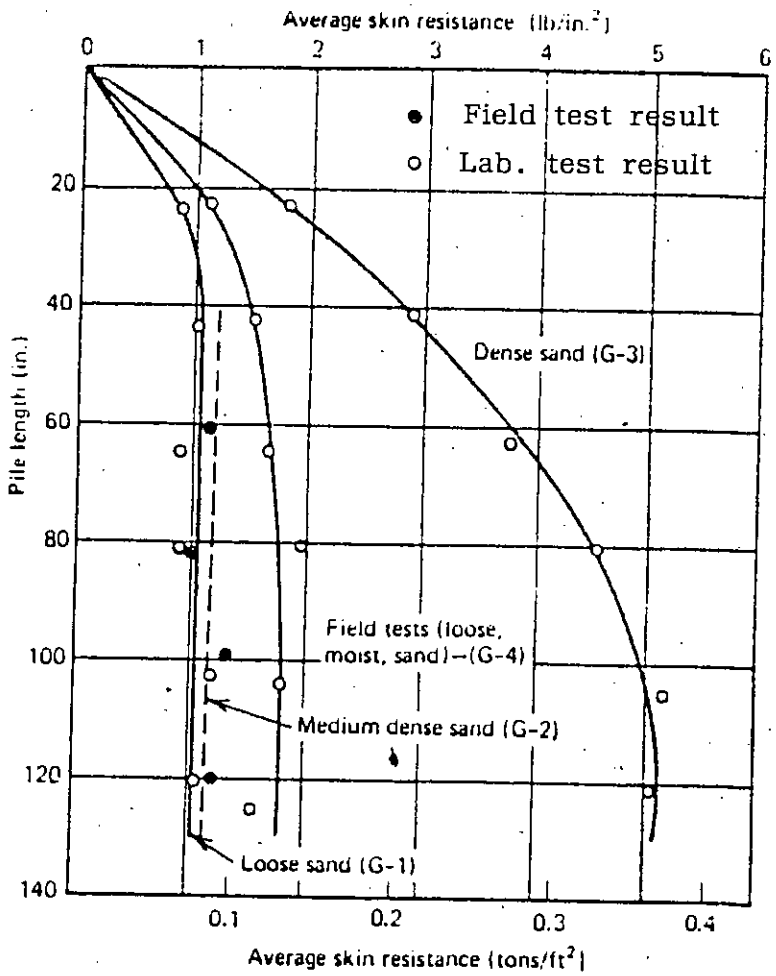


Fig. 2.15 Variation of Skin Resistance with Pile Length (Vesic, 1967).

that tha vertical stresses are due to the effective load from overburden material. Extensive research by Vesic (1967) reveals that the unit shaft and base resistances of a pile do not necessarily increase linearly with depth, but instead reach almost constant values beyond a certain depth which have been shown in Fig. 2.14 and Fig. 2.15 . This phenomenon was attributed by Vesic to arching and is similar to that considered by Terzaghi (1943a) in relation to tunnels.

Some design approaches have effectively incorporated Vesic's finding by specifying an upper limit to the shaft and base resistances. For example, McClelland et al (1969) have suggested, for medium-dense clean sand, the following design parameters: $\phi = 30°$ ; Coefficient of earth pressure, $K_s = 0.7$ (compression loads) or 0.5 (tension loads), with a maximum value of shaft resistance $f_s$ of 1 ton/ft. (96 $KN/m^2$); and $N_q = 41$. with a maximum base resistance $f_b$ of 100 $ton/ft.^2$ (9.6 $MN/m^2$ ). However, such approach take little account of the nature of the sand and may not accurately reflect the variation of pile capacity with pile penetration.

Coyle and Castello(1981), proposed a new design correlation improving existing correlation between bearing capacity factors and pile soil system parameters. Field load test data from 34 tests were found in the literature, but only 16 of them included both compression and tension test data. So they took those 16 data to develop a better correlation. Comparison of

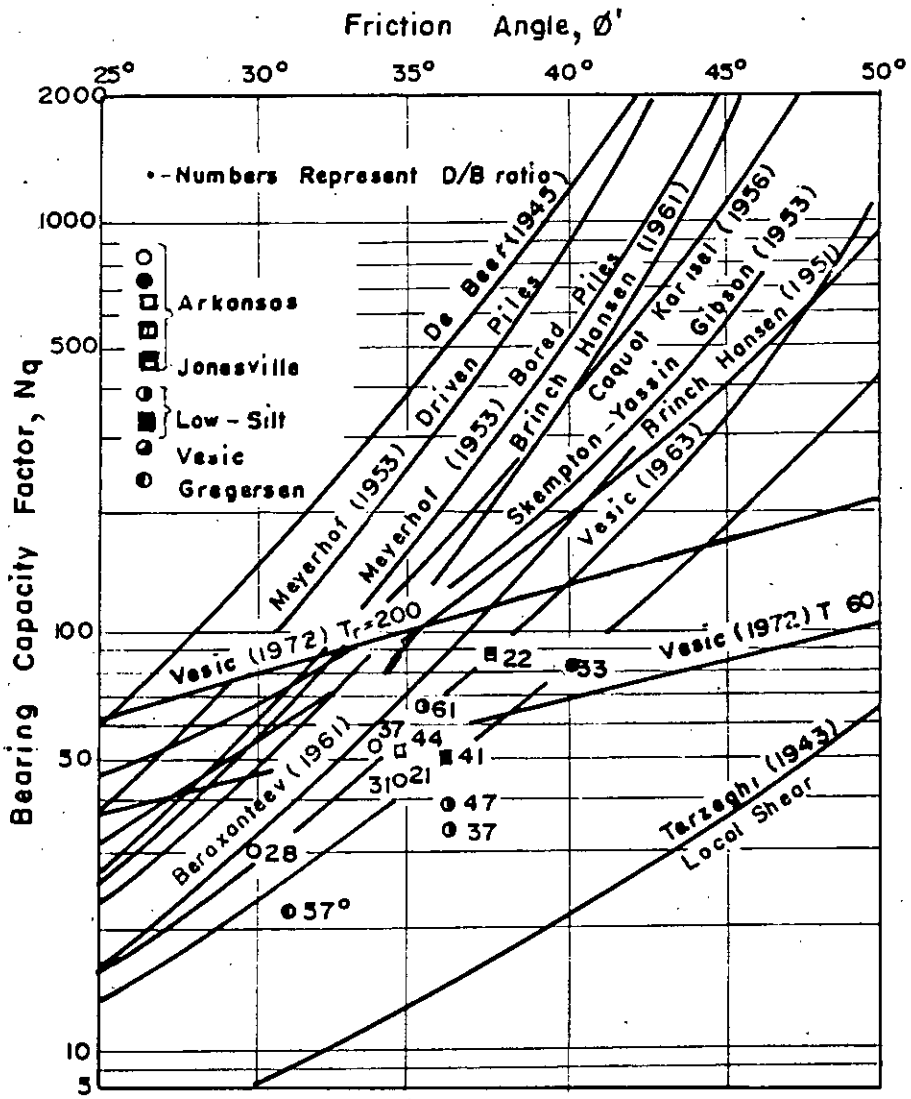


Fig. 2.16 Bearing Factor $N_q$ Versus Ø — Compression / Tension
( Coyle etal, 1981 )

$N_q$ values obtained from field test data and theories is given in figure 2.16 . Curves are plotted for the better known theories, covering a wide range of possible $N_q$ values. Also the $N_q$ values obtained from field test are plotted for the compression/tension data. Tip bearing is separated from the results of compression and tension test data. From the field tip bearing value, $N_q$ values are computed. The results in Fig. 2.16(b) show that none of the theories can be used to predict correct $N_q$ value. Terzaghi's general shear theory also predicts higher $N_q$ value. The measured $N_q$ values deviate widely from the theoretical values. This type of comparison clearly showed the need for improved correlations which include all significant parameters involved in the pile-soil interaction problem.

Coyle and Castello in 1981 used field load test data to develop a new correlation which related the bearing capacity factors to pile geometry parameters and sand properties. Several different combinations of pile parameters and sand properties were investigated during the development of these correlations. The correlations presented were considered the simplest and best for practical usage.

Practical pile designs are based on static cone and standard penetration tests, specially in cohesionless soil. In 1982 Meyerhof analyzed the methods of estimating the ultimate bearing capacity of piles in sand from the results of static cone and standard penetration tests and compared with the results of

load tests on driven and bored piles of different sizes and embedment ratios in the sand stratum. He suggested an empirical reduction factor for the ultimate unit point resistance,

$$R_b = ((B+0.5)/2B)^n < 1 \quad \text{for } B > 0.5 \text{ m} \qquad (2.19)$$

in which B = pile base diameter in meters; and n = an index which may roughly be taken as n = 1 for loose sand, n = 2 for medium dense sand, and n = 3 for dense sand, which is shown in Fig. 2.17.

## 2.5 Analytical Works on Bearing Capacity and Settlement Analysis

Analysis of piles for bearing capacity and settlement may be done by various methods. Such method may be classified into four broad categories:

1. Traditional empirical methods.
2. Load-transfer methods.
3. Methods based on the theory of elasticity
4. Numerical methods (finite element finite, differance method).

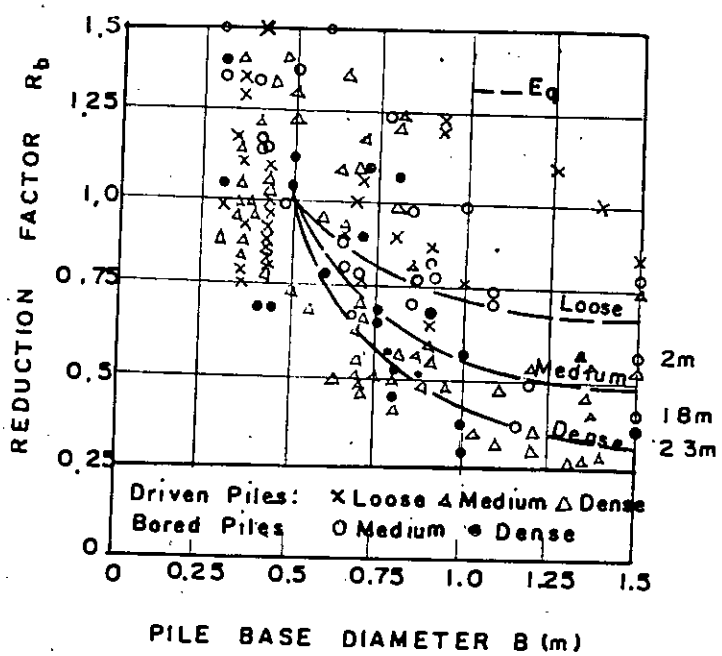


Fig. 2.17 Empirical reduction factor for ultimate point resistance of large diameter piles in sand (Meyerhof, 1983)

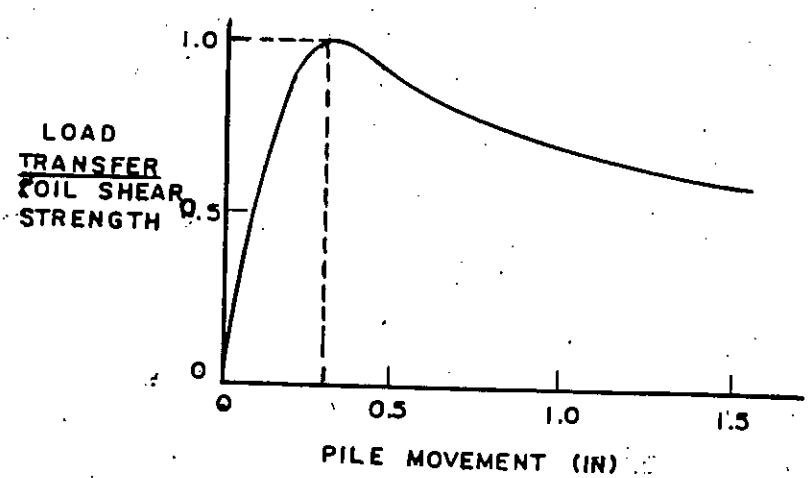


Fig. 2.18 (a) Ratio of load Transfer to soil shear strength versus pile movement.

### 2.5.1 Traditional empirical methods for settlement analysis

Meyerhof (1956) suggested from an analysis of a number of load tests that at loads less than about one third of the ultimate, the settlement (mm) of a pile could be estimated as follows:

$$\rho = d_b/30F \qquad (2.20)$$

where $d_b$ = diameter of pile base (mm)

$F$ = factor of safety ( >3 ) on ultimate load

Focht (1967) examined data from a number of load tests and related the observed settlement, $\rho$ , at the working load to the computed column deformation $\rho_{col}$ at the working load. Focht defined a "movement ratio" as $\rho / \rho_{col}$ and found that for relatively long highly-stressed piles having $\rho_{col}$>8 mm. the movement ratio is of the order of 0.5, where as for relatively rigid piles, having $\rho_{col}$>8 mm, the movement was larger. on the order of 1.0 .

### 2.5.2 Load-transfer methods

This method, proposed by Coyle and Reese (1966), utilizes soil data measured from field tests on instrumented piles and laboratory tests on model piles. The relevant soil data required in this method are curves relating the ratio of the

adhesion (or load-transfer) and the soil shear strength to the pile tip movement. Such curves were first developed by Seed and Reese (1957), and a typical relationship is shown in Fig. 2.18(a).

In actual problems, a number of such relationship may be required to describe the load transfer along the whole length of the pile. The load-transfer method may be summarized as follows:

1. The pile is divided into a number of segments (shown in Fig. 2.18(b)).
2. A small tip movement, $y_T$ is assumed (zero may be selected).
3. The point resistance, $P_T$, caused by this movement is calculated. This may be done approximately by assuming the pile tip to be a rigid circular area and employing the Boussinesq theory (Coyle and Reese,1966)

$$P_T = \frac{2dEy_T}{(1-\nu^2)} \qquad (2.21)$$

where $E, \nu$ are the young's modulus and poisson's ratio of the material beneath the tip, estimated from triaxial tests or other data.

4. A movement, $y_{3T}$ , in the bottom segment at midheight is assumed.

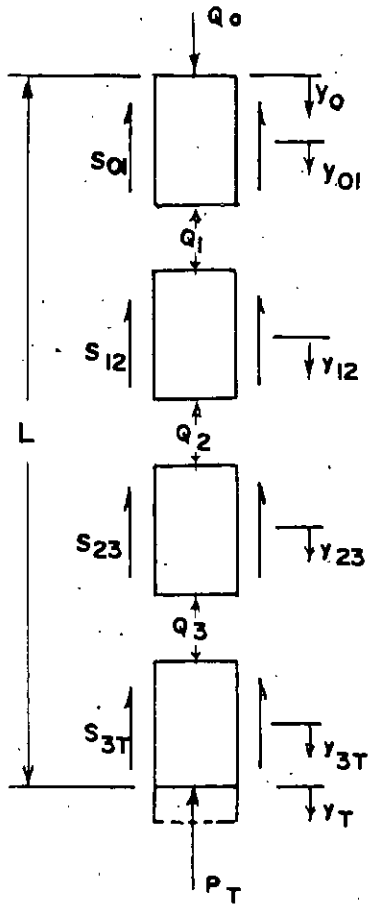


Fig. 2.18 (b) Axially Loaded Pile. (Coyle and Reese, 1966)

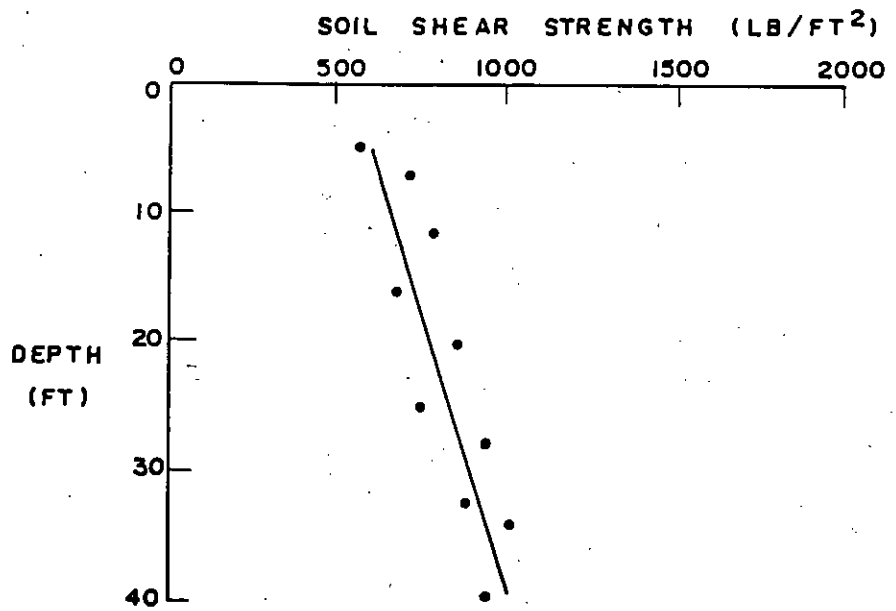


Fig. 2.19 Shear Strength Versus Depth.

5. Using the estimated $y_{3T}$, the appropriate curve of load-transfer/soil-shear-strength versus pile movement is used to find the appropriate ratio.

6. From a curve of shear strength versus depth, (shown in Fig. 2.19), the strength of the soil at the depth of the segment is obtained.

7. The load transfer or adhesion is then calculated as $\tau_a$ = (ratio x shear strength). The load $Q_3$ on the top of segment 3 can be calculated as

$$Q_3 = P_T + \tau_a L_3 P_3 \qquad (2.22)$$

where, $L_3$= length of segment 3

$P_3$= average perimeter of segment 3

8. The elastic deformation at the midpoint of the pile segment (assuming a linear variation of load in the segment) is calculated as

$$y_{3T} = \frac{Q_m}{2} \times \frac{L_3}{2A_3E_p} \qquad (2.23)$$

where $Q_m = (Q_3+P_T)/2$

$A_3$ = area of segment 3

$E_p$ = Pile modulus.

9. The new midheight movement is then given by

$$y'_{3T} = y_T + y_{3T} \qquad (2.24)$$

10. $y'_{3T}$ is compared with the estimated value of $y_{3T}$ from step 4.

11. If the computed movement $y'_{3T}$ does not agree with $y_{3T}$ with in a specified tolerance, step 2 to 10 are repeated and a new midpoint movement calculated.

12. When convergence is achieved, the next segment up is considered, and so on, until a value of load ($Q_0$) and displacement ($y_0$) for the top of the pile are obtained.

The above procedure is then repeated using different assumed tip movements until a series of values of $Q_0$ and $y_0$ are obtained. These values can then be used to plot a computed load-settlement curve.

On the basis of field data on instrumented piles and laboratory tests on model piles, Coyle and Reese derived a series of three average curves of load transfer, shear-strength versus pile-movement curves for various depths, which are shown in Fig. 2.20 .The interpretation of the tests on instrumented piles to obtain these curves was described in detail by Coyle and Reese(1966).

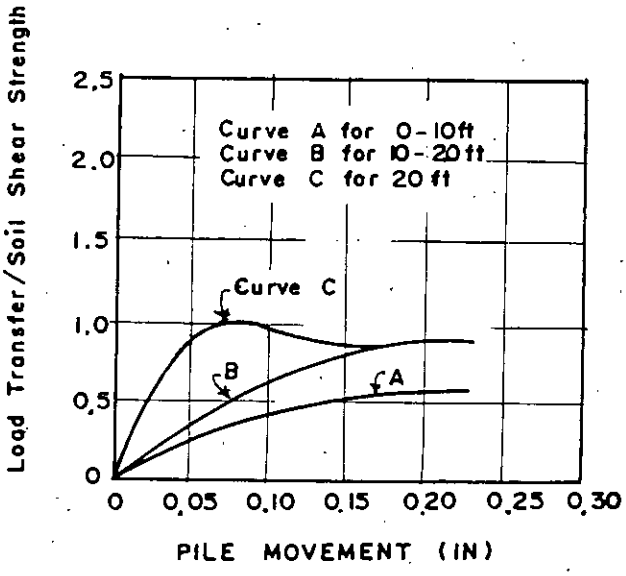


Fig. 2.20 Design load transfer curves for pipe piles in clay (Coyle and Reese, 1966)

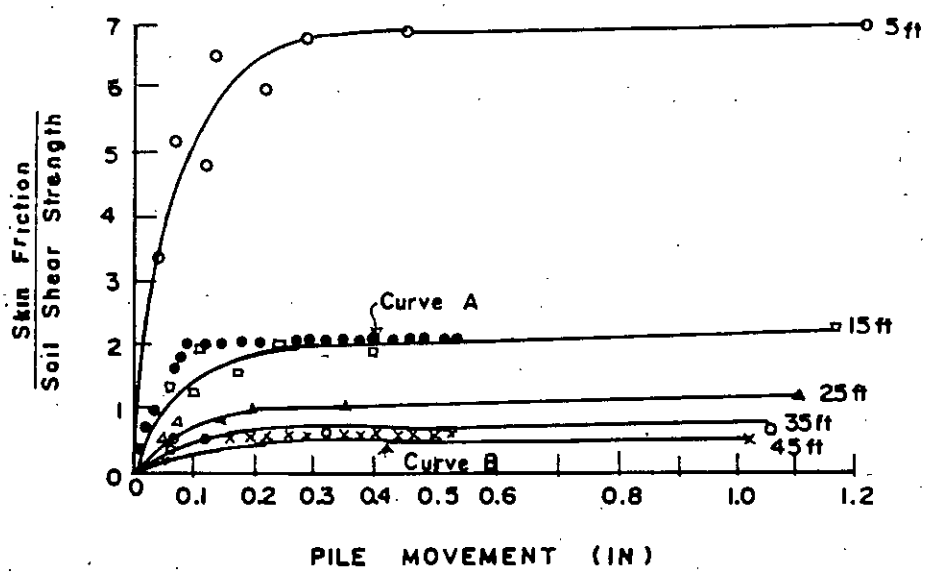


Fig. 2.21 Design load transfer curves for piles in sand (after Coyle and Sulaiman, 1967)

From a series of tests on instrumented pile in sand Coyle and Sulaiman(1967) have presented data on the load-transfer versus movement characteristics for steel piles in saturated sand, shown in Fig. 2.21 . This data suggested that for depths of 0 to 20 ft., curve A, with an upper limit of skin friction of twice the shear strength, can be used. For depths greater than 20 ft., the measured relationships approach curve B, with an upper limit of skin friction of 0.5 times the shear strength.

### 2.5.3 Methods based on the theory of elasticity

In this method the pile is divided into a number of uniformly loaded elements and a solution is obtained by imposing compatibility between the displacements of the pile and the adjacent soil for each element of the pile. The displacements of the pile are obtained by considering the compressibility of the pile under axial loading. The soil displacements are obtained in most cases by using Mindlin's equations for the displacements with in a soil mass caused by loading with in the mass.

D'Appolonia and Romualdi (1963), Thurman and D'Appolonia (1965) assumed the shear stress at each element to be represented by a single point load acting on the axis at the center of each element. Nair (1967) assumed a uniformly loaded circular area at the center of each element. Poulos and Davis (1968), Mattes and Poulos (1969) and considered a shear stress distributed uniformly around the circumference of the pile. The

latter appeared to be the most satisfactory of those numerical methods.

### 2.5.4 Numerical methods

Detailed descriptions of the finite element method have been given by Zienkiewicz (1971) and Desai and Abel (1972). Desai and Christian (1977) discussed comprehensively the use of finite element in geotechnical problems. Desai (1974) considered a pile in sand with a hyperbolic stress-strain response and also used special elements for the pile soil interface.

Balaam et al (1976) used a different type of analysis, in which the finite element method was used to analyze the pile and soil mass separately and then compatibility conditions were imposed to determine the nodal forces and deflections. The possibility of slip at the pile-soil interface is allowed for by specifying a limiting pile-soil shear strength, from which limiting values of nodal force can be calculated.

### 2.5.5 Comparisons between solution from elastic approach and finite element analysis

Balaam et al (1976) obtained elastic solutions of axially loaded piles for the case L/D = 10, K = 100, h/L = 2 and $\nu_s$ = 0.45. Twenty triangular elements were used for the pile and 160 triangular elements were used for the soil. A free outer

boundary was assumed at 35 pile diameters from the pile axis, the base underlying the soil was assumed to be rough and rigid. The settlement at the top of the pile was found to be only 2.00% less than that given by the analysis utilizing Mindlin's equations. Furthermore, the finite-element solution in which the pile and soil are analyzed together as a single mass. Decreasing the number of pile elements to 10 and the soil elements to 120 increases the discrepancy between the finite element solution and the elastic solution to 3.5%. In a parametric study of the settlement of a pile presented by Lee (1973), the solutions are obtained from a finite-element analysis. Table 2.3 shows a comparison between Lee's solutions for a floating pile in a uniform mass and the corresponding solutions from the elastic analysis. In this case the finite element solutions are slightly greater, but generally there is close agreement between the two series of solutions.

A further comparison with Lee's solutions is shown in Table 2.4 , this time for a pile bearing as a stiffer stratum. The agreement is again reasonable.

A comparison between computed load-settlement curves to failure for a pile in a purely cohesive soil is shown in Fig. 2.22 ($P_u$ is the ultimate load capacity). The agreement is generally reasonable, but at loads approaching the ultimate, the settlements given by the finite element analysis are greater than those from the "elastic" approach.

TABLE 2.3 Effect on Pile Displacement , Considering Radial Displacement Compatibility (Mattes and Poulos, 1969)

| Displacement = $\frac{P}{LE_s} I_p$ | | Top Displacement Influence Factor, $I_p$ | |
|---|---|---|---|
| | | Vertical Displacement Compatibility Only | Vertical and radial Displacement Compatibility Only |
| 10 | 100 | 1.793 | 1.782 |
| | 1000 | 1.378 | 1.448 |
| 25 | 100 | 3.559 | 3.542 |
| | 1000 | 3.181 | 3.160 |
| 100 | 100 | 10.670 | 10.488 |
| | 1000 | 5.220 | 5.140 |
| | 20000 | 2.758 | 2.712 |

TABLE 2.4 Comparisons between Elastic and Finite-Element Solutions for Pile Settlement (Lee, 1973)

| Displacement = $\frac{P}{dE_s} I_p$ | | Top Displacement Influence Factor, $I_p$ | |
|---|---|---|---|
| | | Finite Element | Elastic Mindlin Approach |
| L/d | | Floating Pile : Semi-infinite Mass | |
| 3.5 | | 0.267 | 0.258 |
| 5.0 | | 0.211 | 0.205 |
| 10.5 | | 0.115 | 0.112 |
| 15.0 | | 0.103 | 0.100 |
| 19.5 | | 0.094 | 0.092 |
| L/d | Eb/Es | End-Bearing Pile | |
| 5 | 10 | 0.078 | 0.075 |
| | 100 | 0.014 | 0.016 |
| 15 | 100 | 0.020 | 0.020 |

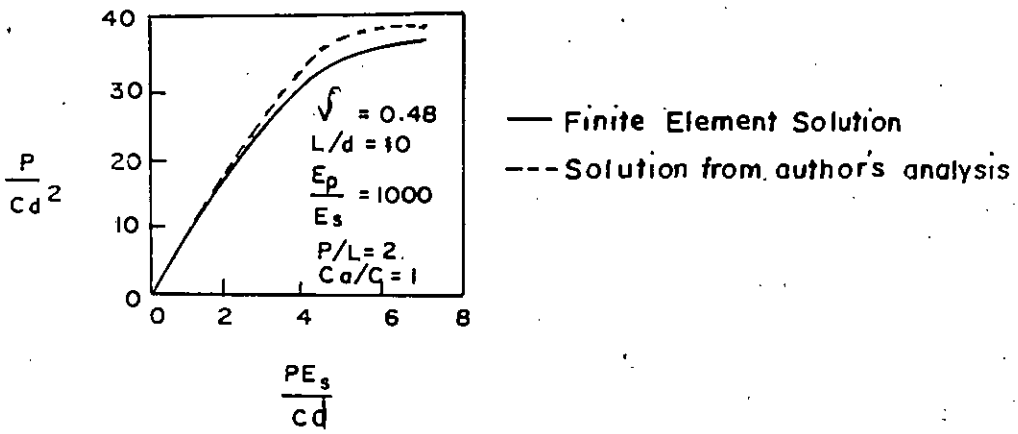


Fig. 2.22 Comparison between load settlement curves to failure. (Lee, 1973)

## 2.6 Main Point from Literature Review

From the literature review it transpires that much works have been done on the accurate prediction, determination and correlation of skin friction and end bearing of a pile. Separate works on skin friction parameters such as, earth pressure coefficient, coefficient of friction etc. have also been done. And bearing capacity factor $N_q$ received a major attention of the researchers.

Other experimental works revealed phenomena like sand arching and linear increment of pile capacity after critical depth.

History of pile design is based on the findings of accurate bearing capacity factor, earth pressure coefficient, coefficient of friction. But knowledge on this aspect seams to be incomplete. It is clear that load transfer mechanism of pile must be known first to simulate or, to predict the load settlement curve for piles. This would require model pile testing in uniform sand bed in order to know the actual load transfer mechanism in a simple and idealized manner.

From literature review of analytical works it is seen that finite element method of analysis can predict closed form solutions for pile top settlement well. So analysis of the problem is hereby recommended by finite element method.

# CHAPTER 3

## RESEARCH SCHEME

### 3.1 Introduction

From literature review it is apparent that load transfer mechanism of a pile must be known first to simulate or predict load settlement curve for the piles. Load transfer mechanism is a highly complex phenomena as it involves many factors such as slips along pile-soil interface and plastic deformation of soil during the progressive loading to failure. So load transfer curves show high degree of nonlinearity and are sensitive to any functional parameter of pile-soil system.

For the sake of idealization, investigations of load transfer mechanism were done in a uniformly laid sand bed only. The model piles are therefore installed in a granular base only in order to simulate a practical situation that is likely to arise in Bangladesh. In Bangladesh most of the piles are likely to rest in a firm sand stratum though there is a cohesive upper layer.

## 3.2 Objective

The research aimed at studying load transfer mechanism in piles installed in granular soils. In course of study of load transfer mechanism some important parametric relations i.e load settlement curve, separation of skin friction etc. were developed. These may be used in reviewing the current design procedure followed for pile foundations.

The research was aimed at interpreting load transfer mechanism based on the following installation and load test results on single piles:

1) A load settlement curve for each set of piles

2) Data relating to distribution of total load into skin friction and tip bearing.

3) Variation of load transfer patterns with respect to pile geometry, placement condition and soil density.

A comparison of the experimental results with currently available theories were also sought.

## 3.3 Soil Used

A Medium dense sand is used for bed preparation. To simulate naturally dry sand, 3% moisture was added thoroughly. The soil is uniformly graded with a uniformity coefficient

ranging from 1.15 to 3.84. Specific gravity of the sand was determined and found to be 2.65. Fig. 3.1 shows its gradation range.

Strength parameters of the sand (internal angle of friction) at various densities were established through standard test procedures and it was 31° for loose sand and 35° for dense sand.

## 3.4 Scheme of Research

The experiment consisted of the following stages of performance:

Uniform sand bed preparation: preparation of uniform sand beds with measurement of densities at different locations in the beds. The beds are prepared in such a way that the densities of different beds are nearly identical.

Determination of density and strength parameters of the sand used in each test: soil parameters, such as specific gravity($G_s$), uniformity coefficient(U), angle of internal friction( $\phi$ )from Direct Shear test, modulus of elasticity of sand($E_s$) are determined.

Pile installation: piles are installed by two methods. Piles drived into an uniformly laid sand bed by applying a static

# PARTICLE SIZE DISTRIBUTION

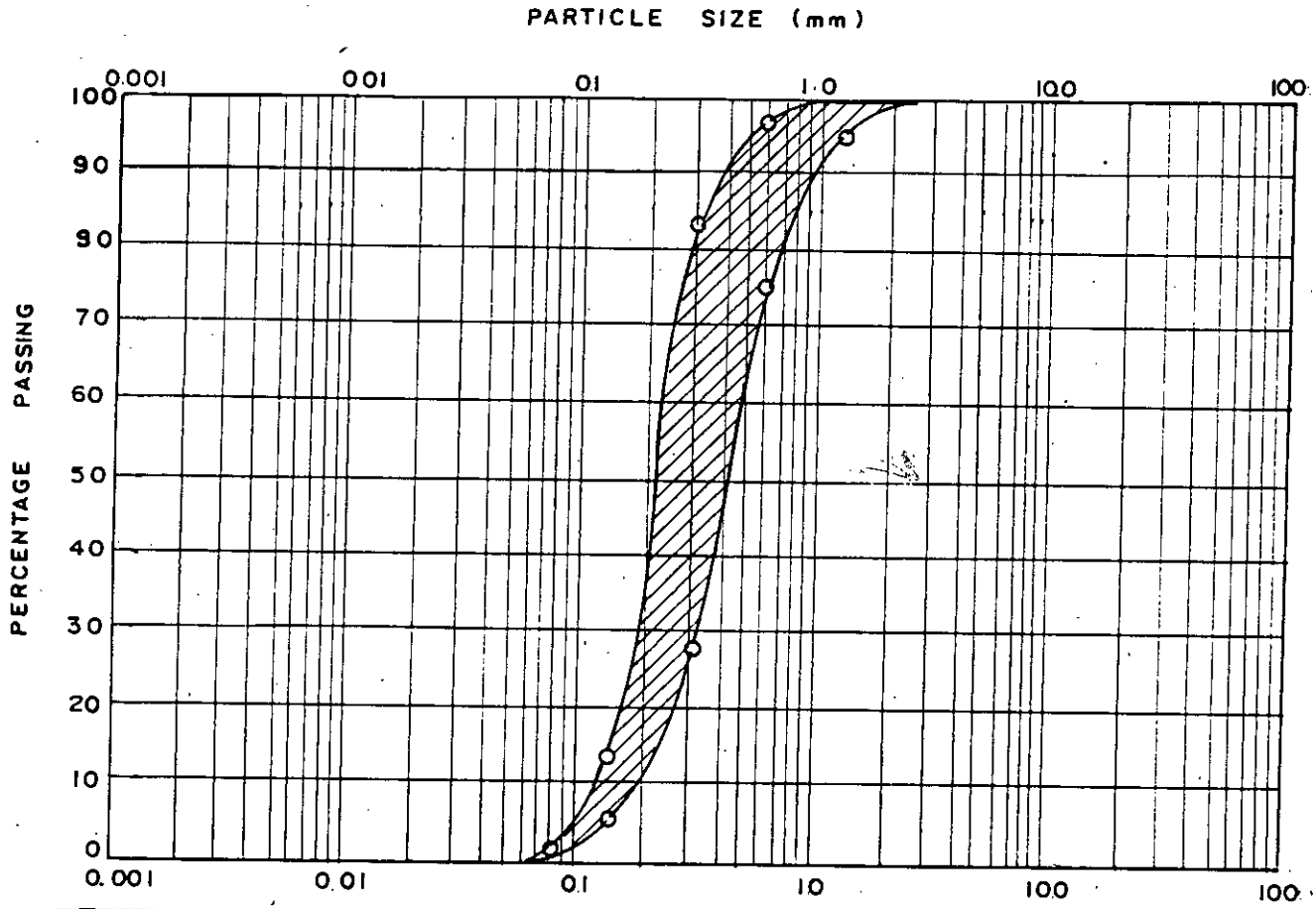


| | FINE | MEDIUM | COARSE | FINE | MEDIUM | COARSE | FINE | MEDIUM | COARSE | |
|---|---|---|---|---|---|---|---|---|---|---|
| Clay | SILT | | | SAND | | | GRAVEL | | | COBBLE |
| | | | | | | | | | | |

$D_{60}$ = 0.22 — 0.5

$D_{10}$ = 0.13 — 0.19

Uniformity Coefficient $u = \frac{D_{60}}{D_{10}}$ = 3.84 — 1.15

Fig. 3.1 Grain Size Distribution Curve.

load is called a displacement pile. When the pile is kept vertical in the tank and then sand is poured to fill the tank, the pile is called a nondisplacement pile.

Axial load test by compression: a pilot test is conducted to check the electrical strain measuring instrument. Then single model pile is tested by displacement and nondisplacement method with the combination of maximum and minimum density of sand. This is repeated for a new diameter of pile.

## 3.5 Specification for Pile Load Test

Pile tests were devised following the method described in ASTM D 1143-74 (standard methods for piles under axial compressive load). Loading was done in the experiment by a direct shear loading device and specified constant rate of penetration (0.03 to 0.10 in/min.) was maintained.

Pile tip movement was measured by a set of strain gauges and average of four strain gauge readings was taken as representative.

All tests were carried out upto a large settlement of pile(upto the diameter of piles). The details of these are discussed in chapter four.

# CHAPTER 4

# LABORATORY INVESTIGATIONS

## 4.1 Introduction

A laboratory programme was developed to assess the load transfer mechanism of a model pile installed in granular soil. As mentioned in the research scheme, this involved in development of a testing tank in which a uniform density sand bed was laid. The uniformity of the sand bed was checked. The details of these arrangements and test procedures are discussed subsequently.

## 4.2 Preparation of Uniform Sand Bed

A steel tank (2ft. x 2ft. x 2ft.) was available in the Geotechnical Engineering Laboratory . The tank was made of steel frame and galvanized iron sheets. Because sufficient rigidity of the sidewalls required to simulate field condition (i.e maintaining $K_o$ condition). As maximum pile diameter for this research was 2 inches and pressure bulbs below pile tip is assumed to extend upto 3D. So a 24 inches deep steel tank was considered to serve well for the purpose. For further detail of the tank see Salahuddin(1986).

For the preparation of uniform bed of sand, nine cubic feet of uniformly graded sand are used.The sand contained materials passing No. 16 sieve and those retained on No. 100 sieve. Fig. 3.1 shows the grain size distribution. A hopper and a hopper carrier (a trolley) were also available for uniform sand placement (Salahuddin, 1986). Details of sheet work for making hopper is shown in Fig. 4.1 . Arrangement for placing hopper on trolley and dropping sand from a specific height is shown in Fig. 4.2.

## 4.3 Evaluation of Soil Properties

Soils used in the sand bed were tested for grain size analysis in accordance to ASTM D422-63(1972) to establish the gradation; fineness modulas and uniformity coefficient. The latter ranged from 1.15 to 3.84. Direct shear test (ASTM D 3080-72) was carried out to find out the angle of internal friction ($\phi$) at various densities. At loose state it was 31° and at dense state it was 35°.

Cycling loading triaxial tests were conducted to determine the modulus of elasticity of sand, which was used in numerical analysis of the problem. For each density of soil, 3 such tests were conducted at three different confining pressure and the required modulas of elasticity was extrapolated from those three values. One typical stress-strain curve is shown in Fig. 4.3. Modulus of elasticity of soil is taken to be the slope

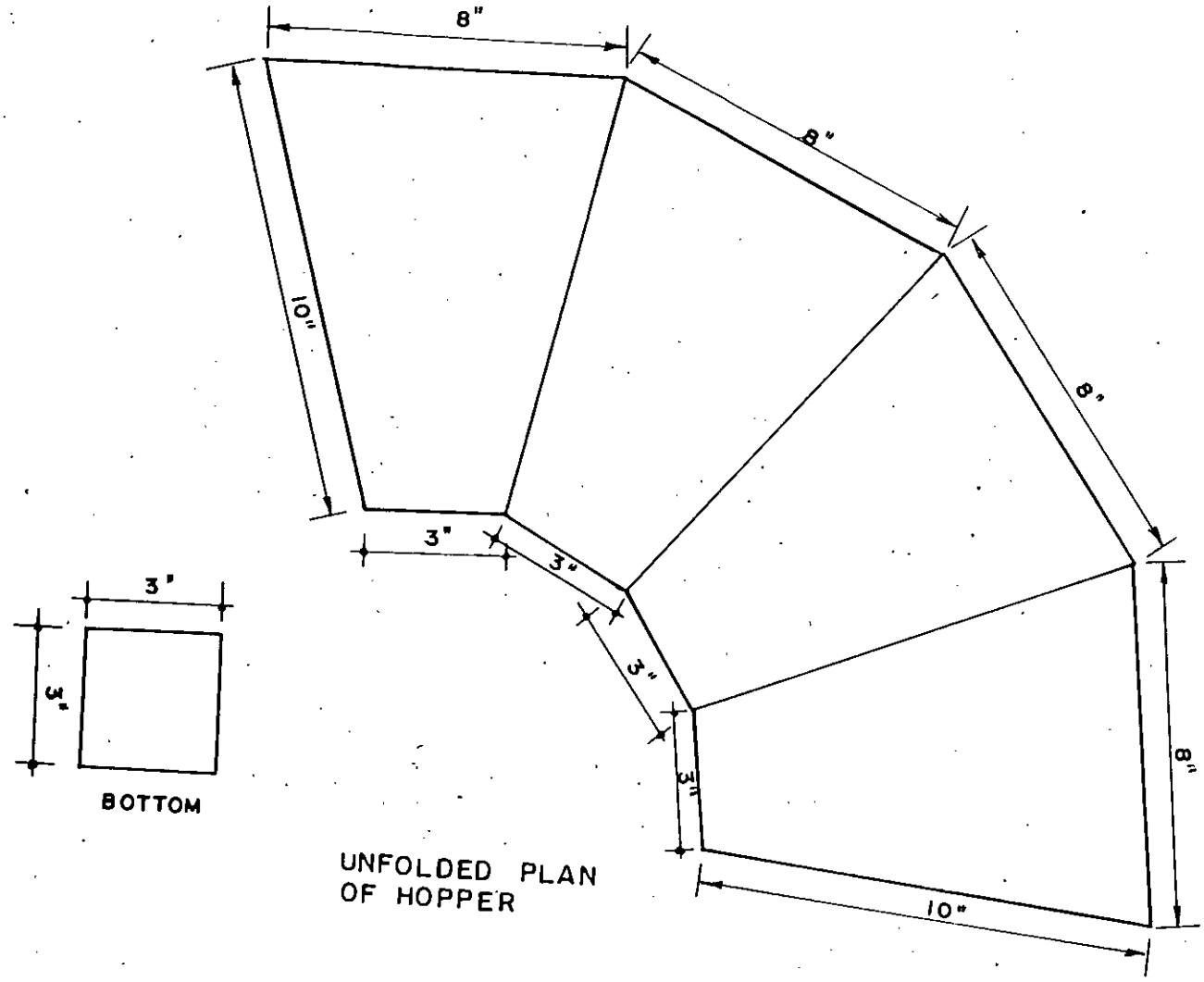


Fig. 4.1 Details of sheet work for making hopper ( Salahuddin, 1986 )

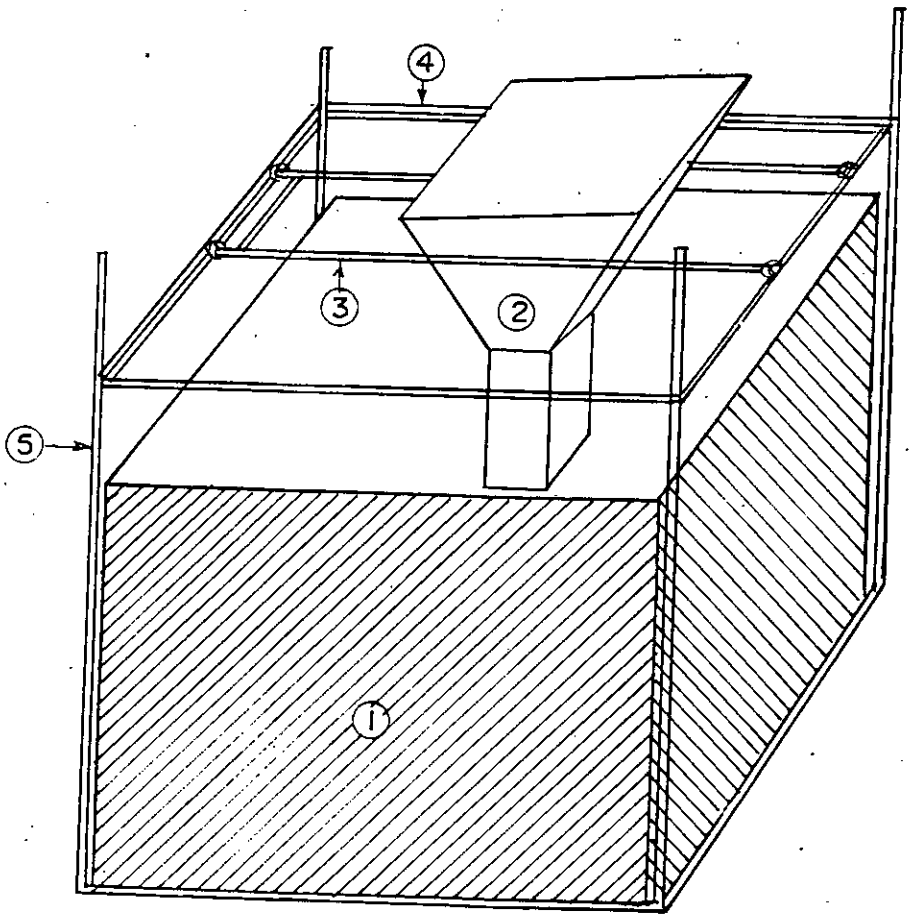


① Sand Tank (2'x2'x2')

② Hopper

③ Hopper Roller

④ Angle frame for roller support

⑤ Tank frame

Fig. 4.2 Testing Tank

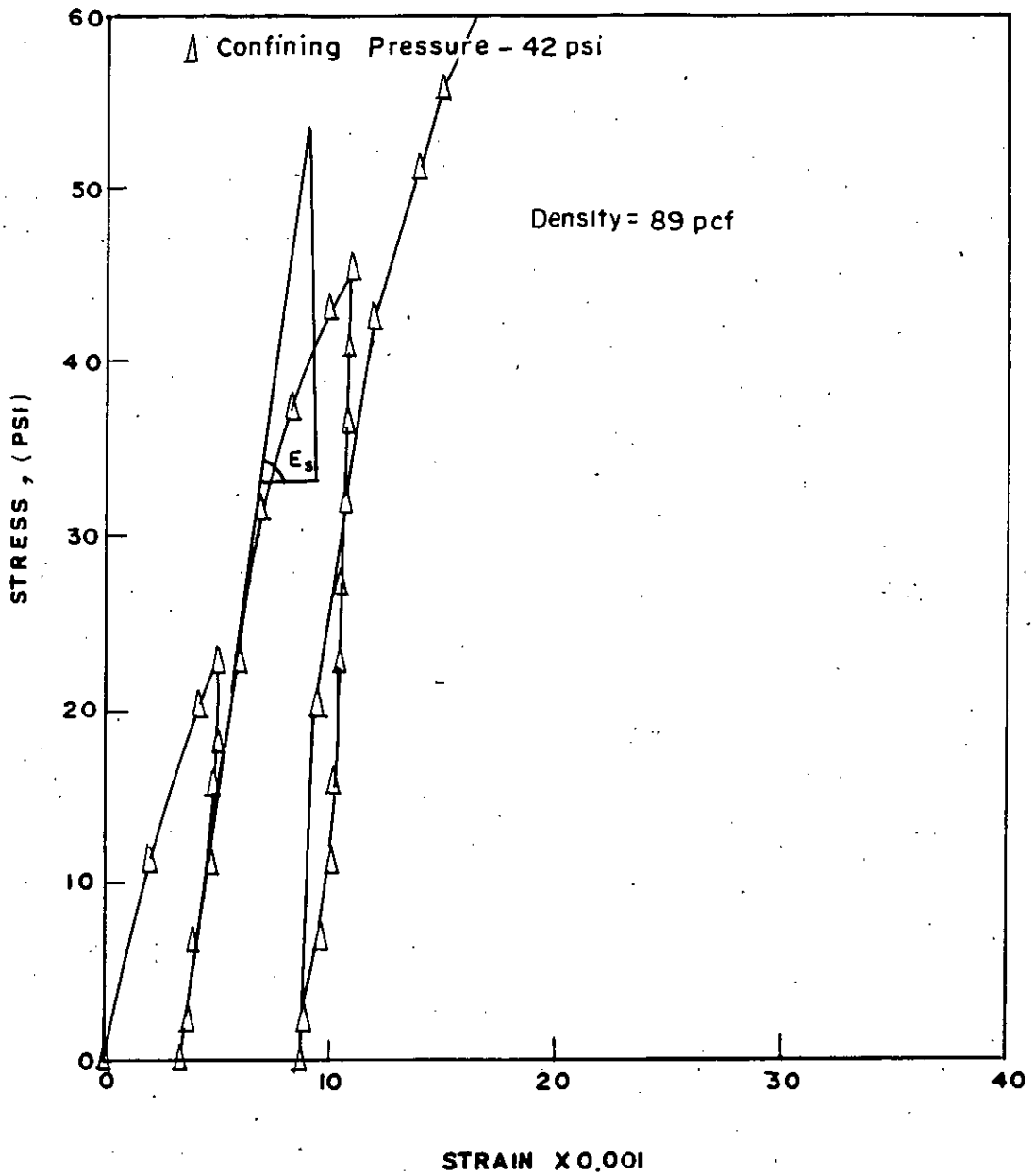


Fig. 4.3 Stress – Strain curve from cyclic loading triaxial test.

of small strain reloading path. Modulus of elasticity for dense condition was 116 psi and for loose condition, it was 70 psi. These are extrapolated modulas of elasticity for an average confining pressure of 0.45 and 0.386 psi respectively.

## 4.4 Measuremant of Strain in Model Piles

In this research three hollow ,one end closed ,model piles were used, each 15" long and the diameters were 0.75", 1.1875" and 2". The thickness of the model piles were 5"/128, 13"/128 and 11"/128 respectively.

As the research aimed at the study of load transfer mechanism, so it needed measuring stress at different depth levels along the pile. Conventional methods of measuring strain could not solve the problem, because it was not sensitive enough to measure very small strain of those model piles. Another reason was that in the conventional method, the instrumentation was not possible without disturbing the sand-pile interface.

So, electric strain gauges were used successfully. The gauges were of TOKYO SOKKI KENKYUJO CO. LTD. Gauge length and resistance were 10 mm and 120 + 0.3 ohms respectively. Figure 4.4 shows how the gauges were installed in aluminum model piles. Here three strain gauges were provided on inner wall of pile, at certain depths; because of the uniformity of compressive stress at that level.

Fig. 4.5 shows the whole arrangement for strain measurement. Here a dummy gauge is used on the same metal for temperature compensation. No. 40 winding wire were used to maintain the connection between the strain gauge and the strain reader (volt meter).

It is important to note that though the wheatstone bridge circuit, used for strain measurement was balanced for temperature compensation, the initial readings were unstable. There was probably other elements of the bridge could be at different starting temperatures (Abedin, 1986). So a minimum of 6 hours was waited for each setting to stabilize the temperature before the experiment was started.

It was observed that degradation of the power supply source to the voltmeter resulted in erratic readings. Hence it was essential to ensure that the battery set used in the voltmeter were sufficiently strong before each set of tests were performed.

## 4.5 Density of Sand Bed in the Test Tank

In the experiment density of soil played an important role in load transfer patterns. It was essential that the density of the sand bed was uniform althroughout. A series of trials ensured that it was possible to obtain a uniform density bed. It was observed that density of sand bed could be related to height

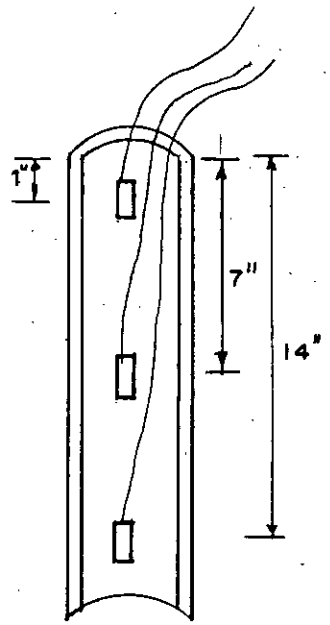


Fig. 4.4 Strain Gauge Setup in piles

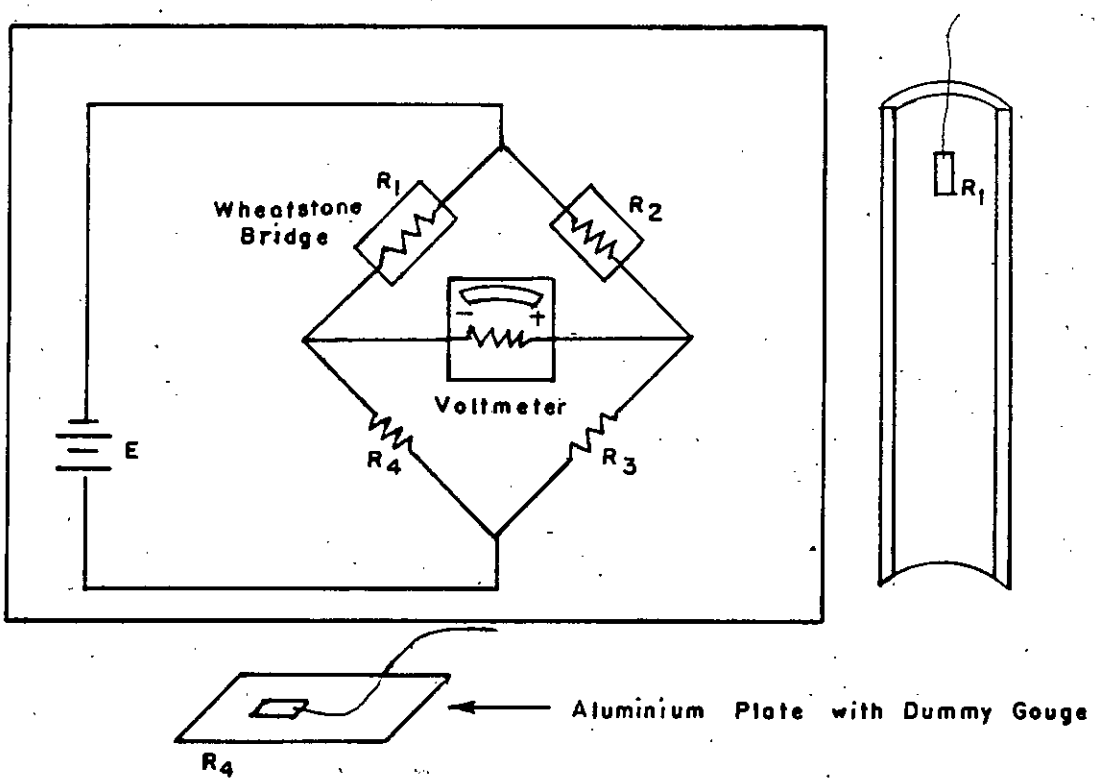


Fig. 4.5 Typical Strain Measuring Arrangement with Temperature Compensation

of fall (Salahuddin, 1986). Other factors such as the manner in which the hopper was charged also affected the density.

### 4.5.1 Density in loose condition

Density in loose condition was achieved by hopper manipulation. Maintaining a 4 inches height of fall of sand from the hopper, a uniform loose sand bed could be obtained. Fig. 4.6 shows an arrangement for maintaining 4" height of fall of sand from the hopper bottom. Sand was fed in the hopper and the hopper disseminated the sand uniformly moving to and fro over a trolley. The frame holding trolley and hopper was raised time to time to maintain 4 inches height of fall of sand. No vibration was allowed in the vicinity of the sand tank, because it could modify the uniformity of sand density. Minimum density that was obtained by this process was about 89 pounds per cubic feet . which fitted well in Fig. 4.7 of Salahuddin( 1986).

### 4.5.2 Density in dense condition

Dense condition was attained by compacting the sand with a standard hammer (10 lb.) after a layer was placed. The sand bed was prepared in five layers. Each layer was of 4.5" thick. Fig. 4.8(b) shows the layering scheme. After the formation of each layer compaction was done by a blowing scheme shown in Fig. 4.8(a). Blowing was devised in this way to get an uniform dense state. Maximum average density obtained by following this process

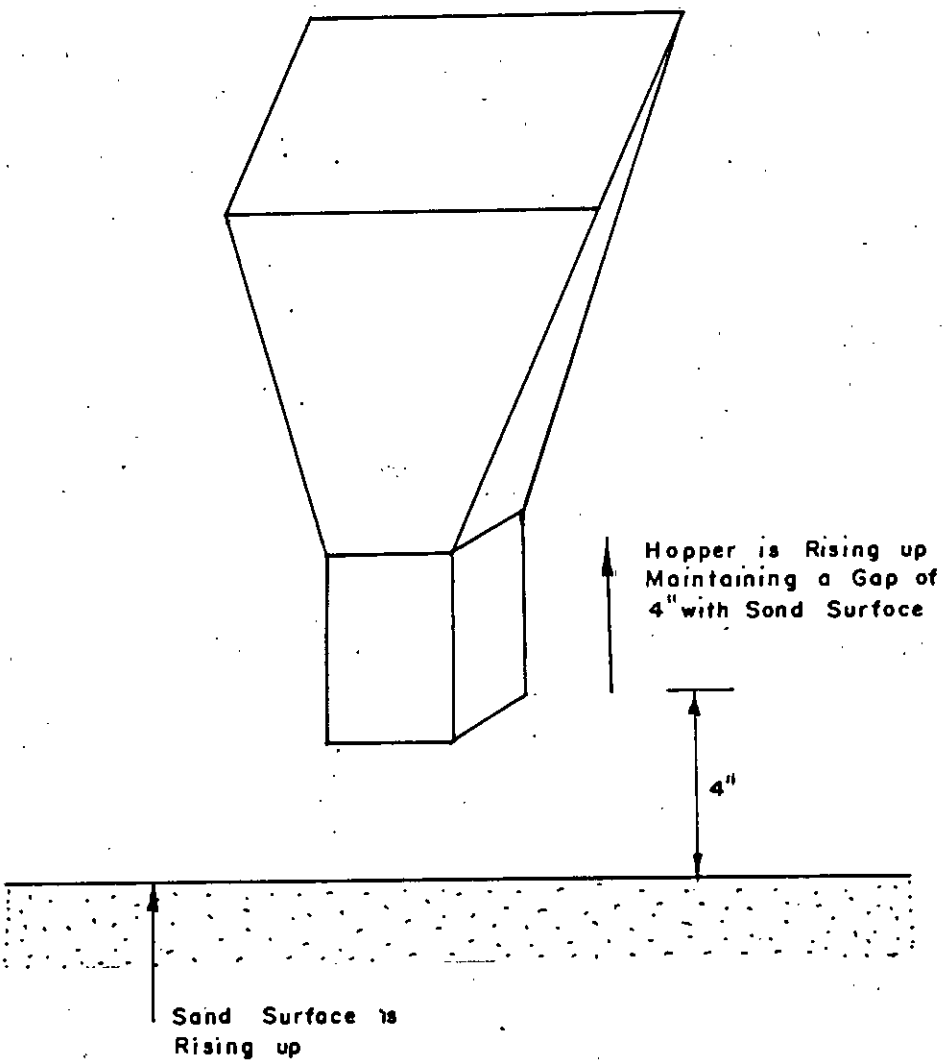


Fig. 4.6 Hopper Manipulation Scheme for Loose State.

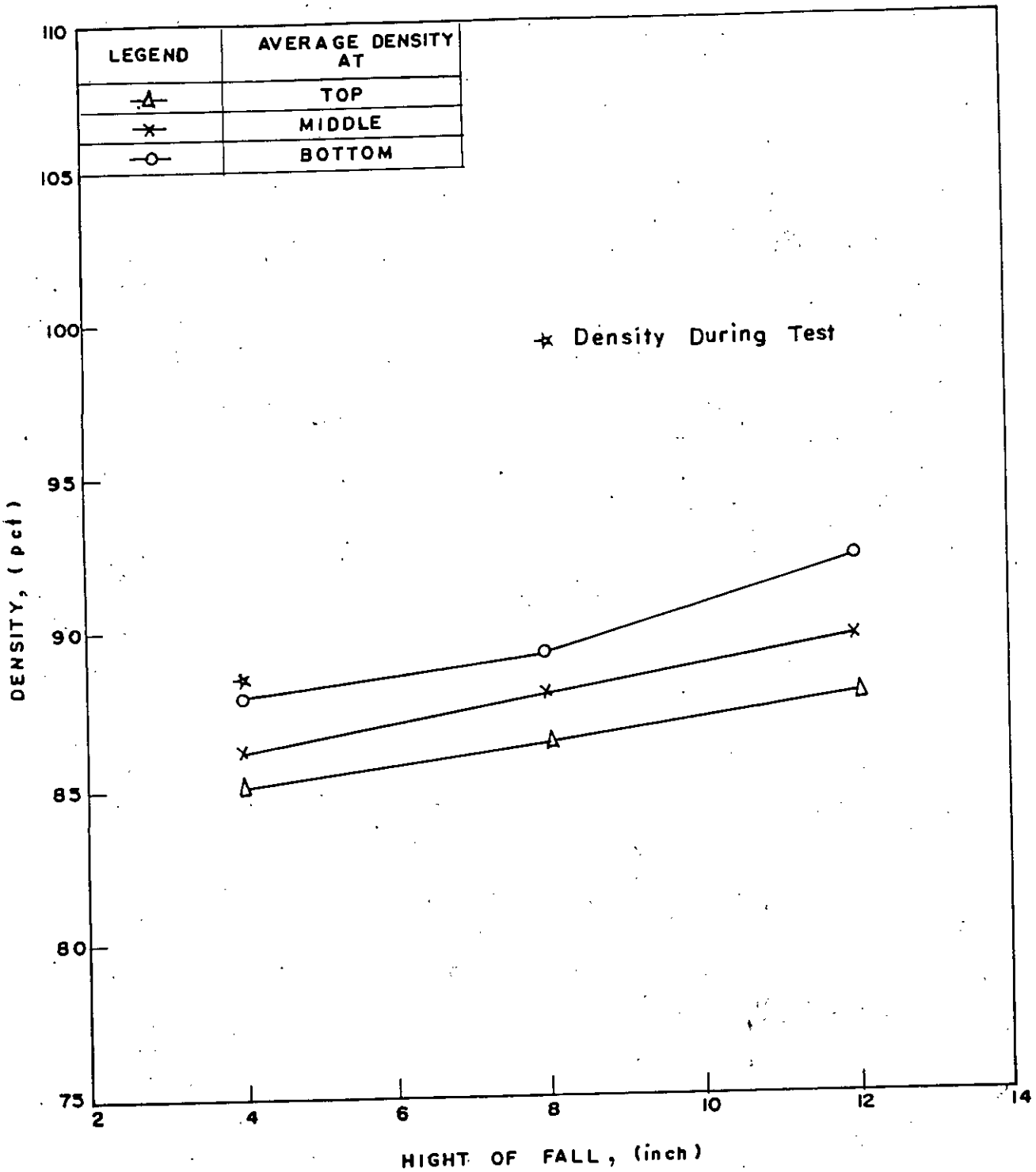


Fig. 4.7 Sand densities at different heights of fall during sand bed preparation, (Salahuddin, 1986)

was 105 pounds per cubic feet.

## 4.6 Rigidity of Model Pile

This research primarily intended to study the transfer of axial load. Initially it is transferred by skin friction. Separation of skin friction from the test was carried out in a indirect way. At a level , h strain ($\varepsilon_p$) was measured by a electronic strain gauge, then skin friction can be separated as follows (Fig. 4.9)

$$\sigma_s = \varepsilon_p * E_p \qquad (4.1)$$

$$P_1 = \sigma_s * A'_p \qquad (4.2)$$

skin friction , $$f_s = (P-P_1)/(1/2*h*A'_p) \qquad (4.3)$$

where, $\varepsilon_p$ = strain in the pile mat.

$E_p$ = modulus of elasticity of pile

$A'_p$ = perimeter of the pile

$P_1$ = acting load at any section

P = Total axial load.

So, modulus of elasticity of pile was needed to be established. For this purpose a short block of the model pile (1 inches in height) was taken in order to avoid slenderness effects. Then it was tested to get a stress-strain curve from where its modulus of elasticity value was calculated, as average of several tests. In Fig. 4.10, it is seen that starting of the curve is nonlinear and concave upward. This was because any

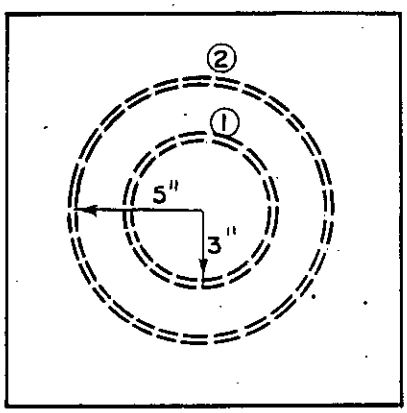


① Blowing Circle 1 (50 Blows)

② Blowing Circle 2 (50 Blows)

Fig. 4.8 (a) Tank Plan Showing Blowing Scheme.

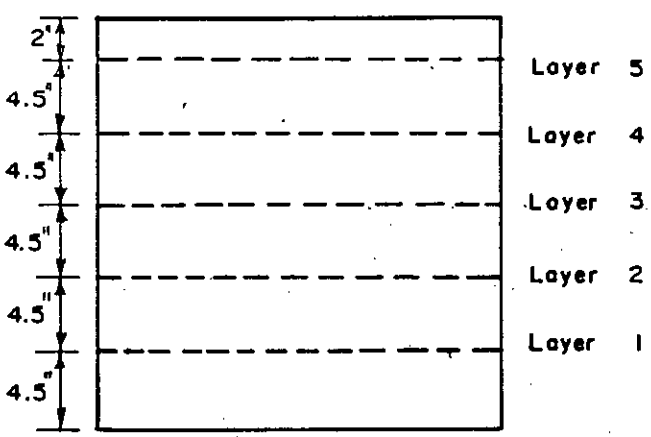


Fig. 4.8 (b) Tank Elevation Showing Layering Scheme.

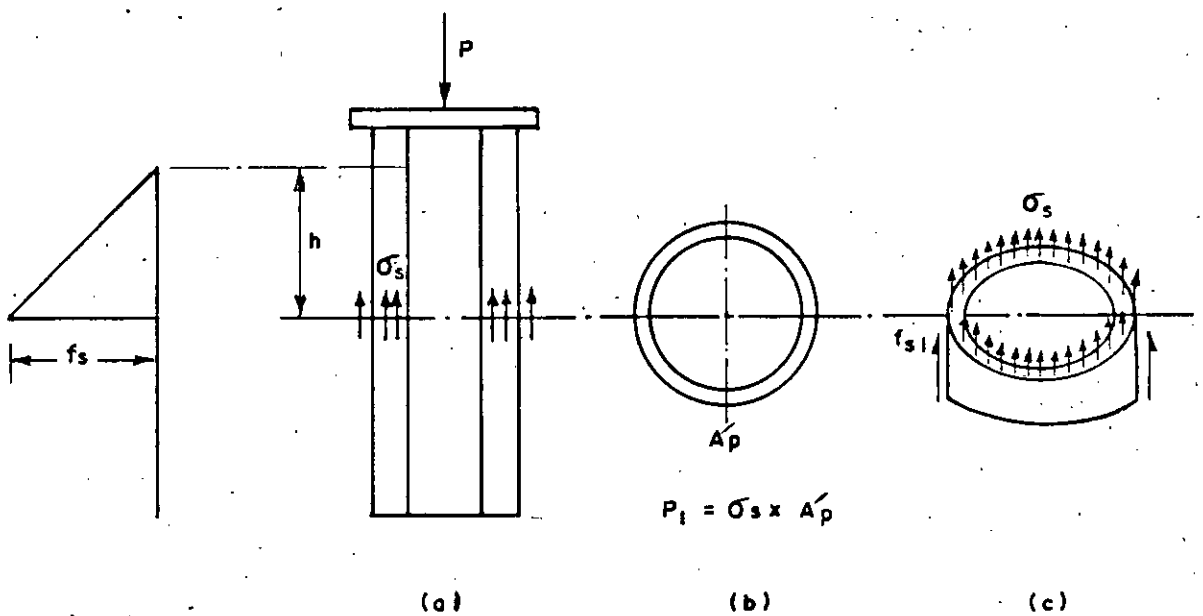


Fig. 4.9 (a), (b), (c) Skin Friction Separation

compression test machine raquires two plates to compress the sample in between. Hence in the test, due to lack of smoothness of surface (both machine plate and pile), load was concentrated on smaller area at the starting of the test. So to ensure full area of pile section under compression higher initial load was applied along with the rubber sleeves on both end of the element.

## 4.7 Pile Placement and Loading Arrangement

All the tests were performed by axial load application. So, to ensure that the pile is axially loaded two sets of wooden bars, all 30" long were used. Each set was set in a criss-cross manner, so that it created a square opening in the middle to let the pile slide in, as shown in Fig. 4.11. Vertical gap between two set of frame was about 5". Combined action of these two frames restrained the pile to remain vertical.

Fig. 4.12 shows the loading arrangements, loading was done by the direct shear box; which was operated manually.

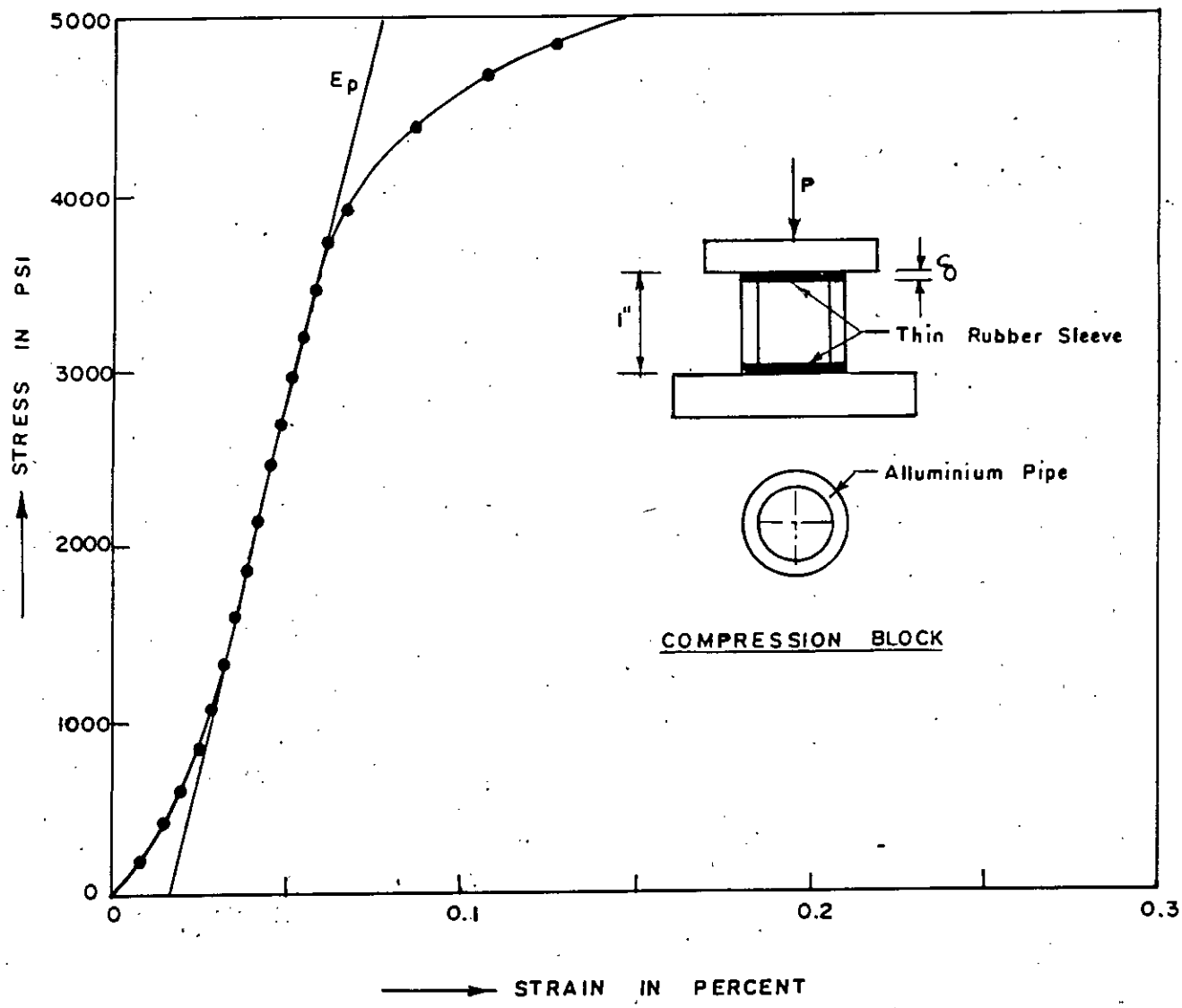


Fig. 4.10 Stress — Strain Curve for Model Pile Element.

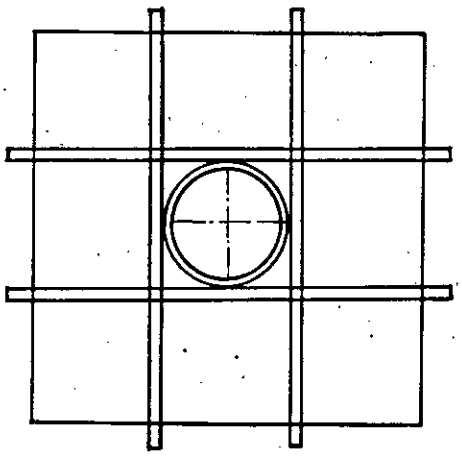

Fig. 4.11 Arrangement to Keep the Pile Vertical.

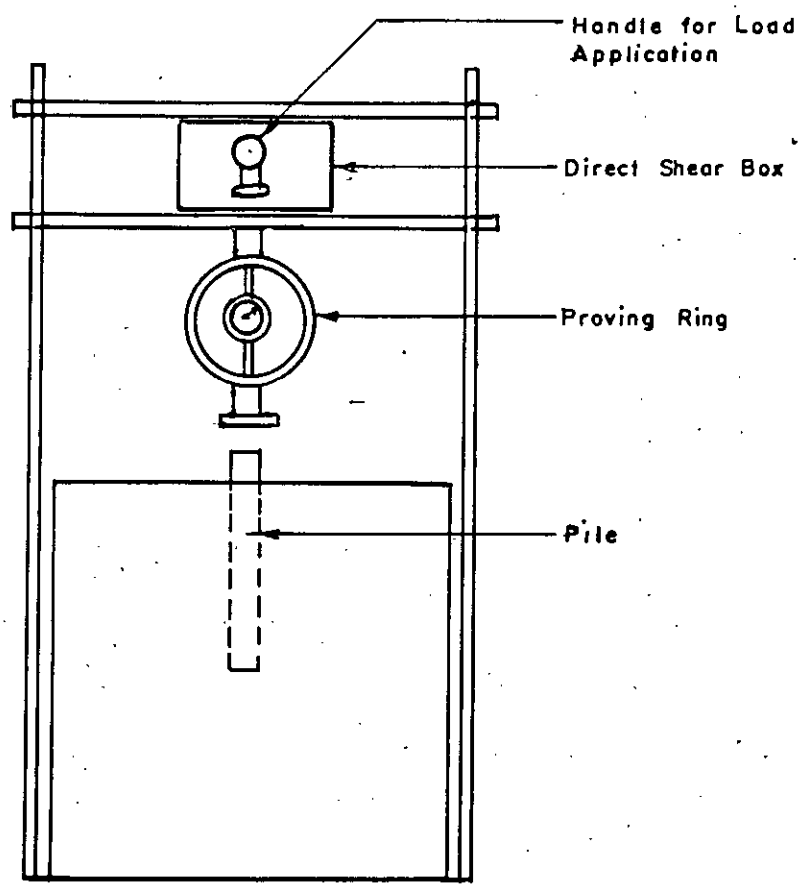


Fig. 4.12 Loading Arrangement.

# CHAPTER 5

## THREE DIMENSIONAL FINITE ELEMENT FORMULATION

### 5.1 Finite Element Formulation

The finite element method is a numerical and powerful technique to solve, approximating a continuum as an assembly of discrete elements. A three dimensional 8-noded brick or hexa hedral element(Fig. 5.1) (Zienkiewicz,1971; Desai and Abel,1972) as been used here. The natural coordinates r,s and t with the origin of the system is taken as the centroid of the element (Fig. 5.1). The relation between the local and global co-ordinate system can be expressed in the following way:

$$\begin{Bmatrix} x \\ y \\ z \end{Bmatrix} \qquad \begin{bmatrix} \{N^T\} & \{0\} & \{0\} \\ \{0\} & \{N^T\} & \{0\} \\ \{0\} & \{0\} & \{N^T\} \end{bmatrix} \begin{Bmatrix} X_n \\ Y_n \\ Z_n \end{Bmatrix} \quad ..(5.1)$$

where $\{N^T\} = [N_1, N_2, N_3, N_4, N_5 \ldots\ldots\ldots\ldots N_8]$

$\{X_n\}^T = [X_1, X_2, X_3, X_4, X_5 \ldots\ldots\ldots\ldots X_8]$

The interpolation functions are obtained from

$$N_i = 1/8(1 + rr_i)(1 + ss_i)(1 + tt_i) \quad \ldots\ldots\ldots(5.2)$$

where i stands for the node number in the element.

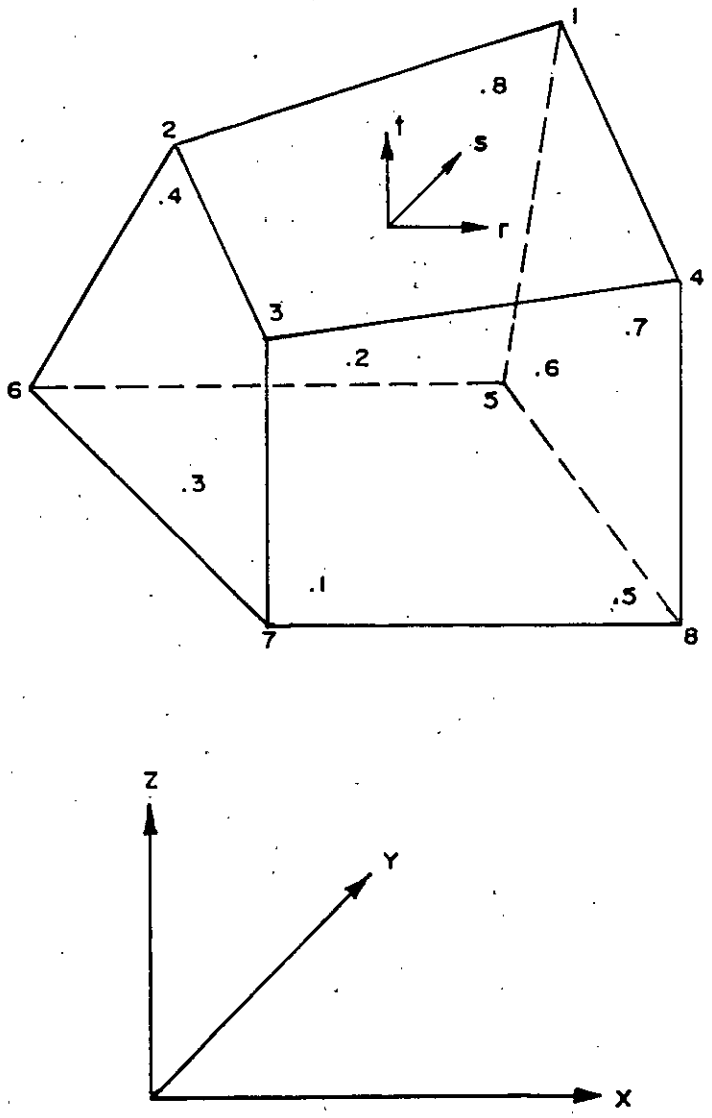


Fig. 5.1 Basic Hexahedral Finite Element.

The components of displacement at any point in the element can be expressed in terms of the interpolation functions and the nodal displacement vector as follows,

$$\{u\} = [N]\{q\} \quad \text{.....(5.3)}$$

where $\{u\}^T = \{u, v, w\}$

$$\{q\} = \{u_1, v_1, w_1, u_2, v_2, w_2 \ldots\ldots u_8, v_8, w_8\}$$

$$[N] = \begin{bmatrix} N_1 & 0 & 0 & N_2 & 0 & 0 & \ldots\ldots\ldots\ldots & N_8 & 0 & 0 \\ 0 & N_1 & 0 & 0 & N_2 & 0 & \ldots\ldots\ldots\ldots & 0 & N_8 & 0 \\ 0 & 0 & N_1 & 0 & 0 & N_2 & \ldots\ldots\ldots\ldots & 0 & 0 & N_8 \end{bmatrix}$$

### 5.1.1 Strain-Displacement Relationship

The strain component at a point in the element are given by

$$\{\varepsilon\} = \begin{Bmatrix} \varepsilon_x \\ \varepsilon_y \\ \varepsilon_z \\ \gamma_{xy} \\ \gamma_{yz} \\ \gamma_{zx} \end{Bmatrix} = \begin{Bmatrix} \delta u/\delta x \\ \delta v/\delta y \\ \delta w/\delta z \\ \delta u/\delta y + \delta v/\delta x \\ \delta v/\delta z + \delta w/\delta y \\ \delta w/\delta x + \delta u/\delta z \end{Bmatrix} = [B1][B2]\ldots.[B8]\{q\} = [B]\{q\} \text{..(5.4)}$$

where [B] = strain displacement transformation matrix..

The strain displacement transformation matrix can be expressed as

$$[B_i] = \begin{bmatrix} \delta N_i/\delta x & 0 & 0 \\ 0 & \delta N_i/\delta y & 0 \\ 0 & 0 & \delta N_i/\delta z \\ \delta N_i/\delta y & \delta N_i/\delta x & 0 \\ 0 & \delta N_i/\delta z & \delta N_i/\delta y \\ \delta N_i/\delta z & 0 & \delta N_i/\delta x \end{bmatrix} \quad \text{.....(5.5)}$$

To evaluate the global derivatives of the shape functions, it is required to establish a transformation relationship from the global to local co-ordinates. It can be done by using Jacobeaie Matrix. By using the chain rule of differentiation it can be found

$$\frac{\delta}{\delta r} = \frac{\delta}{\delta x}\frac{\delta x}{\delta r} + \frac{\delta}{\delta y}\frac{\delta y}{\delta r} + \frac{\delta}{\delta z}\frac{\delta z}{\delta r}$$

$$\frac{\delta}{\delta s} = \frac{\delta}{\delta x}\frac{\delta x}{\delta s} + \frac{\delta}{\delta y}\frac{\delta y}{\delta s} + \frac{\delta}{\delta z}\frac{\delta z}{\delta s} \qquad ..(5.6a)$$

$$\frac{\delta}{\delta t} = \frac{\delta}{\delta x}\frac{\delta x}{\delta t} + \frac{\delta}{\delta y}\frac{\delta y}{\delta t} + \frac{\delta}{\delta z}\frac{\delta z}{\delta t}$$

In matrix notation

$$\begin{Bmatrix} \frac{\delta}{\delta r} \\ \frac{\delta}{\delta s} \\ \frac{\delta}{\delta t} \end{Bmatrix} = \begin{bmatrix} \frac{\delta x}{\delta r} & \frac{\delta y}{\delta r} & \frac{\delta z}{\delta r} \\ \frac{\delta x}{\delta s} & \frac{\delta y}{\delta s} & \frac{\delta z}{\delta s} \\ \frac{\delta x}{\delta t} & \frac{\delta y}{\delta t} & \frac{\delta z}{\delta t} \end{bmatrix} \begin{Bmatrix} \frac{\delta}{\delta x} \\ \frac{\delta}{\delta y} \\ \frac{\delta}{\delta z} \end{Bmatrix} \qquad .....(5.6b)$$

$$[J] = \begin{bmatrix} \frac{\delta x}{\delta r} & \frac{\delta y}{\delta r} & \frac{\delta z}{\delta r} \\ \frac{\delta x}{\delta s} & \frac{\delta y}{\delta s} & \frac{\delta z}{\delta s} \\ \frac{\delta x}{\delta t} & \frac{\delta y}{\delta t} & \frac{\delta z}{\delta t} \end{bmatrix} \qquad .....(5.6c)$$

where [J] is the Jacobian matrix. So the global derivative can be obtained as

$$\begin{Bmatrix} \frac{\delta}{\delta x} \\ \frac{\delta}{\delta y} \\ \frac{\delta}{\delta z} \end{Bmatrix} = [J]^{-1} \begin{Bmatrix} \frac{\delta}{\delta r} \\ \frac{\delta}{\delta s} \\ \frac{\delta}{\delta t} \end{Bmatrix} \qquad \text{.....(5.6d)}$$

Therefore,

$$[B_i] = \begin{bmatrix} 1 & 0 & 0 & 0 & 0 & 0 & 0 & 0 & 0 \\ 0 & 0 & 0 & 0 & 1 & 0 & 0 & 0 & 0 \\ 0 & 0 & 0 & 0 & 0 & 0 & 0 & 0 & 1 \\ 0 & 1 & 0 & 1 & 0 & 0 & 0 & 0 & 0 \\ 0 & 0 & 0 & 0 & 0 & 1 & 0 & 1 & 0 \\ 0 & 0 & 1 & 0 & 0 & 0 & 1 & 0 & 0 \end{bmatrix} \begin{bmatrix} [J]^{-1} & [0] & [0] \\ [0] & [J]^{-1} & [0] \\ [0] & [0] & [J]^{-1} \end{bmatrix} \begin{bmatrix} \{N_i\} & \{0\} & \{0\} \\ \{0\} & \{N_i\} & \{0\} \\ \{0\} & \{0\} & \{N_i\} \end{bmatrix}$$

...(5.7)

where $[N_i]^T = \left[ \frac{\delta N_i}{\delta r} \quad \frac{\delta N_i}{\delta s} \quad \frac{\delta N_i}{\delta t} \right]$

$$= 1/8[r_i(1 + ss_i)(1 + tt_i),\ s_i(1 + tt_i)(1 + tt_i),$$
$$t_i(1 + rr_i)(1 + ss_i)]$$

### 5.1.2 Stress-strain relationship

Stress-strain relation of a continuous media can be expressed as follows

$$\{\sigma\} = [C]\{\varepsilon\} \quad \text{.....(5.8a)}$$

where [C] = stress-strain matrix.

Expanding equation (5.8a),

$$\begin{Bmatrix} \sigma_x \\ \sigma_y \\ \sigma_z \\ \tau_y \\ \tau_z \\ \tau_x \end{Bmatrix} = \frac{E}{(1+\nu)(1-2\nu)} \begin{bmatrix} (1-\nu) & \nu & \nu & 0 & 0 & 0 \\ & (1-\nu) & \nu & 0 & 0 & 0 \\ & & (1-\nu) & 0 & 0 & 0 \\ & & & (1-2\nu)/2 & 0 & 0 \\ & \text{Symmetrical} & & & (1-2\nu)/2 & 0 \\ & & & & & (1-2\nu)/2 \end{bmatrix} \begin{Bmatrix} \varepsilon_x \\ \varepsilon_y \\ \varepsilon_z \\ \gamma_{xy} \\ \gamma_{yz} \\ \gamma_{zx} \end{Bmatrix}$$

$$\{\sigma\} = [C][B]\{q\} \quad \text{.....(5.8b)}$$

In equation (5.8b) it is observed that [C] is the property matrix of the media, [B] is determinable from the geometry of the element. Only {q} is left, which is determined from the following relation:

$$[K]\{q\} = \{Q\} \quad \text{.....(5.9)}$$

where [K] = element stiffness matrix.

{Q} = element load vector.

## 5.2 Salient Features of the Programme

An available finite element software based on displacement type formulation -"FE2000"(Numerics Corporation, 1983) is used for the current analysis. The analysis is performed assuming linear elastic behaviour of pile soil system. Here 2X2 Gaussian quadrature has been used for integration scheme in the element stiffness formation. Salient features of "FE2000" are given in appendix A.

# CHAPTER 6

## EXPERIMENTAL RESULTS AND DISCUSSION

### 6.1 General

Results of the experiment are presented in both graphical and tabular forms. Load-settlement relation, variation of skin friction along embedded depth, development of coefficient of earth pressure with relative depth are represented graphically. Bearing capacity factors are represented in tabular form. Load-settlement curves are non-dimentionalized to show the uniqueness of all curves. From regression of skin friction data, a skin friction prediction model has been suggested. A rational coefficient of earth pressure has also been suggested. Bearing capacity factors obtained by this experiment have been compared with those of others.

### 6.2 Load Settlement Relation for Test Piles

Fig. 6.1 and Fig. 6.2 show load-settlement relations for piles subjected to vertical loads in loose and dense sands respectively. Three types of piles were installed by two different methods. In one case the piles were installed after the soil was placed in the tank and in the other case the piles were placed in the tank and then the sand was poured to fill the tank.

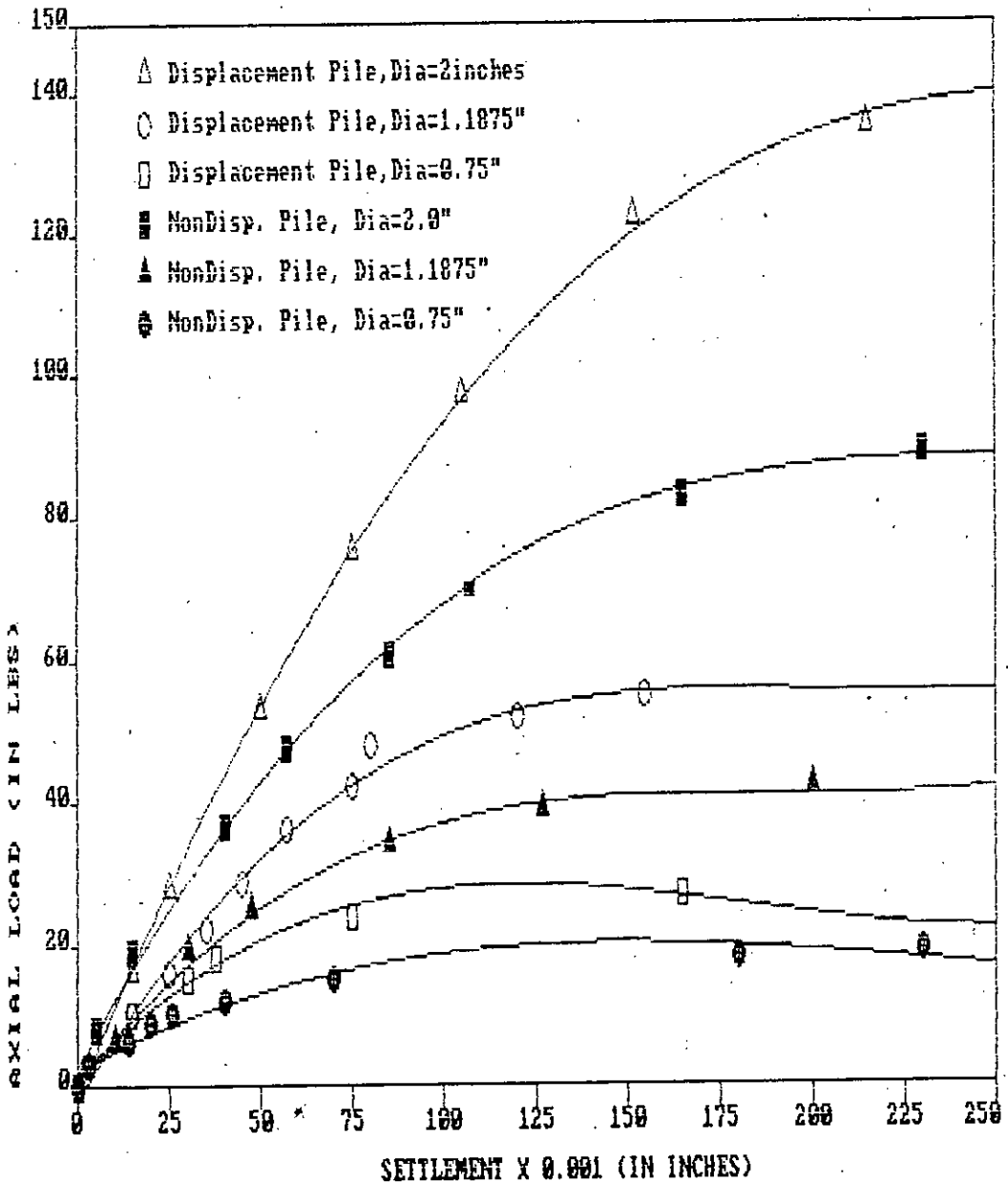


Fig. 6.1 Load-Settlement Curves of Piles in Loose Sand.

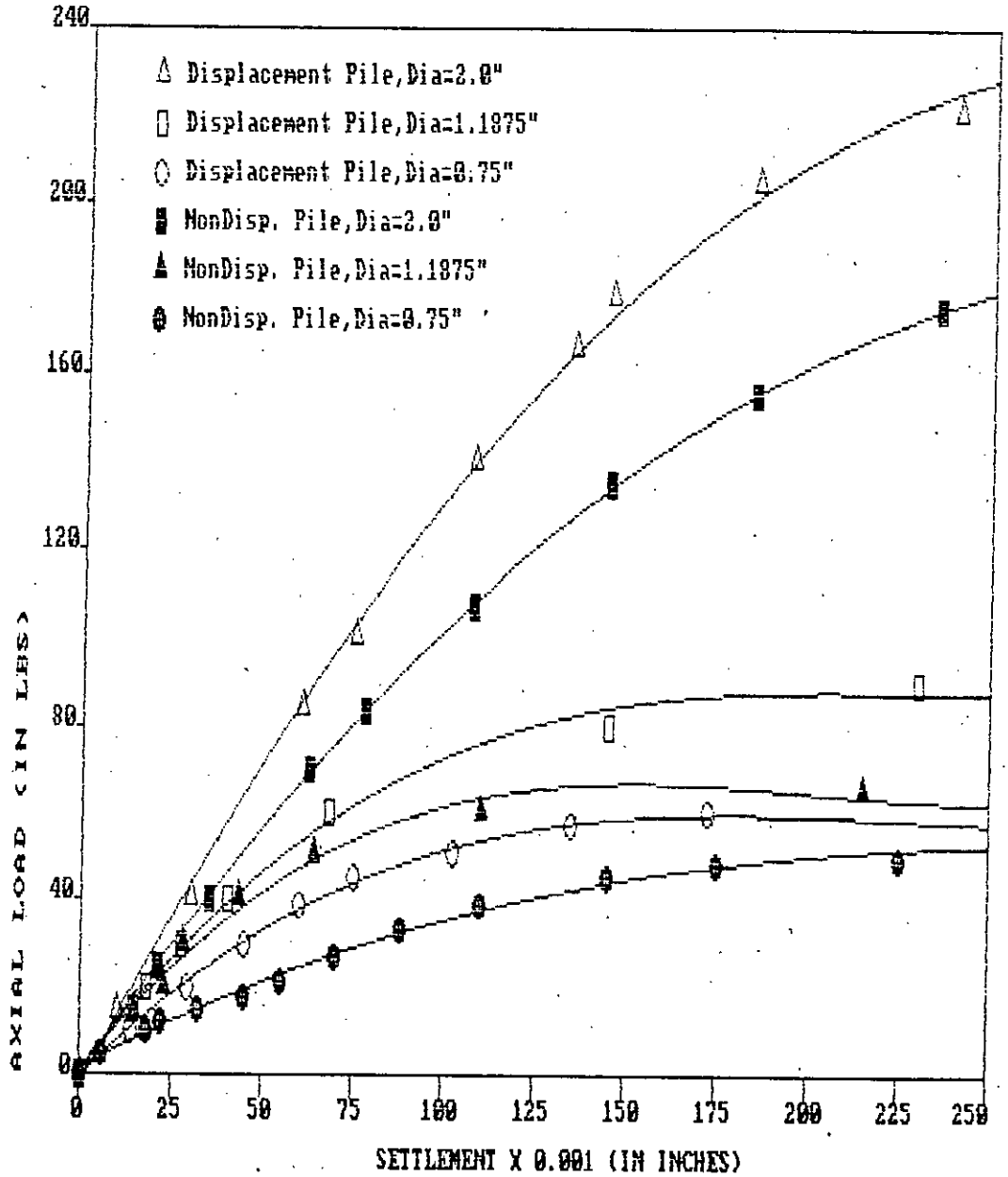


Fig. 6.2 Load-Settlement Curves of Piles in Dense Sand.

The former method is reported as displacement method while the later as non-displacement method of installation.

Data from Fig. 6.1 and 6.2 is replotted in nondimensional form in Fig. 6.3 and 6.4 by dividing axial load at any stage by ultimate load in y-axis and in the x-axis settlement is divided by one tenth of the pile diameter. Here ultimate load is defined as that which causes a settlement of one-tenth of the pile diameter or width (Tomlinson,1980). From the Fig. 6.3. it is observed that piles in loose sand show identical load-settlement response for all types of pile and for both methods of installation . This finding provides a valuable information that all load-settlement relation for piles in loose sand can be represented by a non-dimensional equation relating axial load to ultimate load ratio(load ratio) and settlement ratio(i.e. Settlement/(0.1*diameter of pile)).

There is an increase in pile capacity with increase in the diameter of piles. There is a significant difference in axial load capacity between piles installed with and without displacing the sand. Again as expected, the displacement piles show higher axial capacity than non-displacement piles. This increase in pile capacity for displacement piles can be attributed to sand densification during pile installation. It is also observed from the curves that for larger diameter piles, effect of installation is considerable.

Figure 6.4 shows load ratio versus settlement ratio for piles in dense sand. It can be observed that upto settlement ratio of 1, pile load-settlement response is similar for all types of pile and for both methods of installation as mentionaed earlier for loose sand. But beyond settlement ratio of 1. significant deviation for nondisplacement piles of smaller diameter occurs.

It can also be observed from Fig. 6.3 and 6.4 that the non-dimensional form of the load-settlement relation shown can be considered as parabolic.

## 6.3 Mobilization of Skin Frictional Resistance

In order to study how skin friction is mobilized along pile length the results of displacement piles are considered here. It is expected that during sand filling and bed formation in the non-displacement method some non-uniformity in sand bed may have occurred. Hence the results for this type of installation are not considered for skin friction measurements.

Figure 6.5 through 6.10 show plots of skin friction mobilized at various settlement ratio(expressed as percentage) along different depths of embedments of the pile. Here the skin friction is estimated from the loss of axial load at different lengths of the pile as mentioned in article 4.6. Fig. 6.5 through 6.7 are for loose sand and the rest are for dense sand.

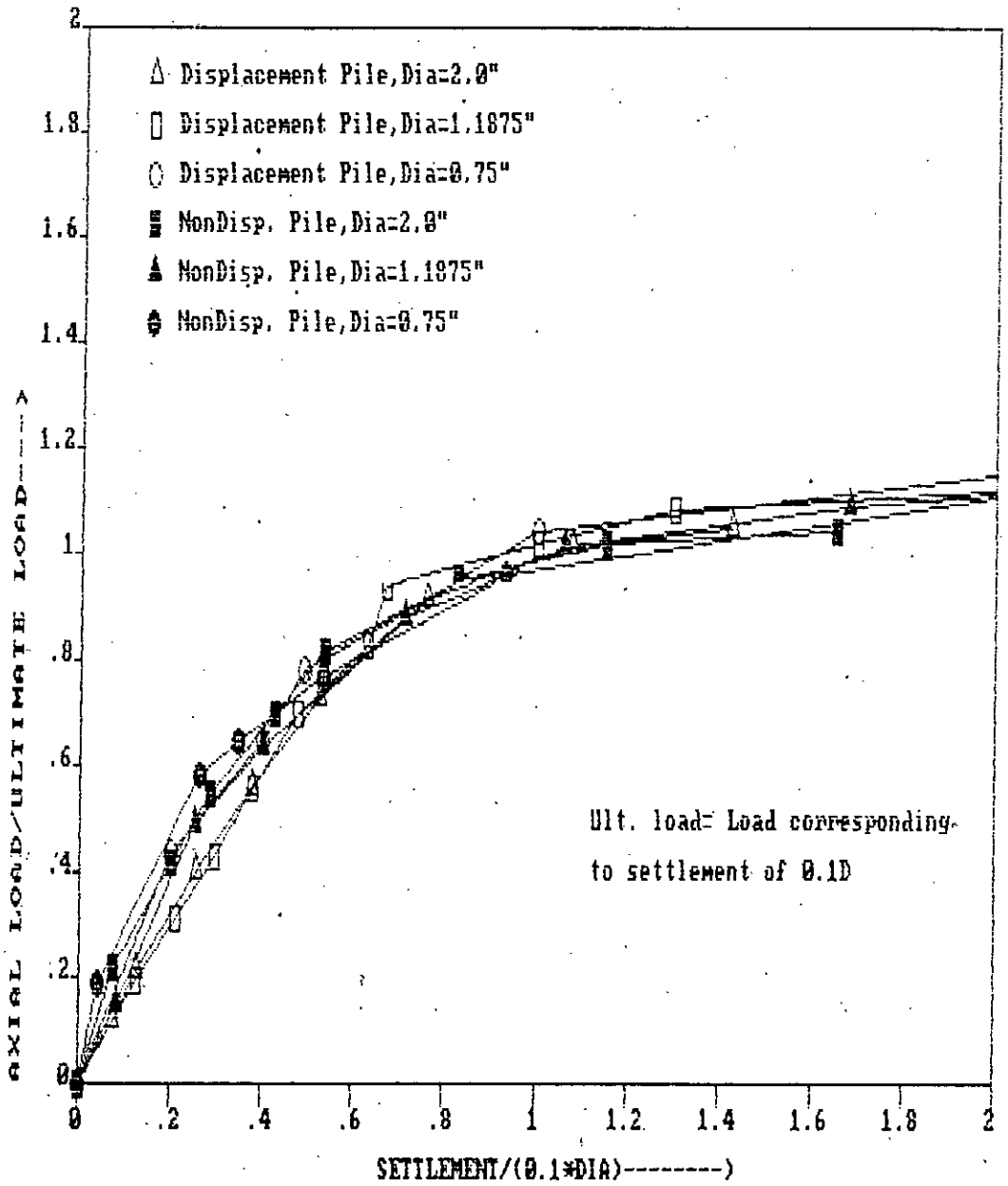


Fig. 6.3 Non-Dimensional Form of Load-Settlement Curves for Loose Sand.

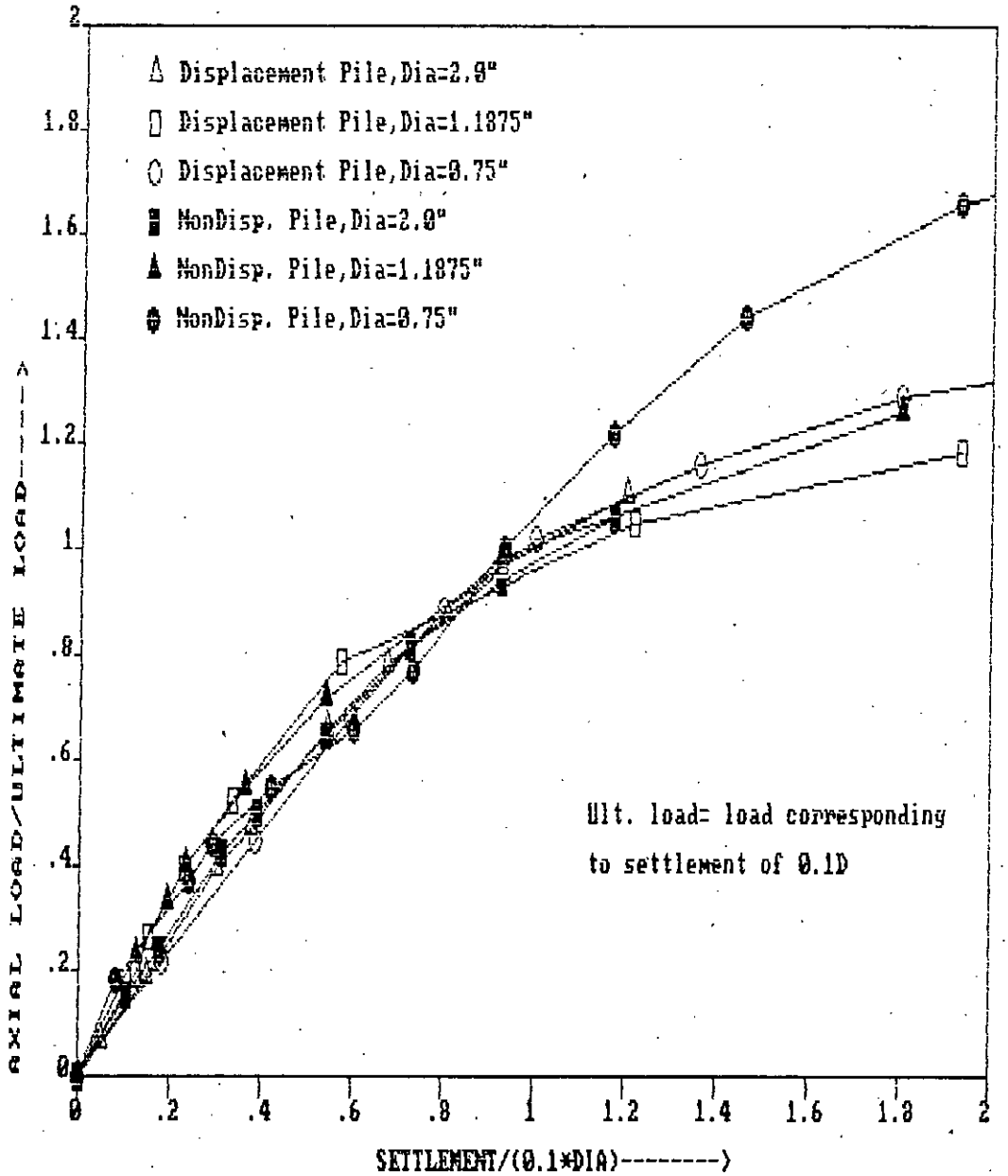


Fig. 6.4 Non-Dimensional Form of Load-Settlement Curves for Dense Sand.

Settlement ratio is the pile penetration divided by one-tenth of the pile diameter expressed as percent. Observation of all the figures indicate that skin friction increases with the pile embedment depth . Also it is seen that there is an increase in skin friction with increased settlement. An observation of the Fig.s 6.5 through 6.10 reveals that in most cases(except 150% curve of Fig.6.5) maximum skin friction is mobilized at settlement ratio of 100%. Skin friction mobilized is less when settlement ratio exceeds 100%. This suggest that a pile movement at 10% of the diameter may be considered as failure displacement. Proper contact at the interface of pile and soil ensure the full mobilization of skin friction. Overburden pressure offers skin frictional resistance through a frictional bond between pile and soil. It could be interpreted as the reduction in skin friction beyond a settlement of 0.1Xpile diameter, may be due to frictional bond failure, resulting in slippage at the pile-soil interface.

It is observed that the skin friction (unit shaft resistance) do not necessarily increase linearly with depth. Initially there is a rate of increase in skin friction with depth which later reduces and attains more or less a constant value. This may be the results of formation of sand arches(Robinsky and Morrison, 1964; Vesic, 1970) along with the settlement mobilization. Sand arches prevent full development of lateral earth pressure.

From the test results of model piles in sand it has been observed that there is an increase in skin friction with the increase in diameter of piles. Existing empirical relation(Meyerhof,1982) shown that skin friction is same for all diameter of pile. This is contrary to the experimental findings.

Here in displacement piles, pile was driven in the ground by displacing certain volume of soil. The rate of volume displacement per foot of sand indicated the rate of densification. Larger diameter pile had higher rate of volume displacement/foot as it had a larger base area. So, larger diameter displacement piles resulted in higher skin friction.

## 6.4 Prediction Model for Skin Frictional Resistance

Skin friction mobilized in a pile shaft at given depth, Z may be considered as(Terzaghi,1943)

$$f = \gamma_s Z K \tan(\delta) \qquad (6.1)$$

Where, $f$ = unit skin friction

$\gamma_s$ = unit weight of soil

$Z$ = depth

$K$ = coefficient of earth pressure

$\delta$ = angle of friction between soil and pile

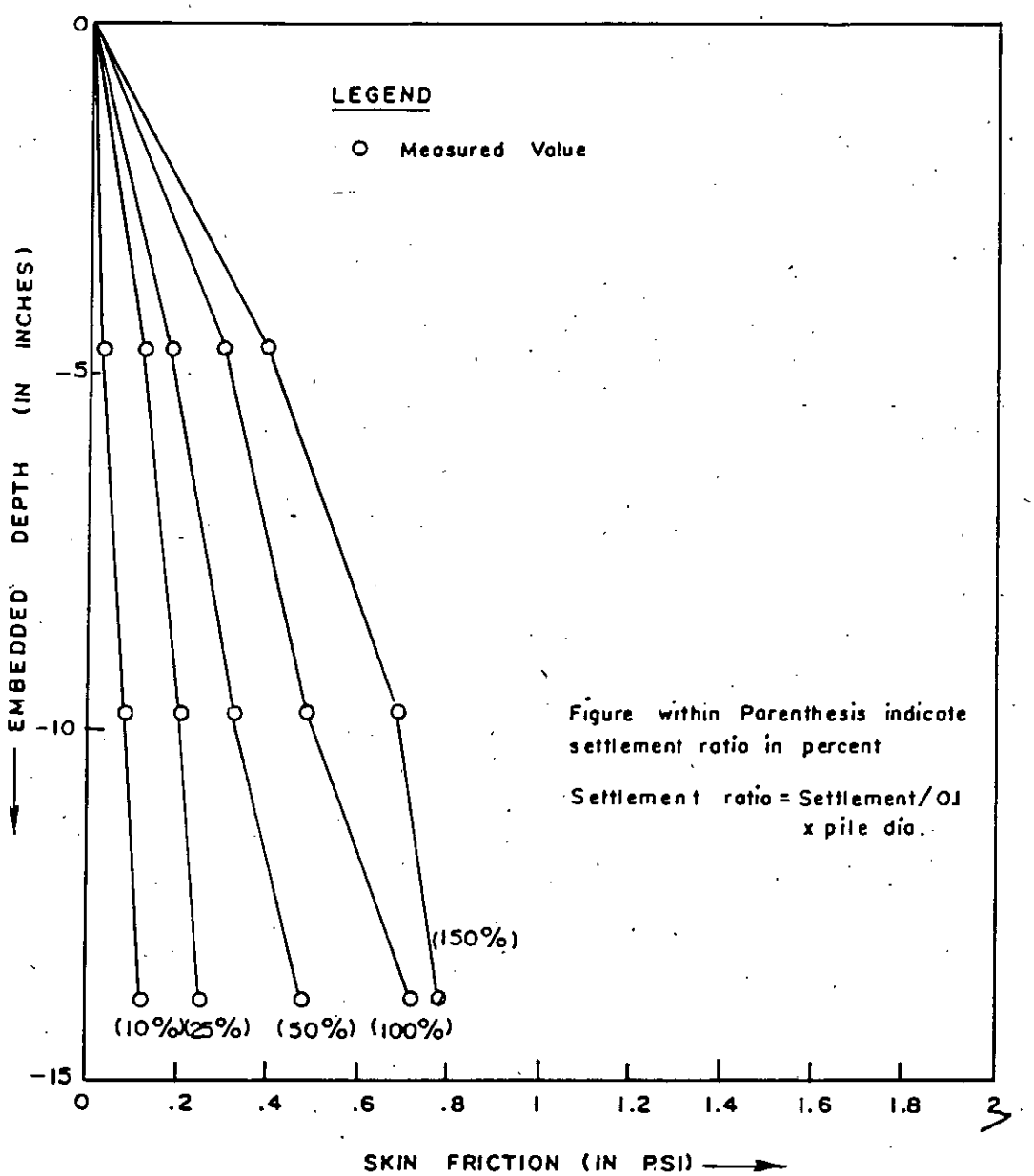


Fig. 6.5 Variation of unit skin friction along depth for displacement piles (dia = 0.75") in loose sand.

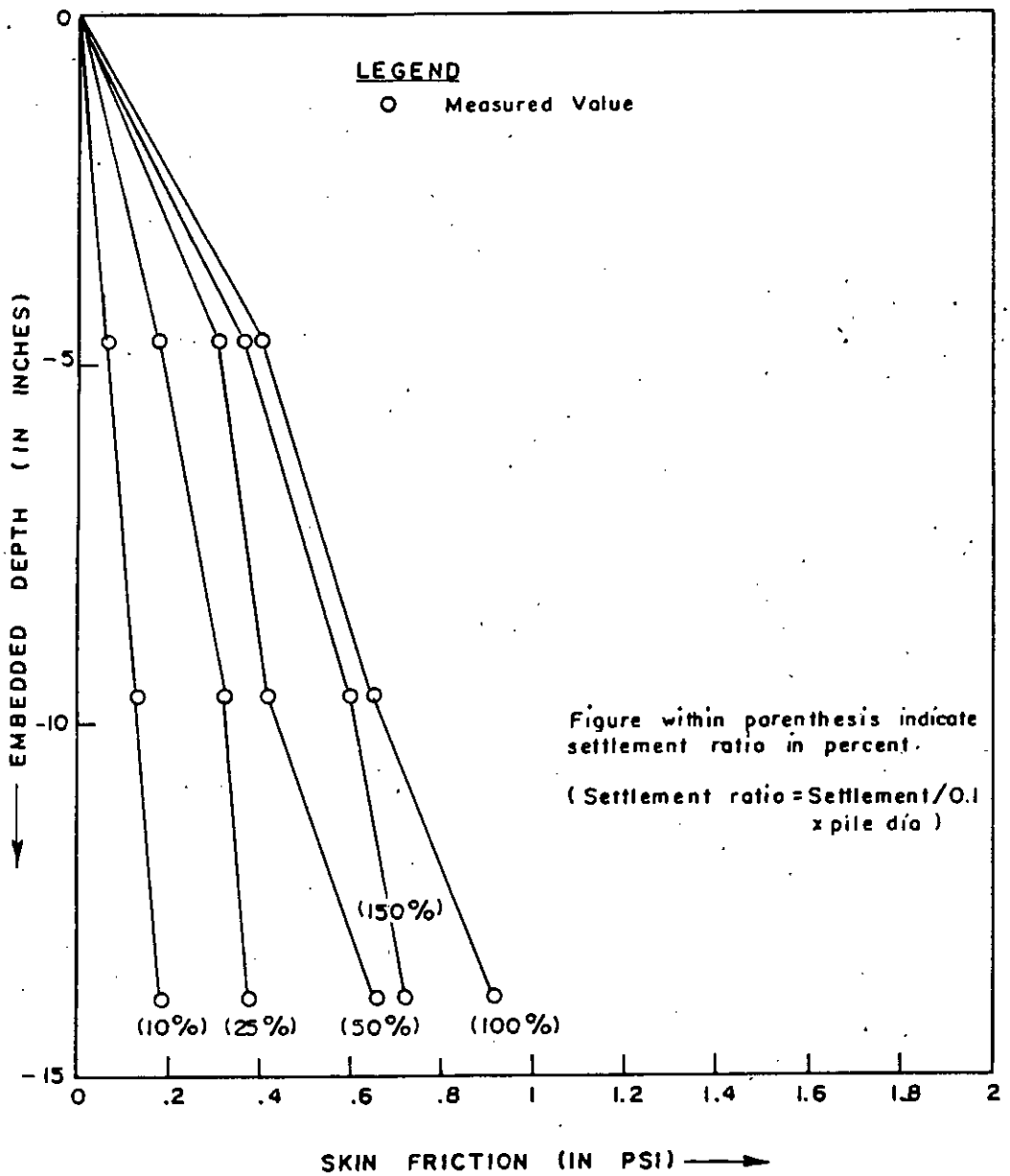


Fig. 6.6 Variation of unit skin friction along depth for displacement piles (dia = 1.1875") in loose sand.

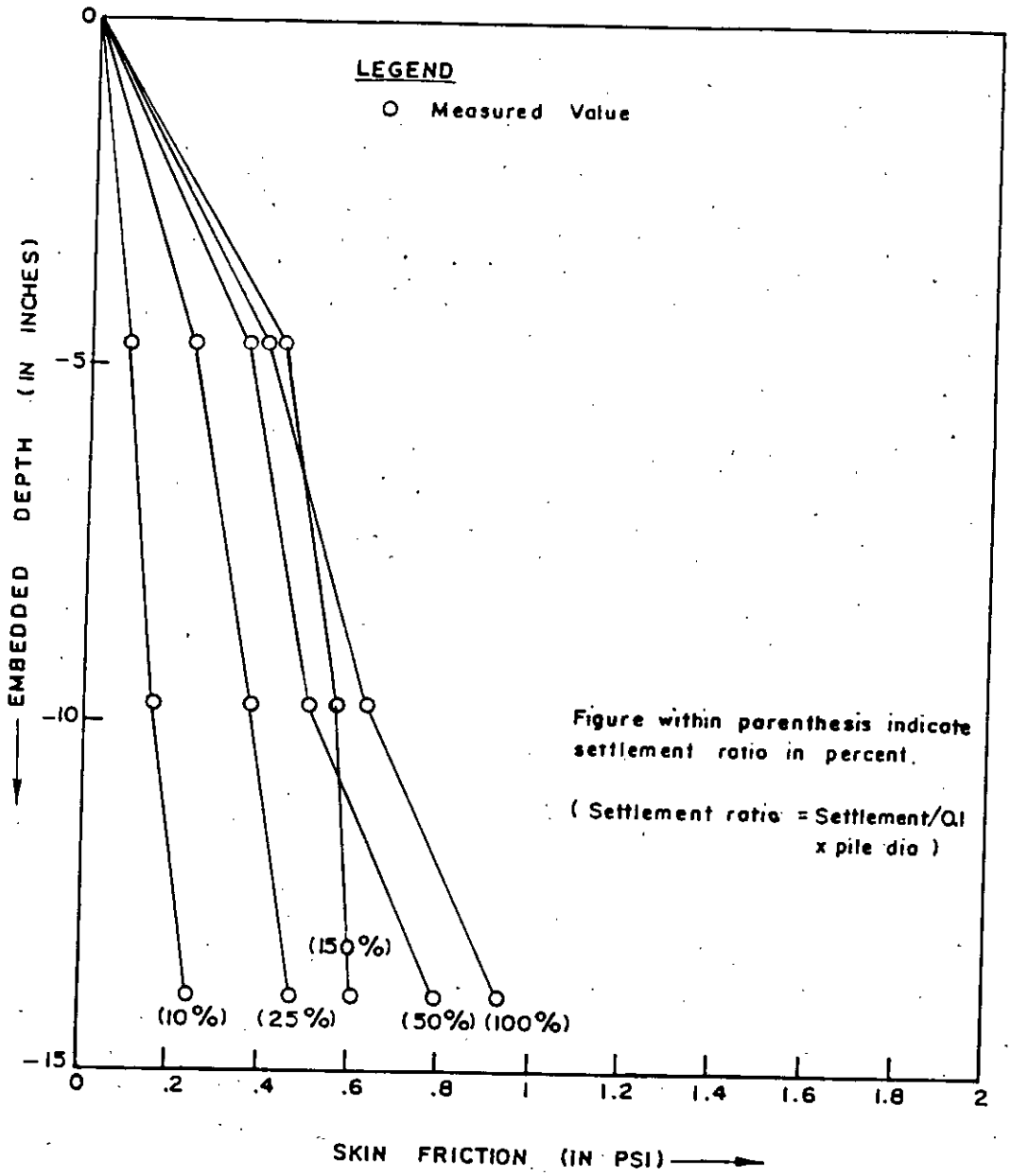


Fig.6.7 Variation of unit skin friction along depth for displacement piles (dia = 2.0") in loose sand.

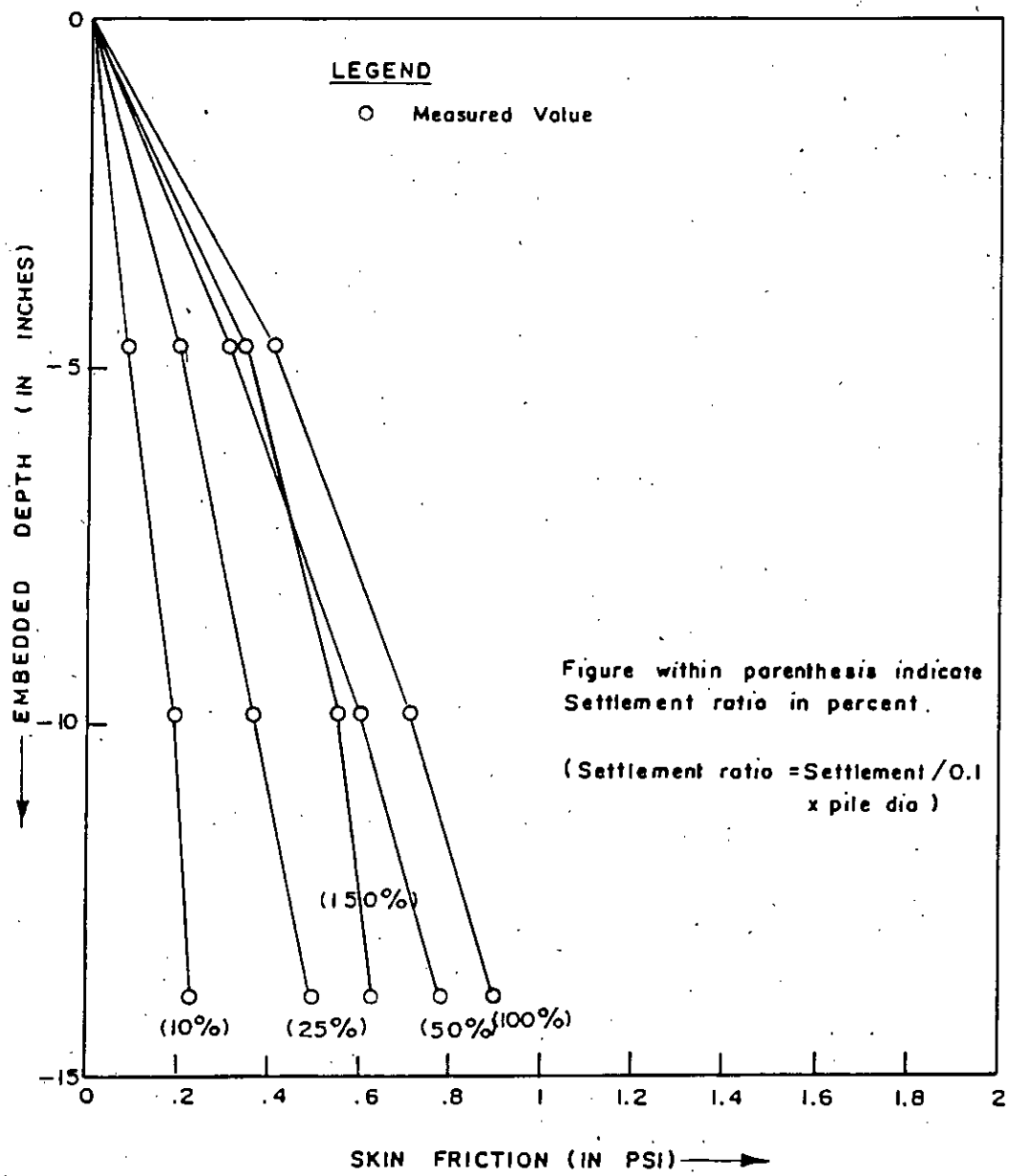


Fig. 6.8 Variation of unit skin friction along depth for displacement pile (dia = 0.75") in dense sand.

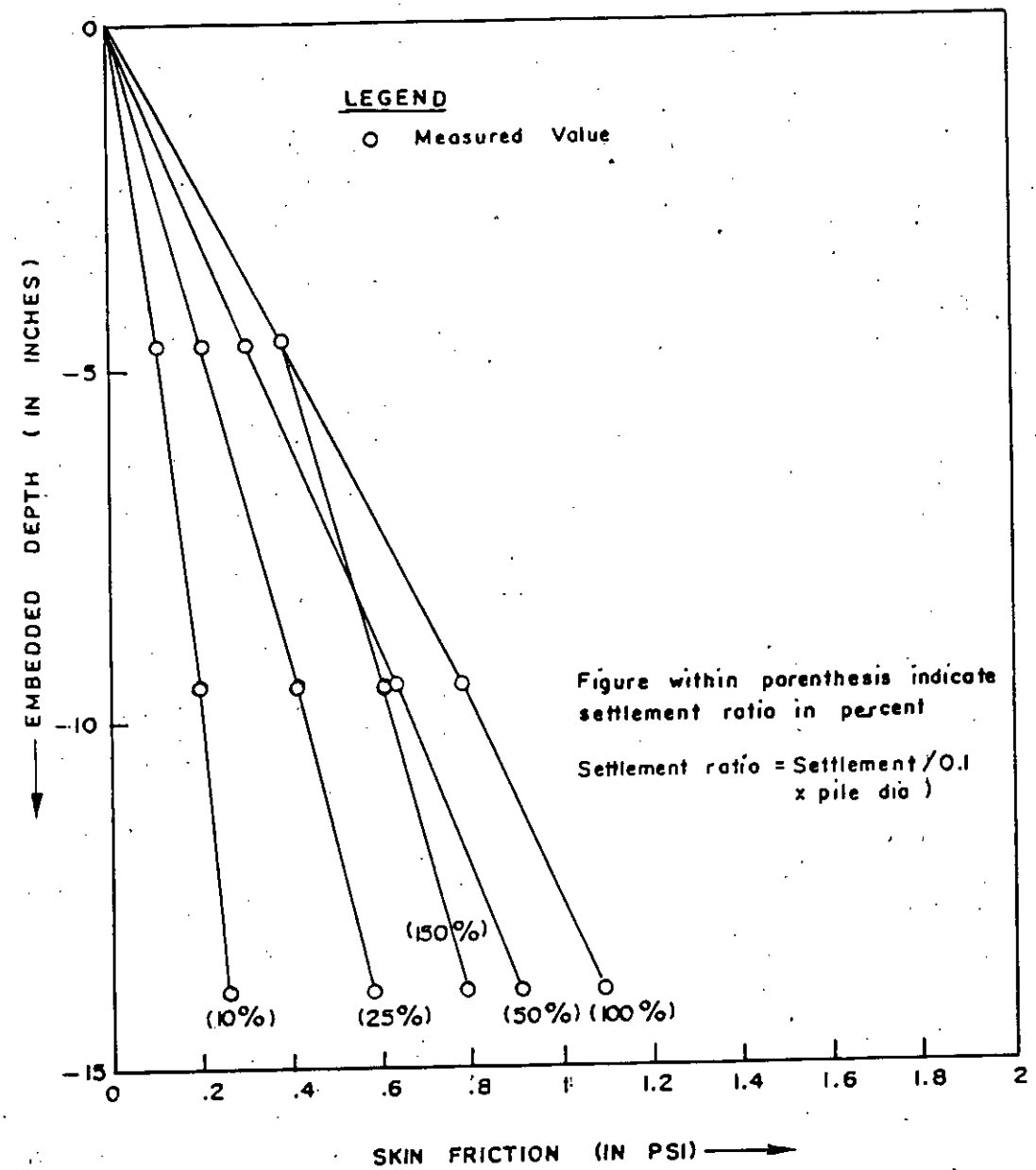


Fig. 6.9 Variation of unit skin friction along depth for displacement pile (dia = 1 1875") in dense sand

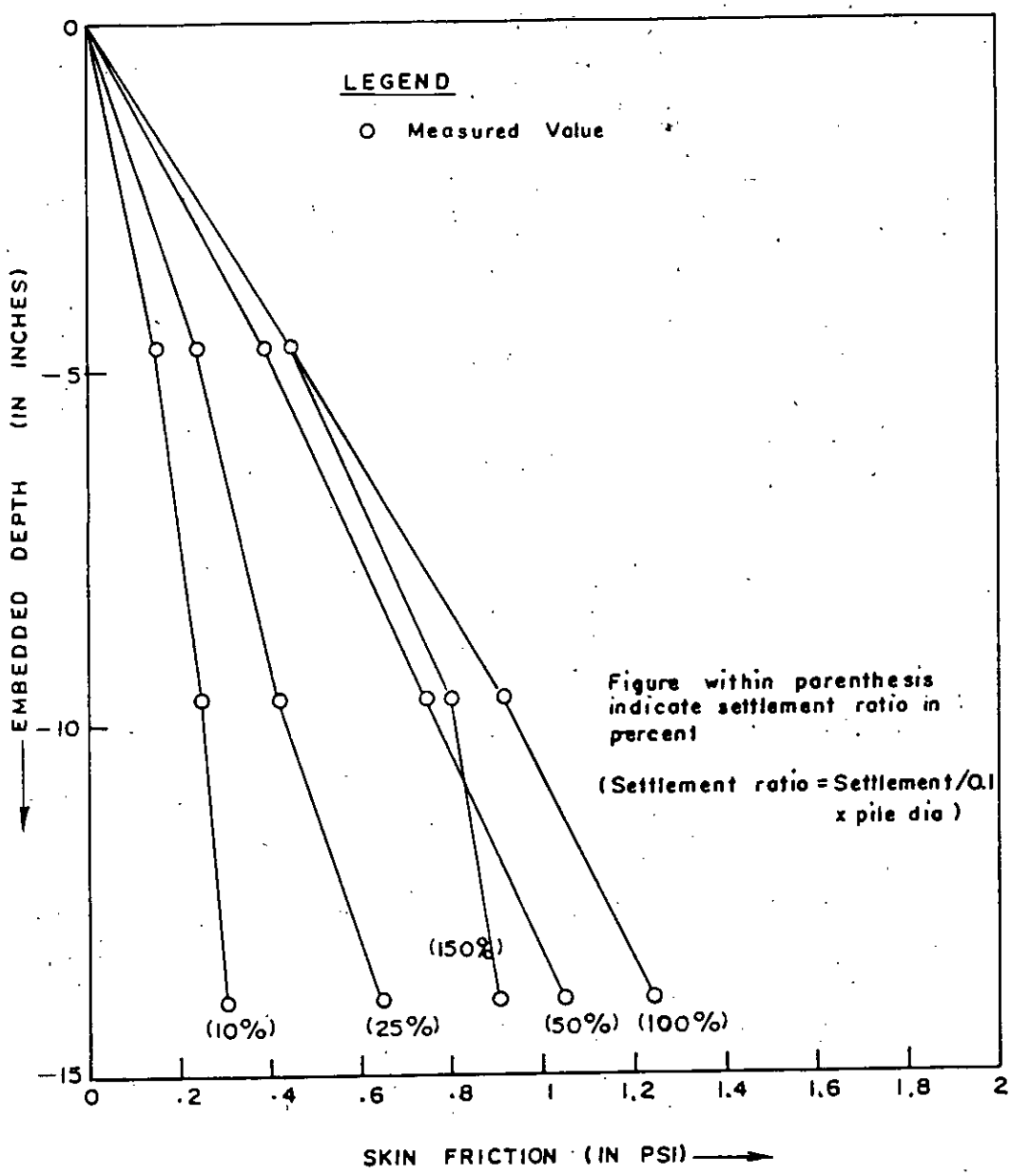


Fig. 6.10 Variation of unit skin friction along depth for displacement piles (dia = 2.0") in dense sand.

Different values of K are suggested by various investigators. In figure 6.11 the variation of this coefficient of earth pressure, K, with relative pile embedment (i.e, Z/L) in loose sand is shown. Fig. 6.12 shows same relation for the dense soil. Fig. 6.13 shows the variation of coefficient of earth pressure, K, at different settlement ratio in loose sand, and Fig.6.14 shows the same variation for dense sand.

From Fig. 6.11 and 6.12 it is observed that the earth pressure coefficient has a general tendency to increase with diameter. At small depth, earth pressure coefficient is higher than earth pressure coefficient at greater depth. In loose sand earth pressure coefficient is higher than in dense sand. According to Szechy(1961), Kerisel(1961), Robinsky and Morrison (1964) and Vesic(1970) dense sand forms arches around pile which prevent full development of earth pressure. This may be the reason of having lower value of coefficient of earth pressure in dense sand than that of loose sand. As these were displacement piles, higher diameter pile densified the sand around the piles during installation; therefore, coefficient of earth pressure is increased with diameter.It is also observed that all the coefficients of earth pressure lie in between that of active and passive earth pressure coefficients.

Observation of Fig. 6.13 and Fig. 6.14 reveals that at settlement ratio of 1, the coefficient of earth pressure reaches the maximum value. This emphasis the consideration that a

settlement of 10% of pile diameter usually taken as failure settlement. These curves also reveal that coefficient of earth pressure increases with the increase in diameter of piles and coefficient of earth pressure in loose sand is greater than that of dense sand.

Tomlinson(1971) suggested that the coefficient of lateral earth pressure should be in between $K_o$ to 1.75. The model pile test results confirm this view. However from the observation of results presented in figures 6.11 through 6.14 it is found that the earth pressure coefficient in dry uniform sand should be an average of active and passive earth pressure. For loose sand a slightly higher value can be considered. In conventional methods of pile design(Tomlinson,1971, Meyerhof,1976, Janbu,1976, Coyle et al,1981) skin friction is determined considering the coefficient of earth pressure at rest (eq. 6.1) which is too conservative as it appears from the above study.

Theoretically skin friction mobilized in a pile may be expressed by the following expression

$$f_{st} = \gamma_s z K_o \tan(\delta) \qquad (6.2)$$

where, $f_{st}$ = theoretical skin friction

$\gamma_s$ = unit weight of soil

$z$ = depth

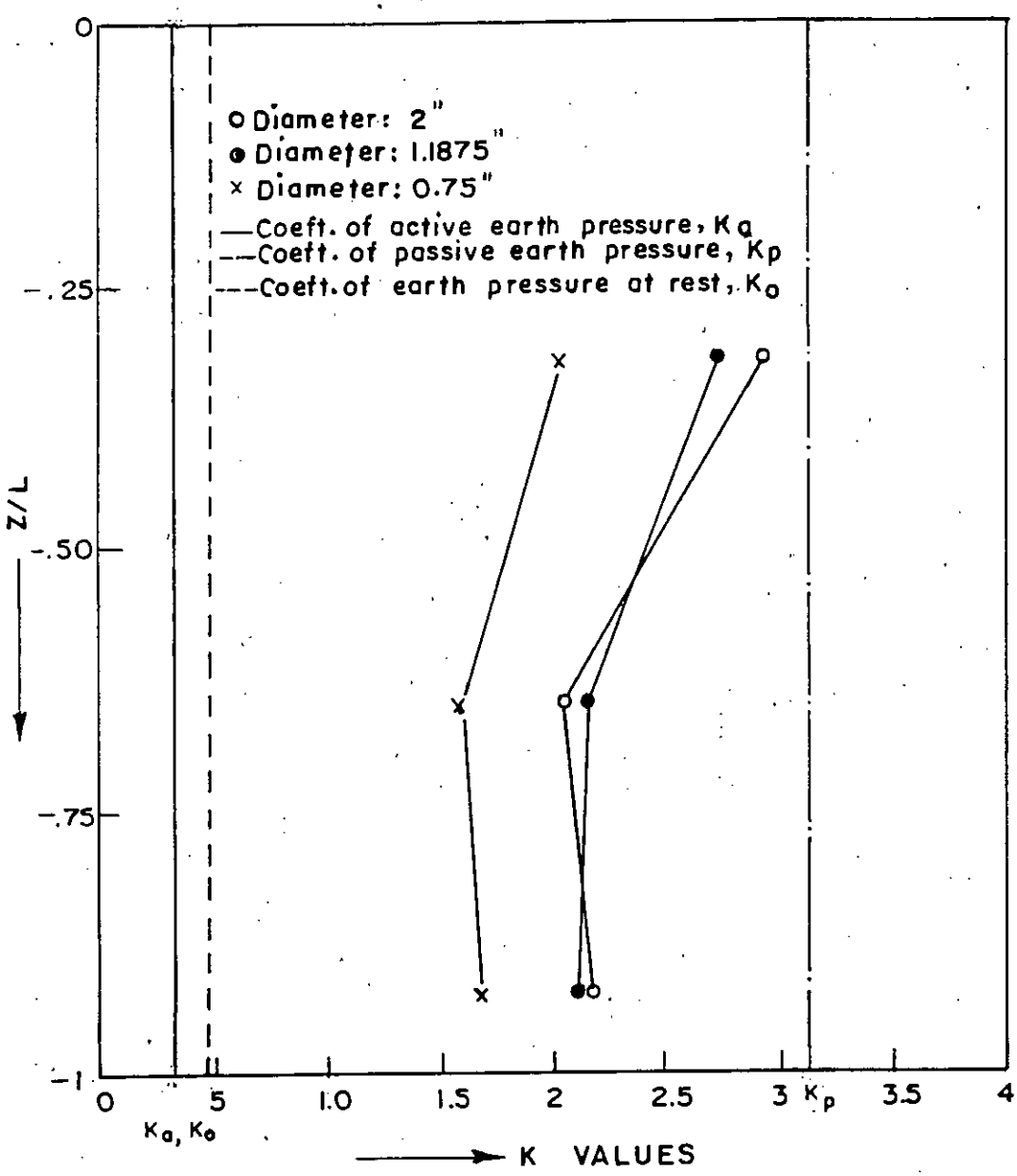


Fig. 6.11 Variation of Coefficient of Earth Pressure with Pile Depth in Loose Sand.

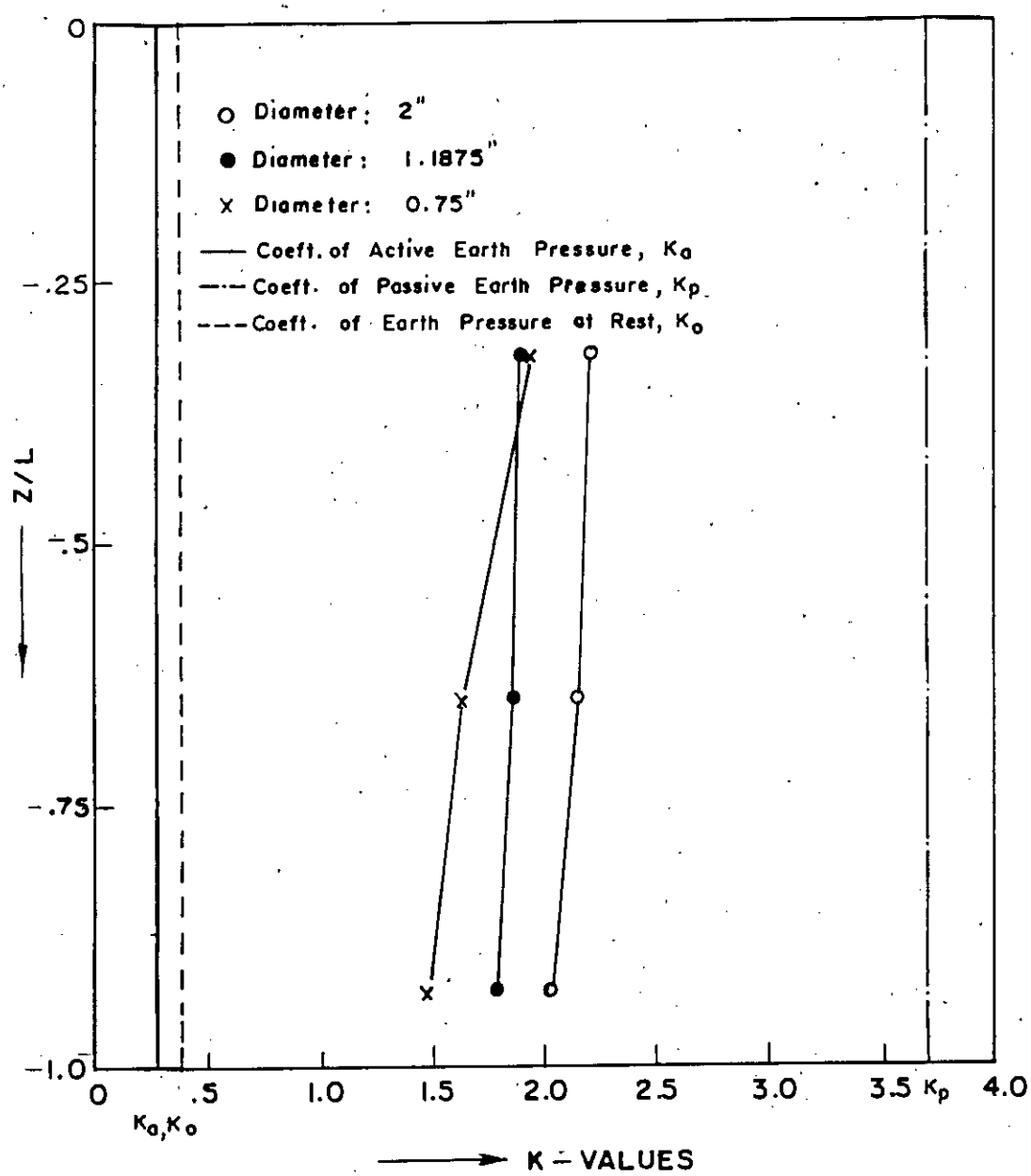


Fig. 6.12 Variation of Coefficient of Earth Pressure with Pile Depth in Dense Sand.

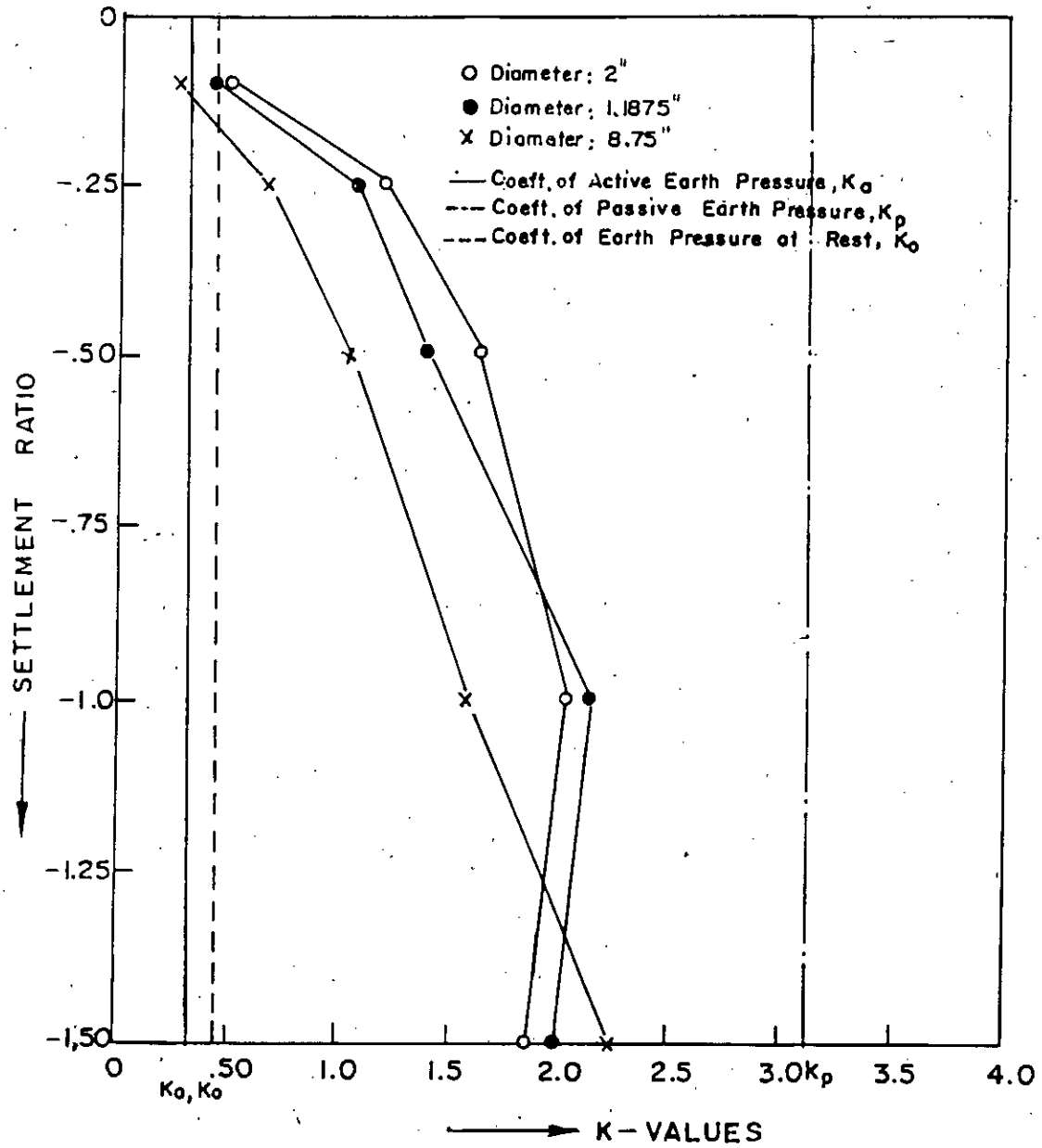


Fig. 6.13 Variation of Coefficient of Earth Pressure with Percent of Failure Settlement in Loose Sand.

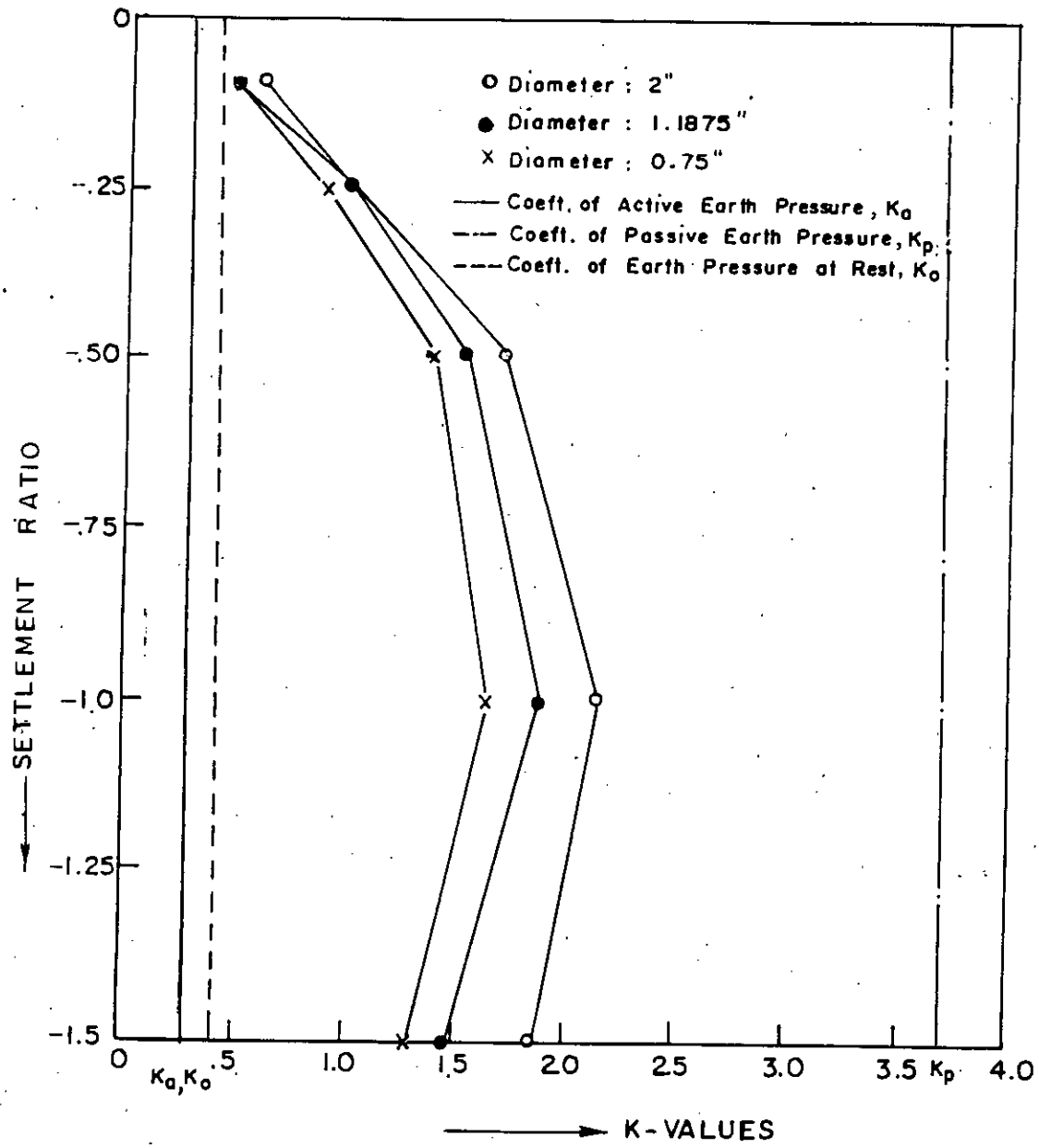


Fig. 6.14 Variation of Coefficient of Earth Pressure with Percent of Failure Settlement in Dense Sand.

$K_o$ = coefficient of earth pressure at rest

$\delta$ = angle of friction between soil and pile.

Results obtained from model pile tests are presented in Table 6.1 . A correlation is developed between calculated and observed skin frictions involving the following parameters.

$$\frac{Fsa}{r \times Fst} = \frac{-Z/L + C_1 \, e^{-C_2 r}}{D_1 \times e^{-D_2 r}} \qquad (6.3)$$

where $$r = \frac{i}{f} = \frac{\text{Any settlement}}{0.1 \times D}$$

Fsa = actual skin friction(psi)

Fst = theoretical ($K_o$) skin friction(psi)

Z/L = embedment depth ratio

For Loose Sand

$C_1 = 105.56 \, e^{-.09(L/D)}$

$C_2 = 2.97 \, e^{-.04(L/D)}$

$D_1 = 26.01 \, e^{-.03(L/D)}$

$D_2 = 1.68 \, e^{-.02(L/D)}$

For Dense Sand

$$C_1 = 124.71\ e^{-.07(L/D)}$$

$$C_2 = 2.55\ e^{-.02(L/D)}$$

$$D_1 = 35.06\ e^{-.05(L/D)}$$

$$D_2 = 1.83\ e^{-.04(L/D)}$$

$$\text{where,} \quad L/D = \frac{\text{Length of pile}}{\text{Diameter of pile}}$$

Fig. 6.15 and Fig. 6.16 contain sample plots, according to the equation (6.3); which satisfactorily predict the observed data. In this regression model, exponential nature of constants are used to incorporate the arching phenomenon of dense sand.

Limitations of the above prediction model are as follows:

1. It is valid upto L/D = 35
2. It is valid upto r = 1.5
3. For a uniformly laid sand bed.

This however, should be of limited use and should be field tested, bearing in mind that, the results used are for model piles in a uniform density bed of a dry sand.

TABLE 6.1(a) Experimental Results of Unit Skin Friction(psi) for Dense Sand.

| L/D | Unit Skin Friction (psi) for Dense Sand at Different Settlement Ratios. | | | | | Pile Depth. (inches) |
|---|---|---|---|---|---|---|
| | 10% | 25% | 50% | 100% | 150% | |
| 20.00 | 0.08 | 0.20 | 0.34 | 0.41 | 0.321 | 4.75 |
| 12.45 | 0.11 | 0.21 | 0.31 | 0.40 | 0.39 | |
| 7.50 | 0.15 | 0.24 | 0.39 | 0.46 | 0.45 | |
| 20.00 | 0.19 | 0.36 | 0.59 | 0.70 | 0.55 | 9.75 |
| 12.45 | 0.21 | 0.425 | 0.65 | 0.80 | 0.63 | |
| 7.50 | 0.25 | 0.42 | 0.75 | 0.92 | 0.81 | |
| 20.00 | 0.23 | 0.50 | 0.78 | 0.91 | 0.63 | 14.00 |
| 12.45 | 0.26 | 0.58 | 0.92 | 1.10 | 0.79 | |
| 7.50 | 0.31 | 0.65 | 1.05 | 1.25 | 0.92 | |

TABLE 6.1(b) Experimental Results of Unit Skin Friction(psi) for Loose Sand.

| L/D | Unit Skin Friction (psi) for Loose Sand at Different Settlement Ratios. | | | | | Pile Depth. (inches) |
|---|---|---|---|---|---|---|
| | 10% | 25% | 50% | 100% | 150% | |
| 20.00 | 0.03 | 0.12 | 0.18 | 0.30 | 0.40 | 4.75 |
| 12.45 | 0.064 | 0.18 | 0.31 | 0.40 | 0.37 | |
| 7.50 | 0.083 | 0.23 | 0.36 | 0.43 | 0.40 | |
| 20.00 | 0.08 | 0.20 | 0.32 | 0.48 | 0.68 | 9.75 |
| 12.45 | 0.13 | 0.32 | 0.42 | 0.65 | 0.60 | |
| 7.50 | 0.15 | 0.37 | 0.50 | 0.62 | 0.56 | |
| 20.00 | 0.12 | 0.25 | 0.48 | 0.73 | 0.78 | 14.00 |
| 12.45 | 0.18 | 0.38 | 0.67 | 0.92 | 0.72 | |
| 7.50 | 0.245 | 0.47 | 0.80 | 0.94 | 0.60 | |

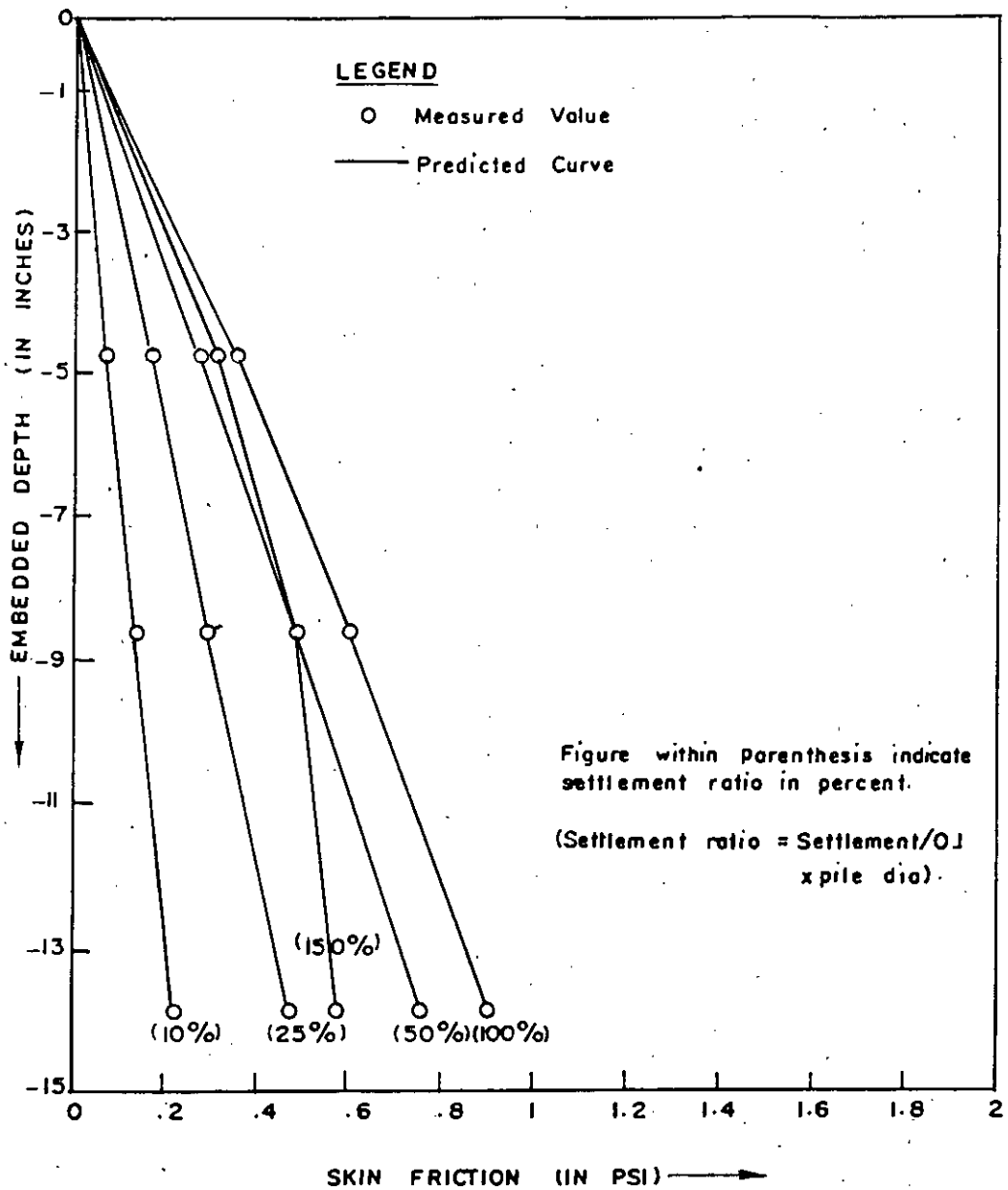


Fig. 6.15 Skin Friction prediction for loose sand from empirical relation (Dia = 2.00")

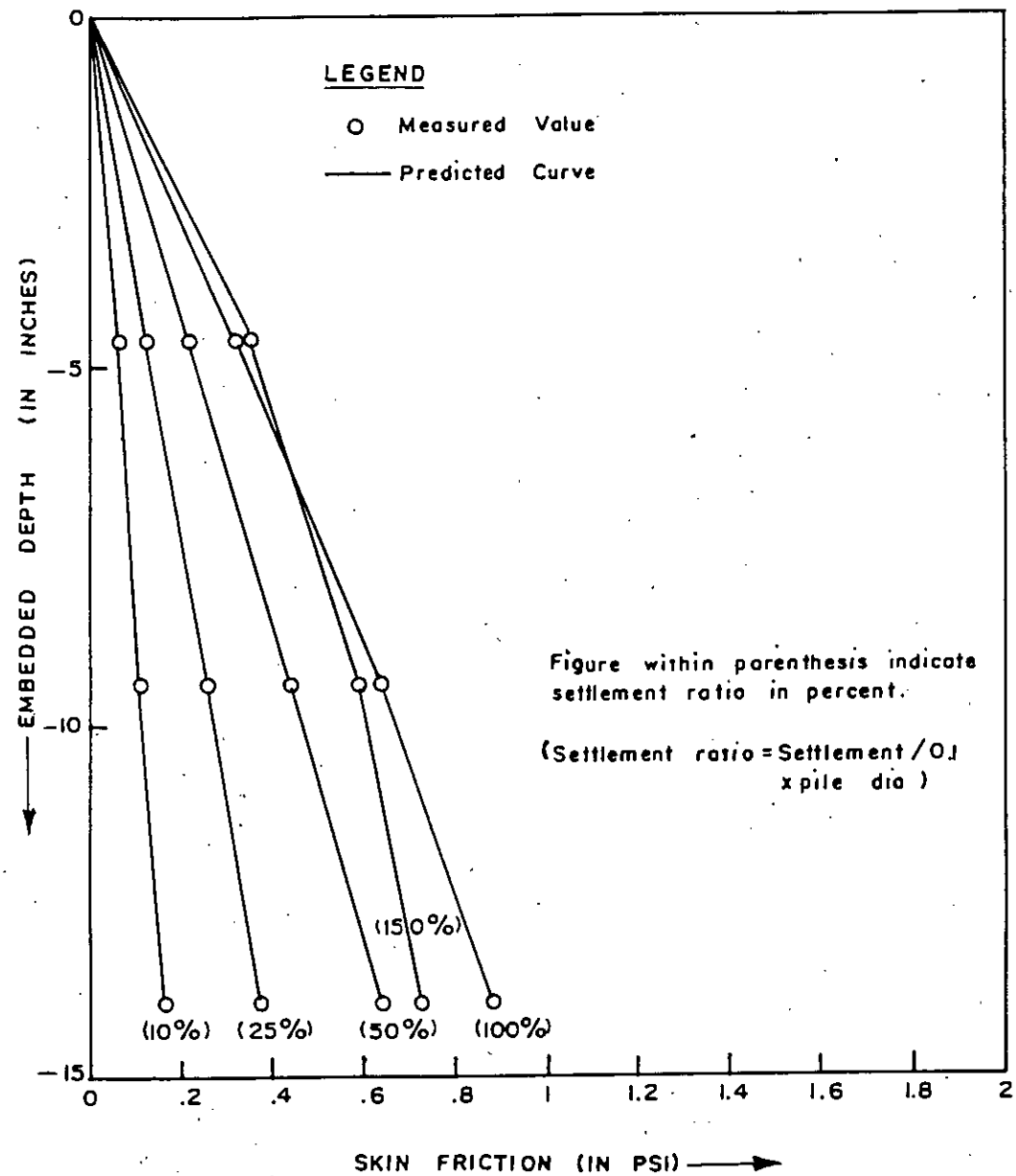


Fig. 6.16 Skin friction prediction for loose sand from empirical relation. ( dia = 1.1875" )

## 6.5 End Bearing of Piles

The bearing capacity factor for a pile can be determined by using equation (2.4)

$$q_o = P_o N_q$$

where $P_o$ = effective overburden pressure

$q_o$ = unit point resistance

$N_q$ = bearing capacity factor

From the effective overburden pressure at pile tip, $P_o$ of model piles, bearing capacity factor, $N_q$ is calculated using equation (2.4) and the values are tabulated in table 6.2. From the table it appears that for loose sand bearing capacity factor is independent of pile diameter. It is also clear from the table that installation process significantly increases bearing capacity factor by densification. In loose sand the difference of $N_q$ between displacement and nondisplacement piles is higher than those values for dense sand. Because dense sand undergoes less densification than the loose condition by the installation procedure as it is already densified.

If a comparison is made between the values of Nq shown in Table 6.2 and the values of Nq from Table 2.2, it is observed that $N_q$ values obtained from this model test are 36.61(displacement pile,loose sand) and 23.47(non-displacement

TABLE 6.2 Bearing Capacity Factors for Model Piles.

| Pile Dia. (inches) | Loose Sand ($\phi = 31^0$) | | Dense Sand ($\phi = 35^0$) | |
|---|---|---|---|---|
| | Displacement Pile | Non-Disp. Pile | Displacement Pile | Non-Disp. Pile |
| 0.75 | 35.40 | 23.90 | 52.36 | 25.25 |
| 1.1875 | 34.44 | 24.74 | 40.77 | 35.59 |
| 2.00 | 39.98 | 21.74 | 50.318 | 42.46 |
| Average $N_q$ Values | 36.61 | 23.47 | 47.81 | 34.43 |

pile,dense sand), which lie between the values obtained by Terzaghi(1943) and that by Vesic(1972). This was also true for dense sand.

# CHAPTER 7

## ANALYSIS AND INTERPRETATION OF FINITE ELEMENT RESULTS

### 7.1 Introduction

A fully three-dimensional finite element analysis is performed for the axially loaded pile soil system. The soil is replaced by an elastic continuum and perfect bonding is assumed between pile and soil interface. Displacements at the head and load distribution and skin friction along the pile length are compared with experimental observations.

### 7.2 Description of Finite Element Model

In this research axially loaded piles were tested in a sand tank of 2ft.X 2ft.X 2ft. size. Due to symmetry of soil-pile system as well as loading only one quarter of the full model has been discretized. Fig. 7.1 shows the discretized system of the problem. There are 124 elements with 220 nodes in the mesh fig. 7.1. The degree - of-freedom(DOF) in the x-direction in the plane ADCB and EFHG are constrained. The DOF in y-direction for the faces ADGH and BCEF are constrained. The plane, DCEG is constrained for the DOF only in vertical(z) direction.

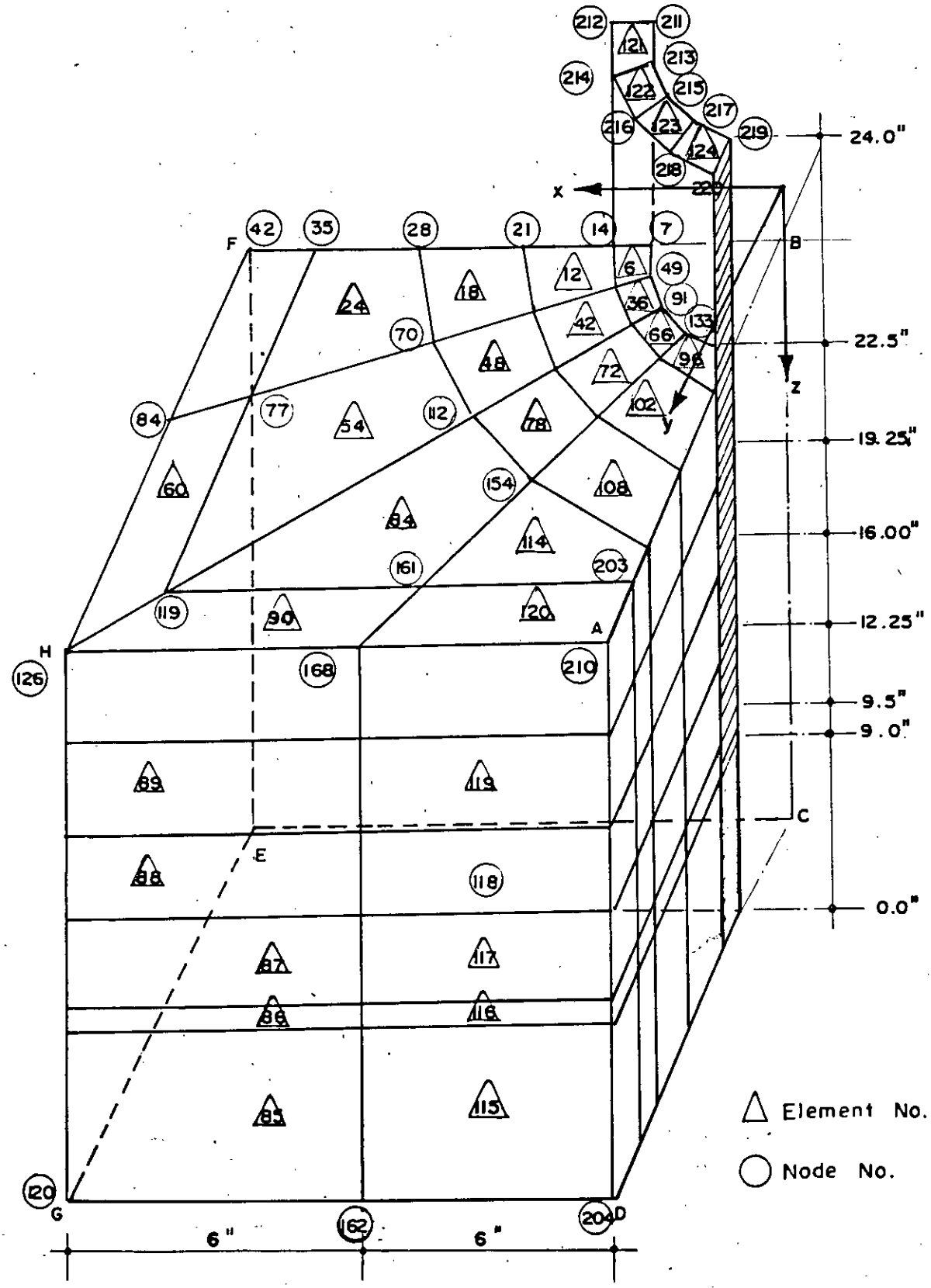


Fig. 7.1 3D Finite Element Mesh Pile in Soil Block.

Here, no interface element is considered as there was no such scope in the present version of "FE2000". As the piles were circular, so to simulate circular curve, small straight lines are considered in place of arcs(shown in Fig. 7.1). The hatched portion in Fig.7.1 indicated pile elements.

In actual model tests load was applied as distributed over the pile x-sectional area and the test was a CRP(constant rate of penetration ) test having a rate of 0.03-0.10 in/min. So here total load is uniformly applied over all top faces of pile(node 211 through 220).

## 7.3 Material Properties

The pile and soil properties were determined by appropriate tests described in chapter 4. Following properties were considered for the present analysis.

Soil modulus at mid depth of pile:

Dense soil : 116 psi.

Loose soil : 70 psi.

Poisson's ratio of pile material :$\nu_p$ = 0.25(assumed)

Poisson's ratio of soil :$\nu_s$ = 0.30(assumed)

Modulus of elasticity of pile : $E_p$= 8.0 X $10^6$ psi

## 7.4 Discussion on Results

### 7.4.1 Load deformation behaviour

Fig. 7.2 shows typical load-settlement curve. Finite element results for one load increment(as it was a linear elastic analysis) have also been plotted on this curve for comparison. Other load-settlement curves for various diameter and installation conditions are given in appendix B.

Observation of these curves show that at lower load there has been a good agreement between FEM and experimental results .But at higher load their variation is significant.

At lower load soil behaves elastically. But with the increase in load,it become nonlinear. Again,when pile penetrate into soil it transfers load to the surrounding soil material by a bond between pile and soil. Higher load induces slippage through breaking of bond (called debonding) and regeneration of bond (called rebonding) also occur due to particle reorientation.All these bonding, debonding, slippage, and rebonding at the interface of pile and soil which contribute significant nonlinearity to the load-settlement curve are ignored in the present study.

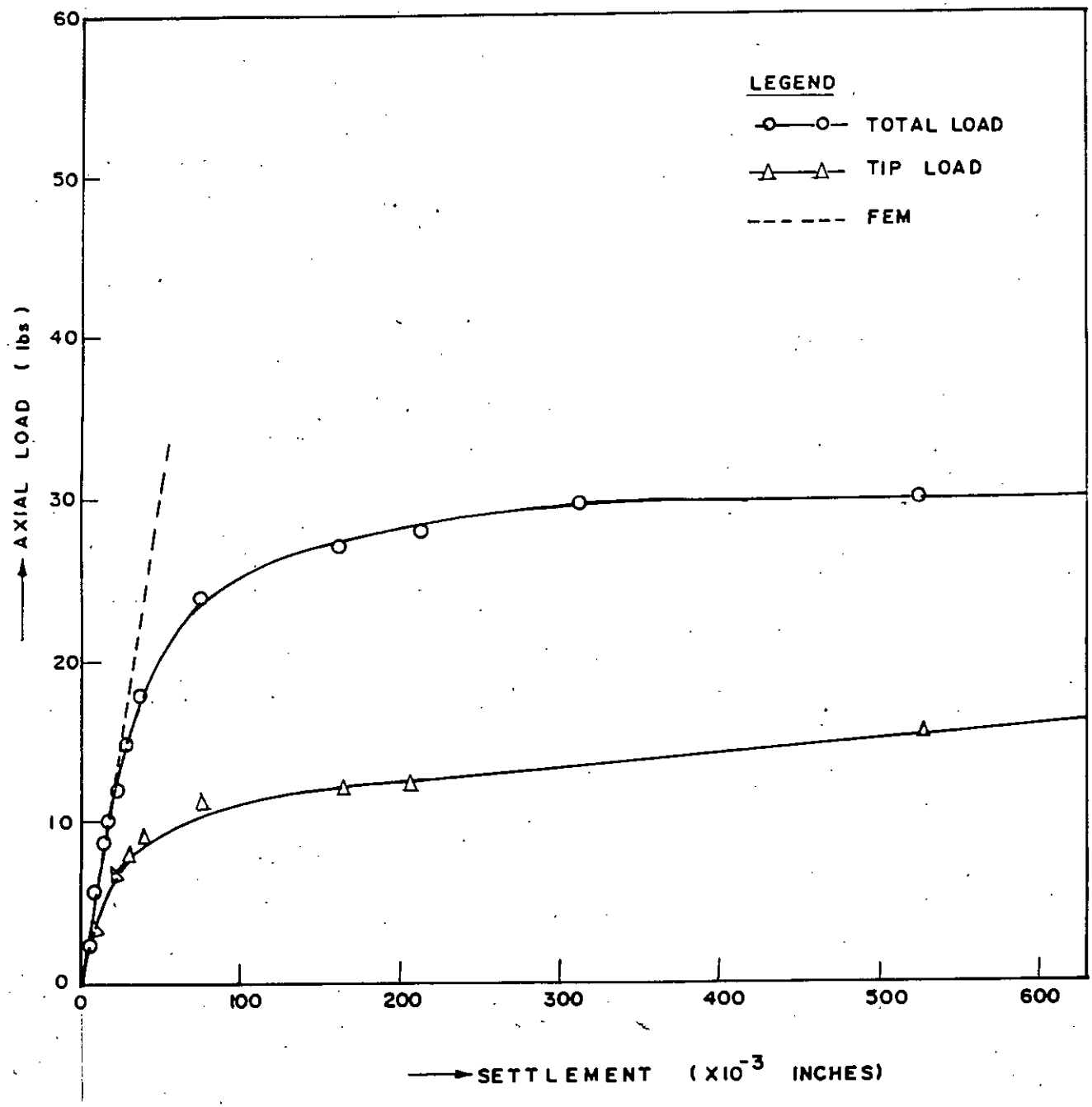


Fig. 7.2 Displacement Piles in Loose Sand. (Dia= 0.75)

### 7.4.2 Stress distribution along the pile

Fig. 7.3 shows the variation of compressive vertical stress ( $\sigma_{zz}$ ) along embedment depth. The finite element results compare well with those of observation for dense sand. The same results are plotted for loose sand in Fig. 7.4.

Fig. 7.3 shows reasonable agreement of vertical stresses between FEM results and measured values for dense sand. But the discrepancy between FEM and measured value in Fig.7.4 is substantial for loose sand.In dense condition the skin resistance offered by sand is higher than the loose sand, so the perfect bonding between sand and pile may be assumed and also only 25% of failure load is applied so the loading may also be assumed essentially within elastic range. In elastic analysis perfect bonding between sand and pile is assumed. Hence in this case comparison between numerical analysis and experimental results are found to be quite satisfactory.

But for the loose condition skin resistance is virtually negligible. Even at 25% of failure load slippage, separation may occur along the pile soil interface. Under this condition observed values of axial load should have been higher than the predicted values which contradicts with the finding(Fig. 7.4). This discrepancy may be due to the fact that soil modulus used in

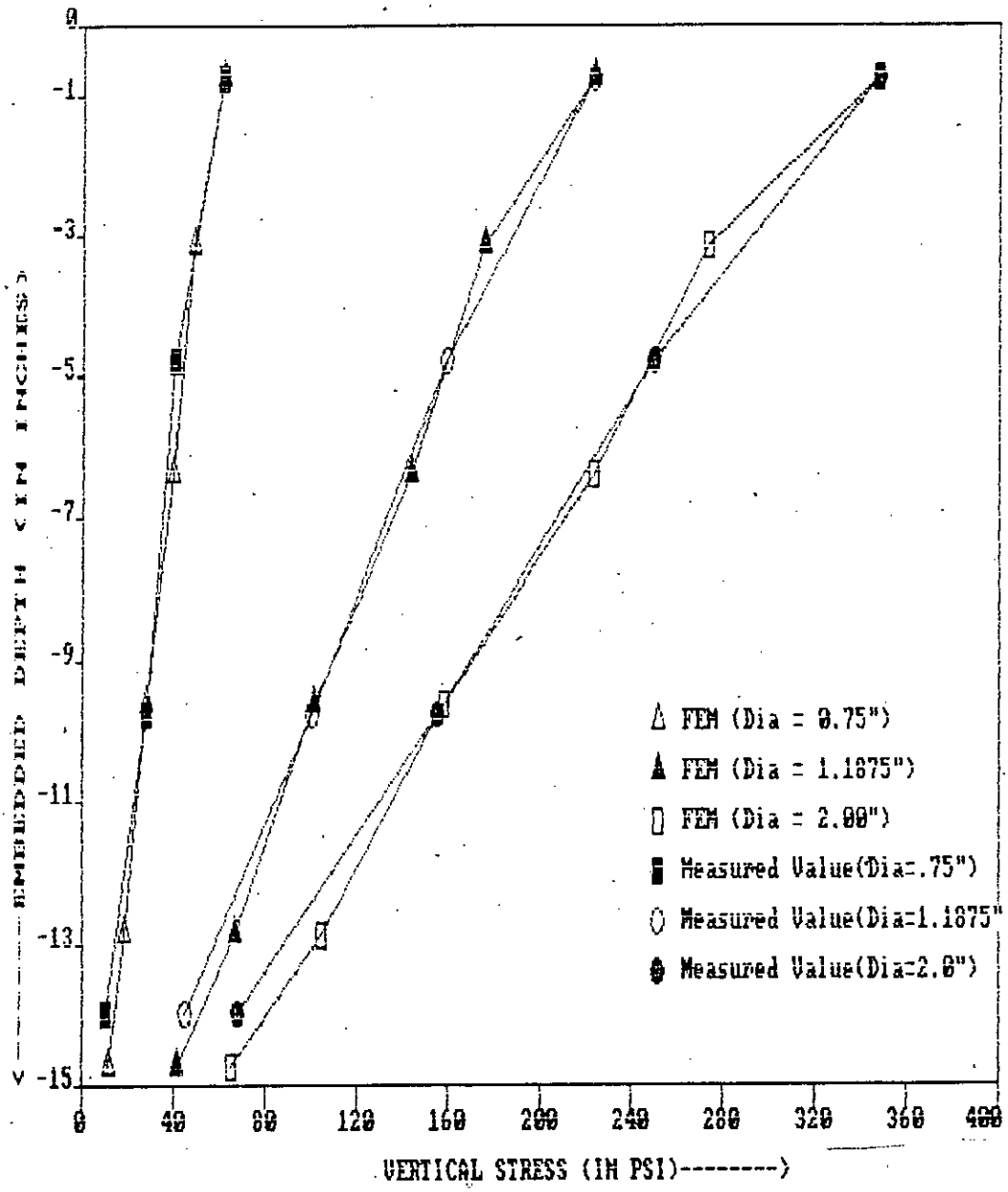


Fig. 7.3 Variation of Vertical Stress ( $\sigma_{zz}$ ) Along Embedment Depth for Displacement Piles in Dense Sand (at 25% of Failure Load).

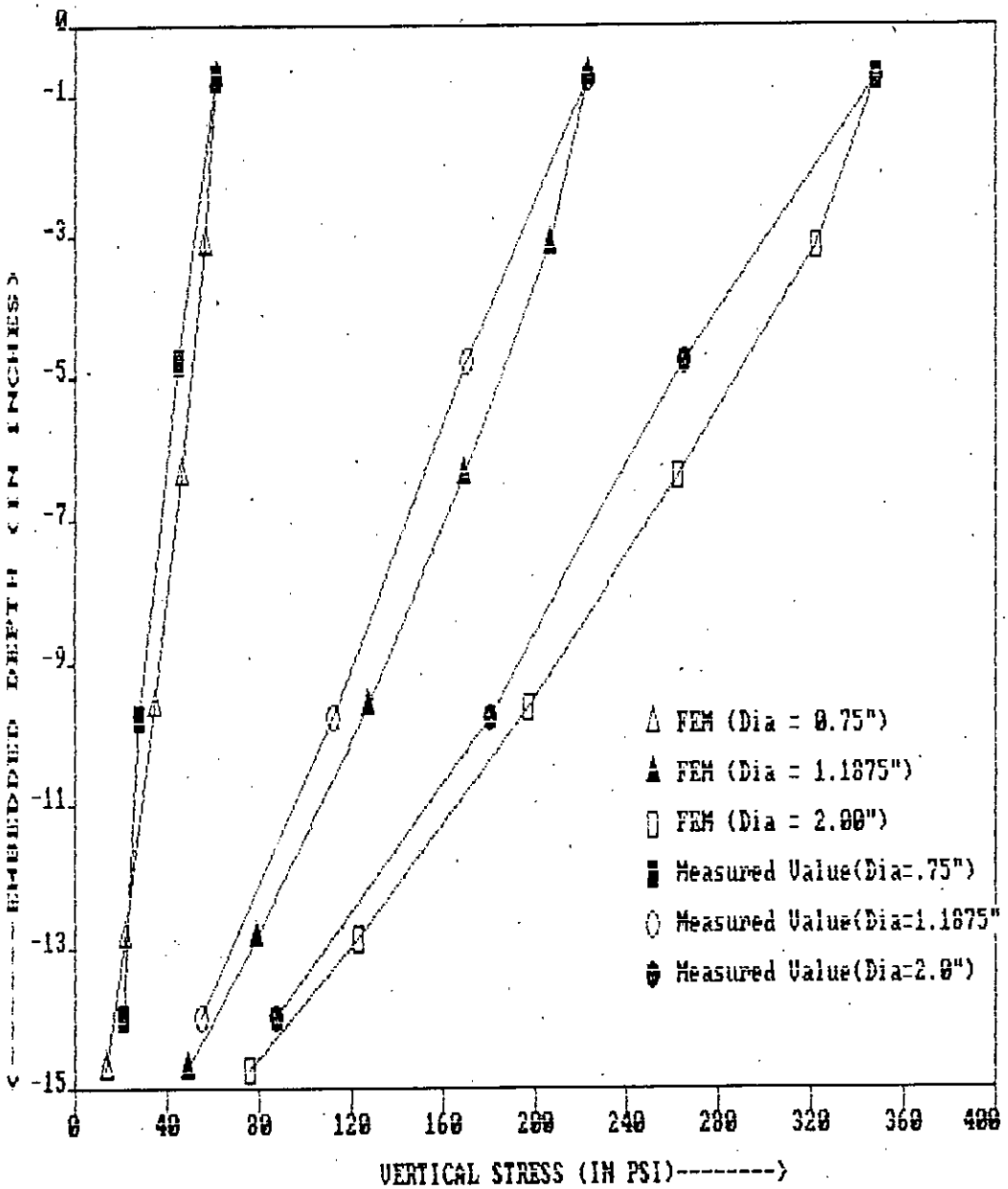


Fig. 7.4 Variation of Vertical Stress ( $\sigma_{zz}$ ) Along Embedment Depth for Displacement Piles in Loose Sand (at 25% of Failure Load).

the analysis is too low.

### 7.4.3 Axial load transfer at failure load

Fig. 7.5 show variation of axial load long embedded depth for dense soil. This curve show a large variation between finite element result and that observed experimentally at failure load. The other curves for all diameter, density and installation conditions are given in appendix B.

At failure load slippage and debonding phenomenon may occur at the pile soil interface. Under this condition load transfer by skin friction will be negligible and the pile itself will carry higher percentage of load. In linear elastic analysis perfect bonding between pile and soil at the interface is assumed, which means significant amount of applied load is transferred by skin friction. If material nonlinearity and interface behaviour(i,e bonding, debonding, slippage phenomenon) had been considered then the predicted values would have been closer to observations.

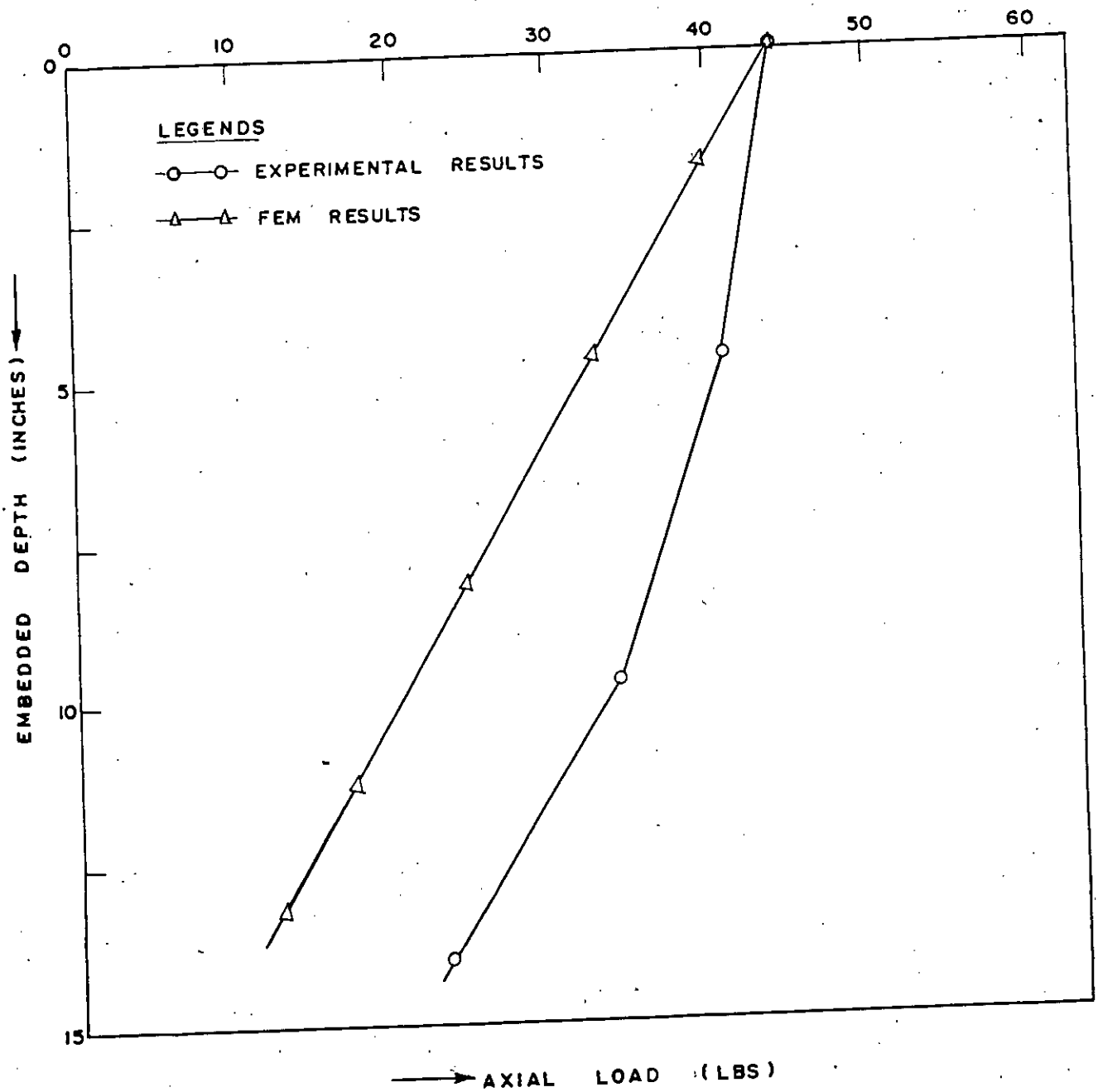


Fig. 7.5 Displacement Piles in Dense Sand (Dia = 0.75")

# CHAPTER 8

## CONCLUSIONS AND RECOMMENDATIONS FOR FURTHER RESEARCH

### 8.1 Conclusions

Model piles of various diameters were installed in uniformly bedded sand deposit and tested in compression. In order to evaluate load transfer mechanism, loads transferred to the pile at various depths were measured by electrical strain gauges. From the results obtained and discussed in preceding chapters, the following conclusion may be made.

1. During transfer of load from pile top, the skin friction developed on the pile shaft does not increase linearly with depth. Frictional resistance increases with depth but the rate of increase decreases with depth and may attain a constant value. This may be attributed to sand arching effect.

2. Skin friction mobilized increases with increase in pile penetration and attains a maximum value at 0.1D penetration where D is the diameter of the pile.

3. For displacement piles, skin frictional resistance increases with diameter of the piles.

4. At low penetration of pile, coefficient of earth pressure is low, which increases to a values close to $(K_a + K_p)/2$ with the increase in penetration (settlement).

5. An empirical model of skin friction is suggested involving L/D, which can incorporate reduction in stress due to sand arching. This model is strictly valid for a uniform bed of dry sand and upto a value of L/D = 35 and r = 1.5.

6. Bearing capacity factor $N_q$, is independent of pile diameter. It depends on relative density of sand and installation condition. Installation effect is higher in loose sand than dense sand.

7. Analytical results with finite element modelling compared to experimental results show very good correlation at very low percentage of settlement ratio. This is due to the fact that soil behaves elastically at a low percentage of strain.

## 8.2 Recommendations for Future Research

In order to enhance the findings of this study on load transfer mechanism and to develop a generalized model of skin friction mobilization, the following additional works may be undertaken in a future research.

1. The load transfer behaviour of piles in sand under saturated condition may be performed. A procedure similar to that followed in this study may be used and additional measurements of pore water pressure will be required.

2. The results obtained may be verified by a prototype in the field.

3. The effect of surface roughness of the pile shaft may be studied by changing the surface condition in model piles or by using piles made of different materials.

4. The study may be extended to include the effect of lateral load in changing pile capacity and skin friction values.

5. Further analytical procedure using nonlinear or elasto-plastic soil-pile system and Finite Element method may be developed to predict pile load transfer under different installation condition.

# REFERENCE


1. ABEDIN, M.Z.(1986), "Eccentrically Loaded Strip Footing on a Sand Layer Overlying a Rigid Stratum", Ph.D Thesis, University of Strathclyde, Glasgow, U.K.

2. BALAAM, N.P., BOOKER, J.R., & POULOS, H.G. (1976), "Analysis of Granular Pile Behaviour Using Finite Elements", Univ. of Sydney Civ. Engg. Res. Rep. R 290, Aust.

3. BISHOP, A.W., COLLINGIDGE, V.H., and O'SULLIVAN, T.P.(1948), "Driving and Loading Tests on Six Precast Concrete Piles in Gravel ", Geotechnique, London, England, Vol. 1, No. 1, June, 1948, pp. 49-58.

4 BIAREZ, J. and GRESILLAN, J.M. (1972), "Essais et Suggestions pour la calcul de la Force Portante des Pieux en Milieu Pulverulent", Geotechnique, London, England, Vol. 22, No.3, Sept., 1972, pp. 433-450.

5. BROMS, B.B. (1966), "Methods of calculating the ultimate Bearing Capacity of Piles -- A Summary", Sols-soils no. 18-19: 21-32.

6. COYLE, H.M. and REESE, L.C.(1966), "Load Transfer for Axially Loaded Piles in Clay" ,Jnl. of Soil Mech. and Engg. Divn., Proceedings of the ASCE, Vol.92, No. SM2,

March, 1966.

7. COYLE, H.M. and SULAIMAN, I.H. (1967). "Skin Friction for Steel Piles in Sand", J.S.M.F.D., ASCE, Vol. 93, SM6: 261-278.

8. COYLE, H. M. and CASTELLO, R. R. (1981), "New Design Correlations for Piles in Sand", Jnl. of Geotechnical Engineering Division, Proceedings of the ASCE, Vol. 107, No. GT7, July, 1981.

9. D'APPOLONIA, E. and ROMUALDI, J.P. (1963), "Load Transfer in End-Bearing steel H-Piles", J.S.M.F.D., ASCE, Vol. 89, SM2: 1-25.

10. DESAI, C.S. (1974)."Numerical Design Analysis for Piles in Sands". Jnl. Geot. Engg. Divn., ASCE, vol. 100, No. GT6, pp. 613- 635.

11. DESAI, C.S. and ABEL, J.F.(1972), "Introduction to the Finite Element Method," New York, Van Nostrand Reinhold.

12. DESAI, C.S. and CHRISTIAN, J.T. (1977), "Numerical Methods in Geotechnical Engineering", McGraw-Hill Book Co., New York, 1977.

13. FOCHT, J.A. (1967) "Discussion to paper by Coyle and Reese", J.S.M.F.D., ASCE, Vol. 93, SM1: 133-138.

14. JANBU, N. (1976), "Static Bearing capacity of Friction Piles", Proceedings, 6th European Conference on SMFE, Vol. 1.2, pp. 479-488.

15. KERISEL, J. (1961), "Fondations Profondes en Milieu Sableux", Proc. 5th Int. Conf. Soil Mechanics and Foundation Engineering, Vol.2 : 73-83.

16. KEZDI, A. (1975), "Pile Foundations", Foundation Engineering Handbook, H.F. Winterkorn and H.Y. Fang, eds., Van Nostrand Reinhold Co., New York, N.Y., 1975, pp. 556-600.

17. LEE, I.K.(1973), "Application of Finite Element Method in Geot. Engg., Part I -- Linear Analysis", Ch. 17 in Finite Element Techniques -- A Short Course of Fundamentals and Application, Univ. of N.S.W., Aust.

18. MC CLELLAND, B., FOCHT, J.A. and EMRICH, W.J. (1969), "Problems in Design and Installation of offshore Piles", Journal of the Soil Mechanics and Foundation Divn., ASCE, Vol. 95, SM6, pp. 1419-1514.

19. MATTES, N.S. and POULOS, H. G.(1969), "Settlement of Single Compressible Pile", Jnl. of Soil Mech. and

Foundation Engg. Div., Vol. 95, No. SM1, January, 1969.

20. MEYERHOF, G.G.(1951), "The Ultimate Bearing Capacity of Foundations", Geotechnique, London, England, Vol. 2, No. 4, 1951, p. 301.

21. MEYERHOF, G.G. (1953), "The Bearing Capacity of Foundations Under Eccentric and Inclined Loads", 3rd. Int. Conf. on Soil Mechanics and Foundation Engineering, Vol. 1, pp. 440-445.

22. MAYER, F and L'HERMINIER, R.(1953), "La Pouvoir Portant des Piaux en Milieu Coherent", Proceedings of the III International Conferance on Soil Mechanics and Foundation Engineering, Vol. 2, 1953, pp. 60-65.

23. MEYERHOF, G.G.(1956), "Penetration Tests and Bearing Capacity of Cohesionless Soils", J.S.M.F.D., ASCE, Vol. 82, SM1, pp. 1-19.

24. MEYERHOF, G. G.(1959), "Compaction of Sands and Bearing Capacity of Piles", Journal of the Soil Mechanics and Foundation Division, ASCE, Vol. 85, No. SM6, Proc. Paper 2292, Dec., 1959, pp.1-29.

25. MEYERHOF, G.G..(1976), "Bearing Capacity and Settlement of Pile foundations", J.G.E.D, ASCE, Vol. 102, GT3, March, pp. 195-228.

26. MEYERHOF, G.G.(1982), "Scale Effects of Ultimate Pile Capacity", Jnl. of Geotech. Engg., ASCE, vol. 109, No. 6, pp. 797-806.

27. NAIR, K. (1967), "Load-Settlement and Load Transfer Characteristics of a Friction Pile Subject to Vertical Load", Proc. 3rd Pan-Amer. Conf., S.M. & F.E., 1: 565-590.

28. NORDLUND, R. L.(1963), "Bearing Capacity of Piles in Cohesionless Soils", Journal of the Soil Mechanics and Foundation Division, ASCE, Vol. 89, No. SM3, Proc. Paper 3506, May, 1963, pp. 1-35.

29. NUMERICS CORPORATION(1983), "FE2000" A Computer Program for Finite Element Analysis.

30. POULOS, H.G. and DAVIS, E.H.(1968), " The Settlement Behaviour of Singles Axially Loaded Incompressible Piles and Piers", Geotechnique, 18: 351-371.

31. POTYONDY, J.G. (1961), "Skin Friction Between Various Soils and Construction Materials", Geotechnique, London, England, Vol.2, No. 4, Dec., 1961, pp. 339-353.

32. PRANDTL, L. (1920), "Uber die Harte Plastischer Korper", Nachr. Kgl. Ges. Wiss. Gottingen, Math. Phys. Klasse.

33. REISSNER, H. (1924), "Zum Erddruckproblem", Proc. 1st. Intern. Congr. Applied Mechanics, Delft (Holland).

34. ROBINSKY, E.I. and MORRISON, C.F. (1964), "Sand Displacement and Compaction Around Model Friction Piles", Canadian Geotechnical Journal, Toronto, Ontario, Canada, Vol. 1, No.2. Mar., 1964, pp.81-93.

35. SALAHUDDIN, M. (1986), "Laboratory Evaluation of Torque and Uplift Capacity Relations for Screw Piles in Granular Soil", an M.Sc. Thesis, Civil Engg. Dept., BUET, July, 1986.

36. SEED, H.B. and REESE, L.C. (1957), "The Action of Soft Clay Along Friction Piles", Transactions, ASCE, Vol. 122, 1957.

37. SZECHY, C. (1961), "The Effect of Vibration and Driving Upon the Voids in Granular Soils Surrounding a Pile", Proceeding of the V Int. Conf. on Soil Mechanics and Foundation Engineering, Vol.2, 1961, pp.161-164.

38. TERZAGHI, K. (1943), "Theoretical Soil Mechanics", John, Wiley and Sons, Inc. New York, N.Y., 1943, pp. 42-143.

39. TERZAGHI, K. (1943a), "A liner Plate Tunnel on the Chicago (Ill.) Subway", Trans. American Society of Civil Engineers, Vol. 108, pp. 970-1007.

40. THORNBURN, S. and R. MACVICAR, (1971), "Pile Load Tests to Failure in the Clyde Alluvium", Conf. on Behaviour of Piles, ICE, pp. 1-8.

41. THURMAN, A. G., and D' APPOLONIA, E.(1964), "Prediction of Pile Action by a Computer Method", Proceeding Conf. on Deep Foundations, Mexico, December, 1964.

42. THURMAN, A.G. and D, APPOLONIA, G.E.(1965), "Computed Movement of Friction and End-Bearing Piles Embedded in Uniform and Stratified Soils," Proc. 6th Int. Conf. S.M. & F.E., Vol. 2: 323-327.

43. TOMLINSON, M.J.(1971), "Pile Design and Construction Practice", A View Point Publication, London, pp. 210-216.

44. TOMLINSON, M.J.(1980), "Foundation Design and Construction", A Pitman International Text, Fourth Edition, pp.375.

45. VESIC, A.S. (1967), "A Study of Bearing Capaoity of Deep Foundations", Final Rep., Proj. 8-189, School of Civil Engg., Georgia Inst. Tech., Atlanta, Ga.

46. VESIC, A.S. (1968), "Load Transfer, Lateral Loads and Group Actions of Deep Foundation", Performance of Deep Foundations, STP444, American Society for Testing Materials, June, 1968, pp. 5-14.

47. VESIC, A.S. (1970), "Tests on Instrumented Piles, Ogeeche River Site", Journal of the Soil Mechanics and Foundation Division, ASCE, Vol. 96, No. SM3, Proc. Paper 7170, March, 1970, pp. 561-583.

48. VESIC, A.S. (1972), "Expansion of Cavities in Infinite Soil Mass", Vol. 98, No. SM3, Proc. Paper 8790, March, 1972, pp. 265-290.

49. VESIC, A.S. (1975), "Principles of Pile Foundation Design", Soil Mechanics Series no. 38., School of Engineering, Duke University, Durham, N.C., pp. 48.

50. VESIC, A.S. (1977), "Design of Pile Foundations", NCHRP Synthesis of Highway Practice No.42, Transportation Research Board, 2977.

51. VIJAYVERGIA, V.N. and JOHN A. FOCHT, Jr. (1972), "A New Way to Predict Capacity of Piles in Clay", OTC Paper 1718, 4th Offshore Technology Conference, Houston, Tex.

52. ZIENKIEWICZ, O.C. (1971), "The Finite Element Method in Engineering Science", McGraw-Hill Book Co., Second Edition, London,1971.

# APPENDIX-A

# SALIENT FEATURES OF FE2000

FE2000 is developed by Numerics Corporation, beginning in 1983. It is continually enhanced to reflect the evolving needs of advanced engineering applications. It is supported by Numerics Corporation and its sublicensees with hotline support and consulting.

It is the only general purpose Finite Element Analysis (FEA) programme to be written since microcomputers became available to the engineering community. FE2000's modern software architecture makes it portable with full capability from microcomputers to super-computers.

It is currently about 75,000 lines of Fortran. yet its modular design allows it to run with full capability even on a PC with 512 K of memory.

It uses a BLOCKED PROFILE MATRIX SOLVER, so that problem size is not limited by available memory. The solver allows different nodes to have different degrees of freedom, and keeps track of the instantaneous bandwidth for each equation.

It is able to solve very large problems. The IBM-PC version allows problems upto 10,500 degrees of freedom (DOF), with a peak bandwidth of 1750.

It has a built-in, AUTOMATIC BANDWIDTH MINIMIZER. Models can be made using arbitrary node and element numbers without sacrificing efficiency of solution.

It monitors round off decay during equation solving, and informs user of any precision loss that may have occurred.

It is designed to solve static, dynamic and heat transfer problems.

It has a library of 45 different elements to choose from, to allow modeling of almost any geometric configuration.

# APPENDIX-B

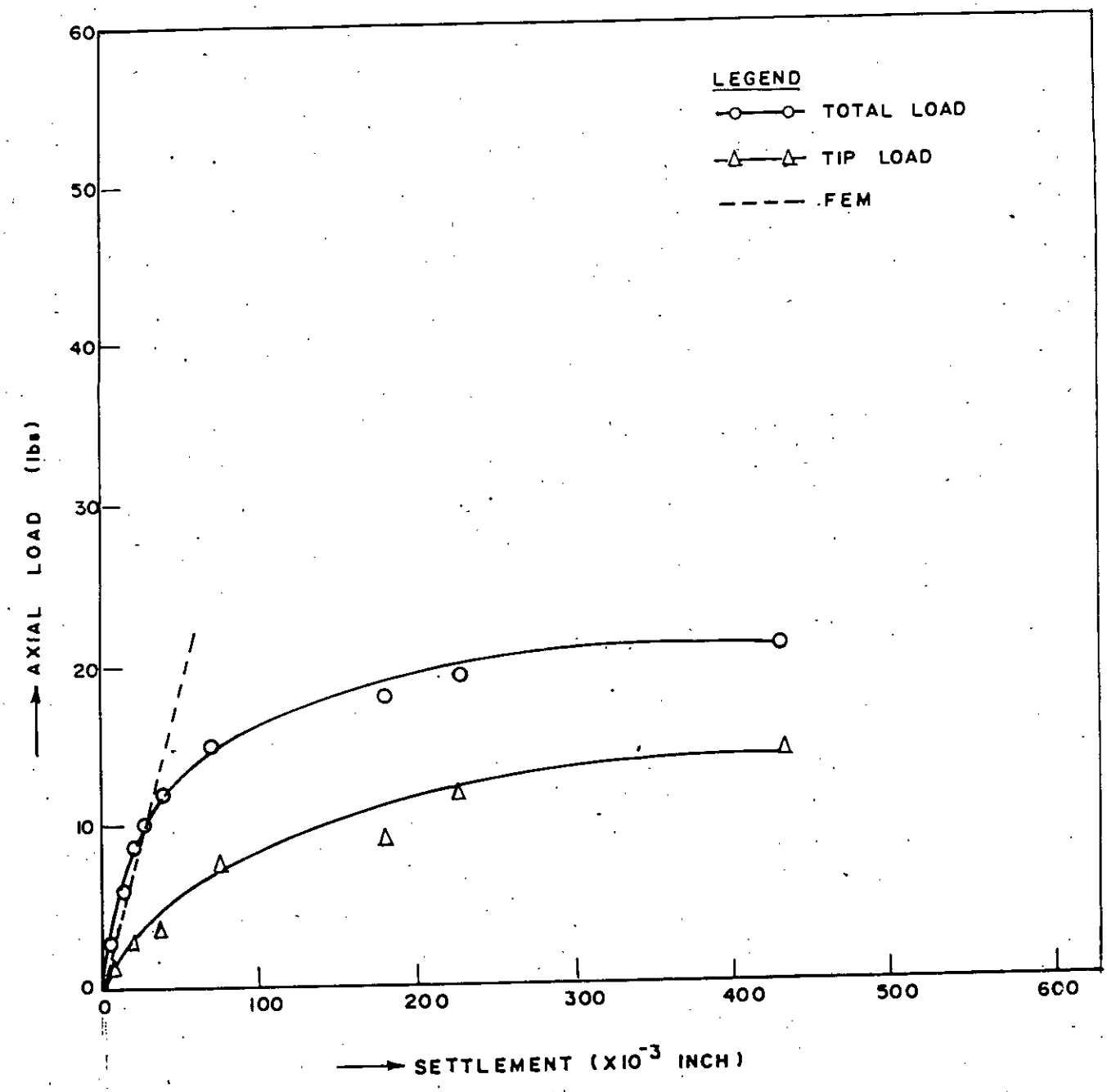


Fig. B.1) Nondisplacement Piles in Loose Sand ( Dia = 0.75")

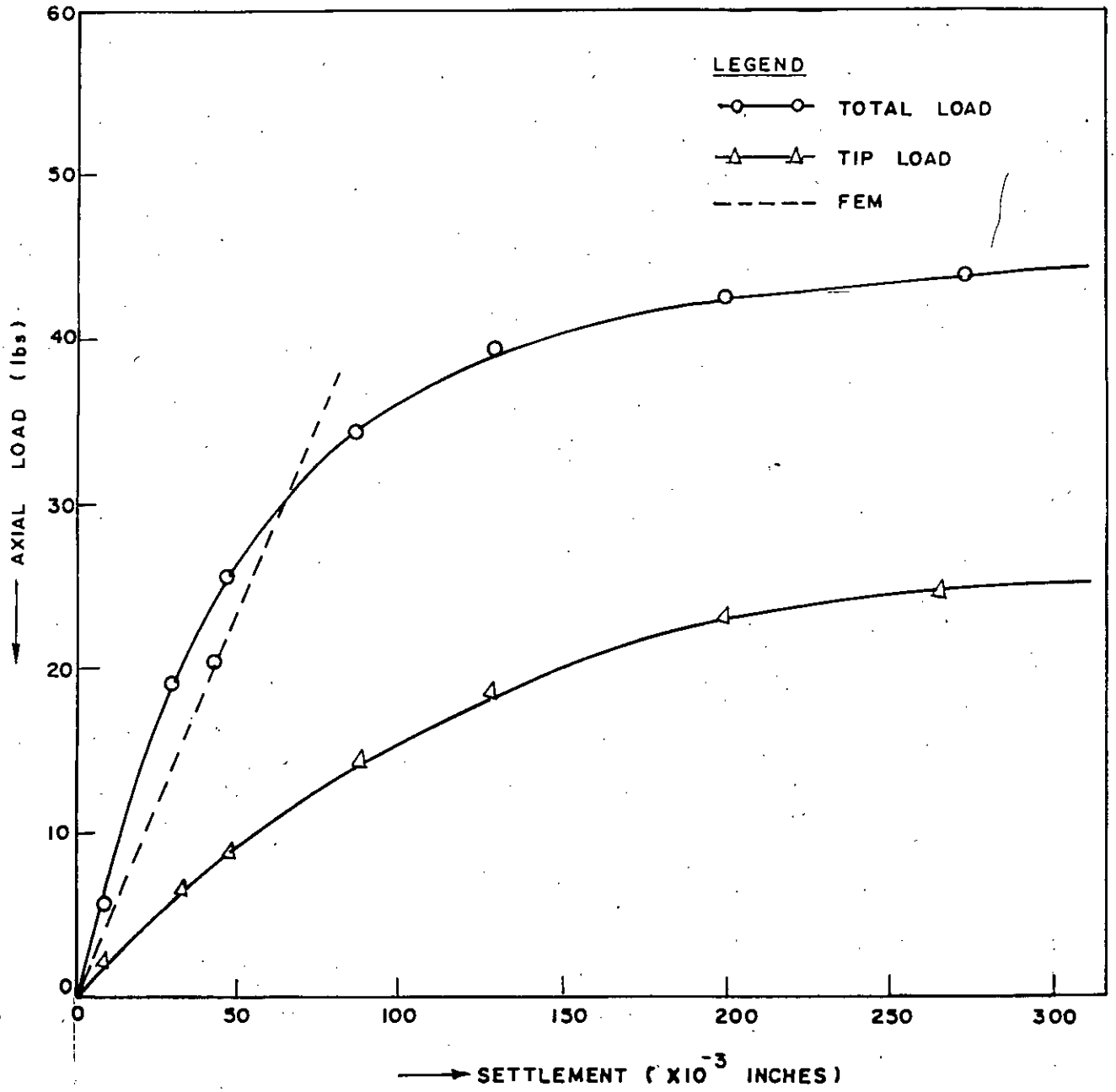


Fig. 5.2 Nondisplacement Piles in Loose Sand ( Dia = 1.1875 )

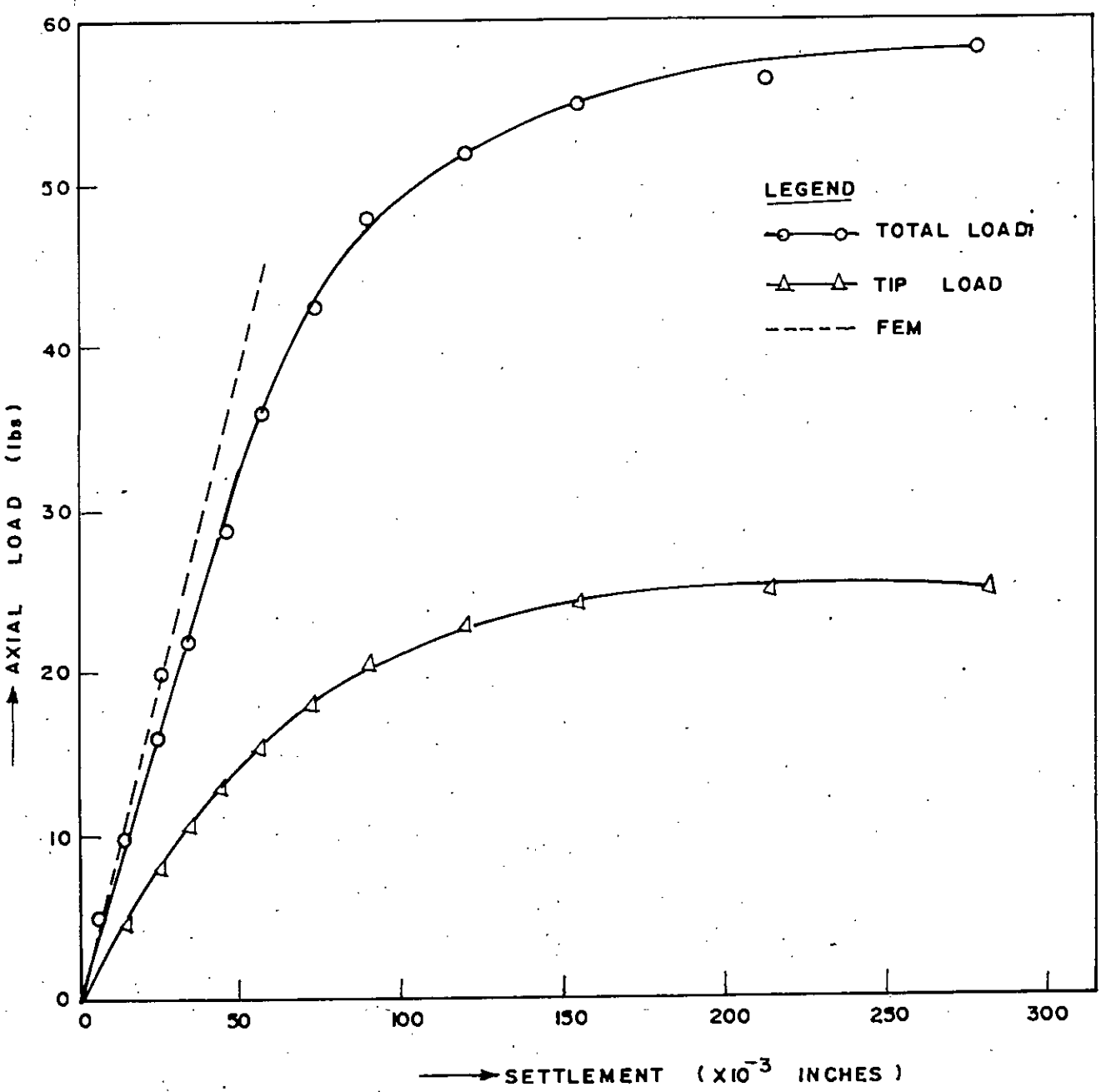


Fig. 8.33 Displacement Piles in Loose Sand (Dia = 1.1875")

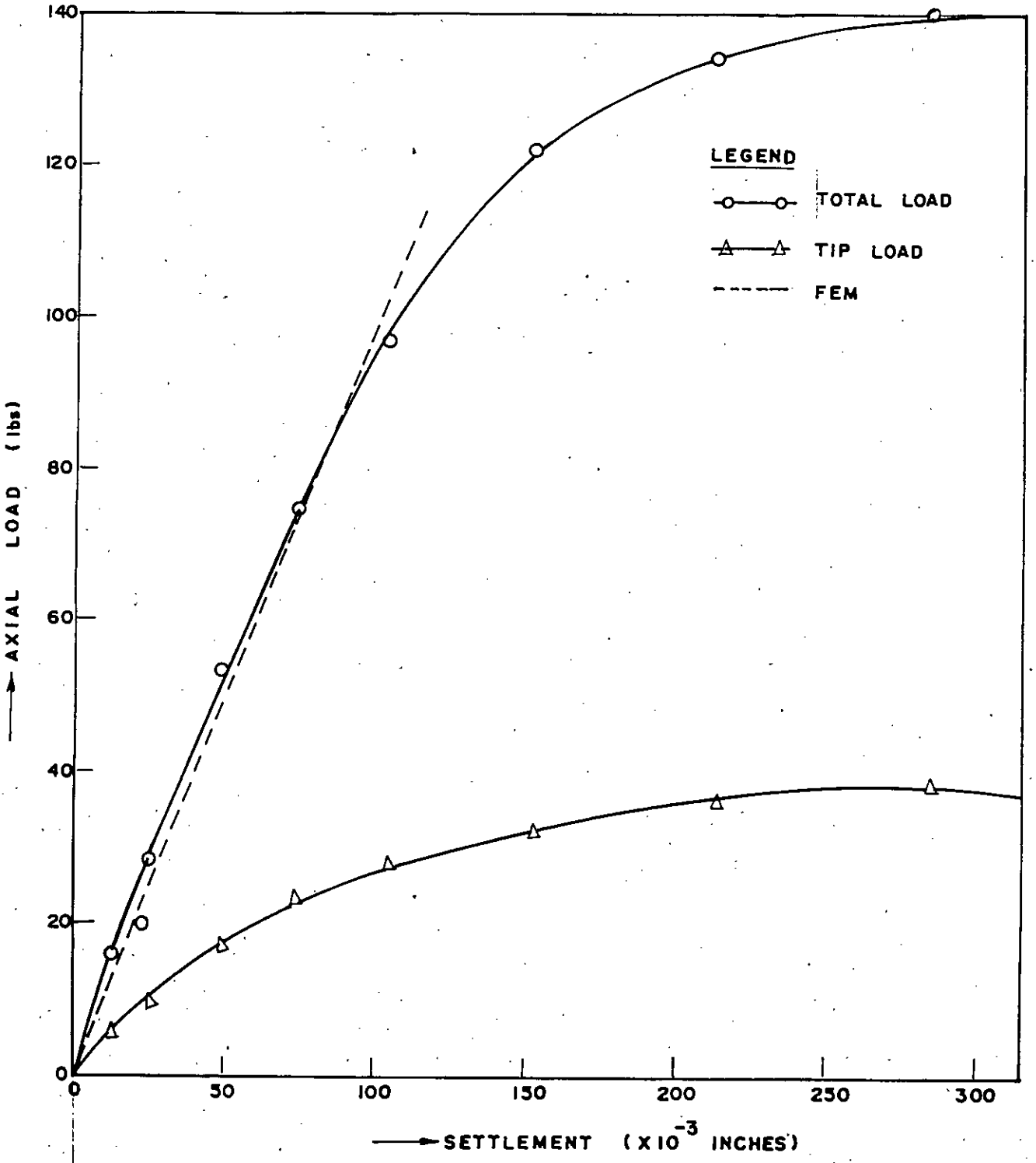


Fig. B.4 Displacement Piles in Loose Sand. (Dia = 2")

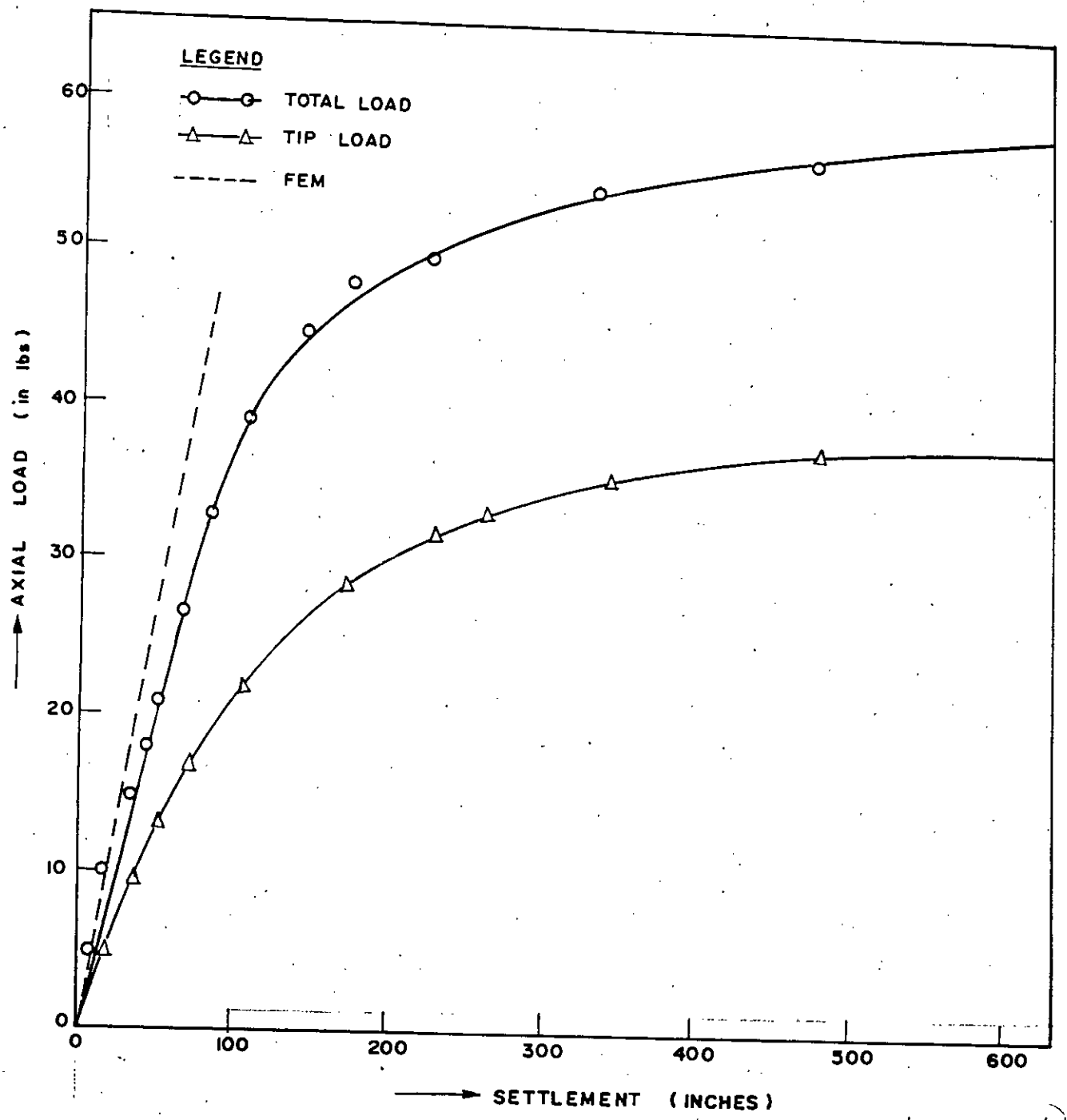


Fig. B.5.5 Nondisplacement Piles (Single) in Dense Sand (Dia = 0.75")

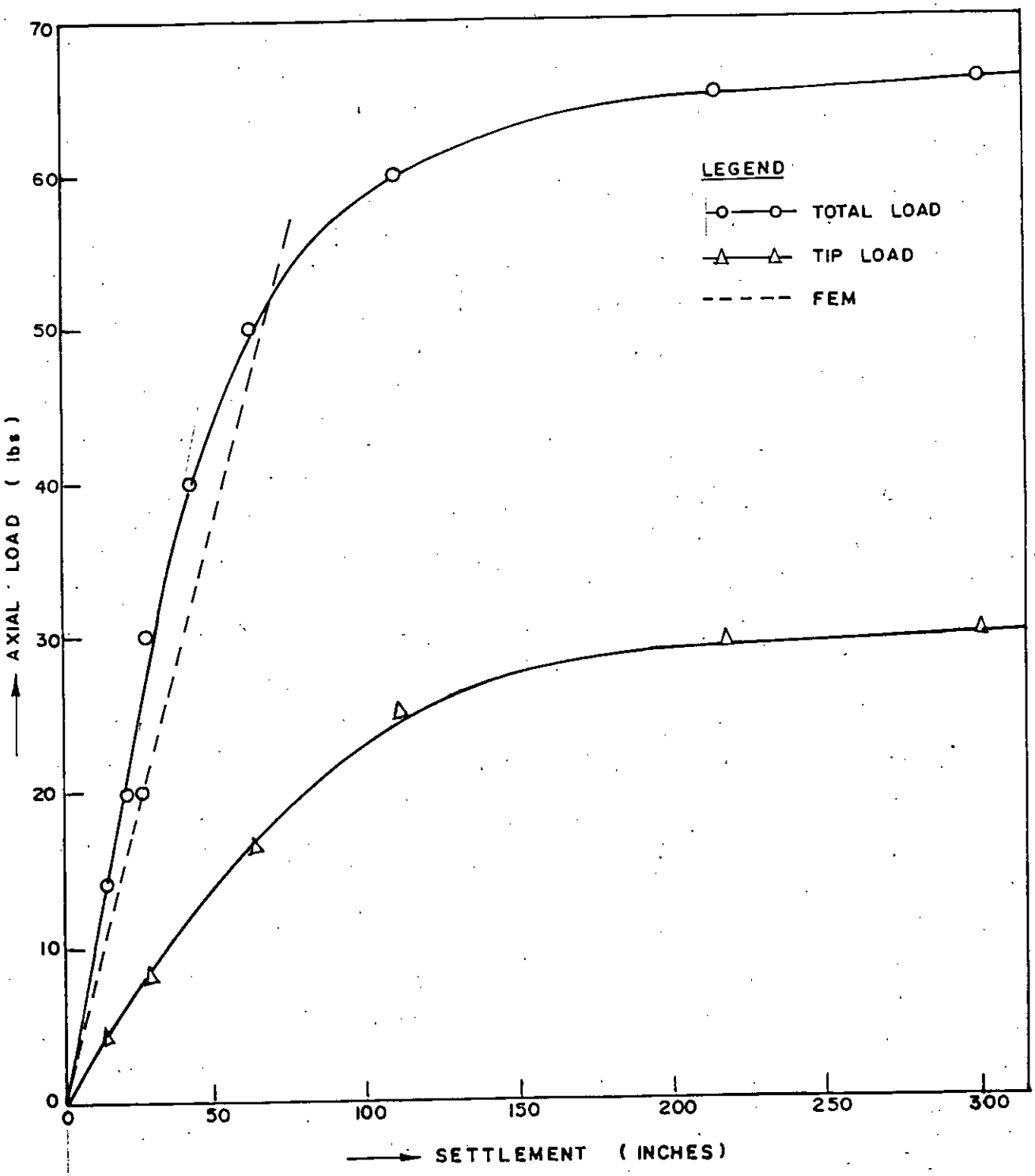


Fig. B.6 Nondisplacement Piles in Dense Sand (Dia = 1.1875")

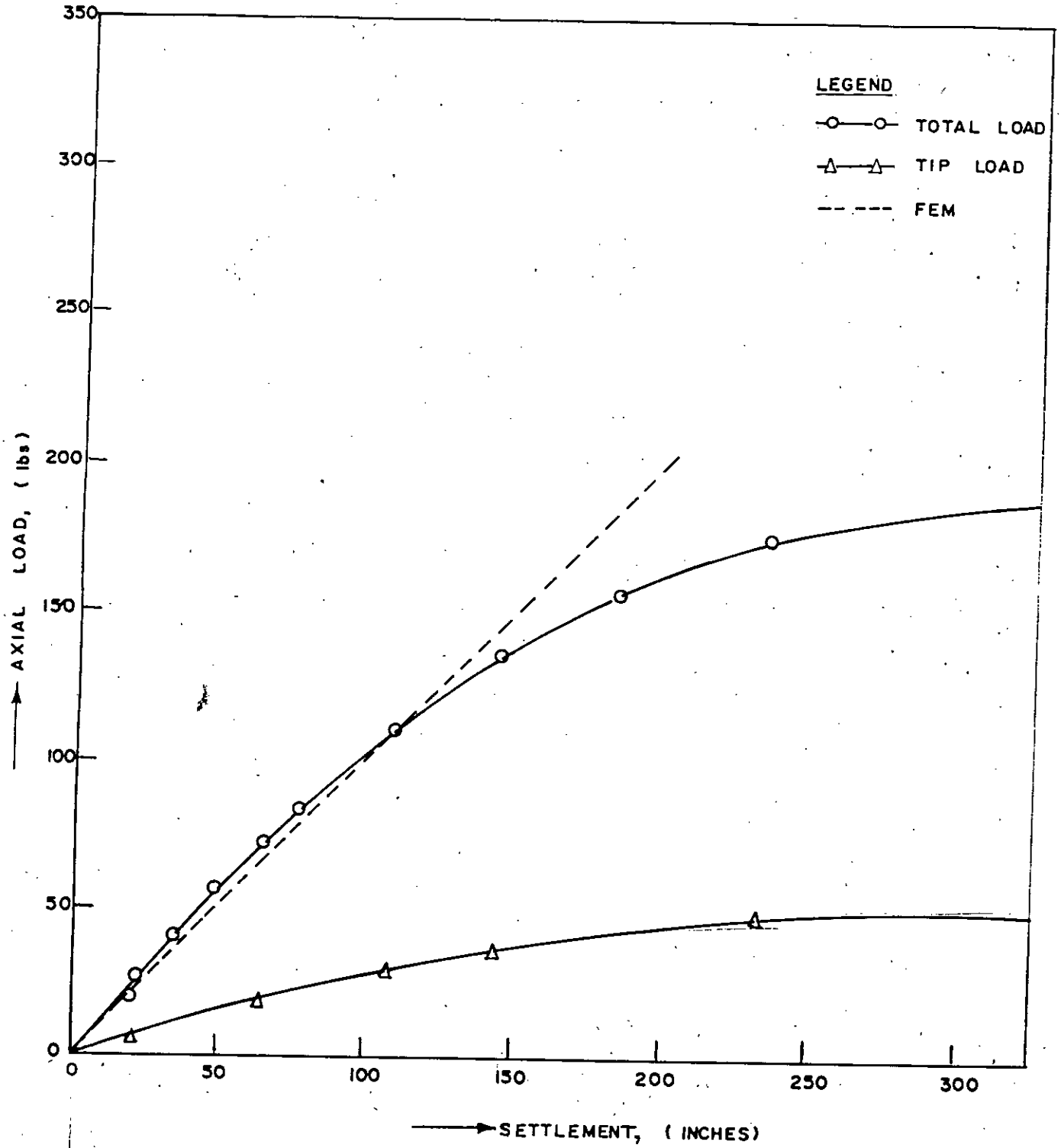


Fig. B.7 Nondisplacement Piles in Dense Sand. ( Dia =2.0")

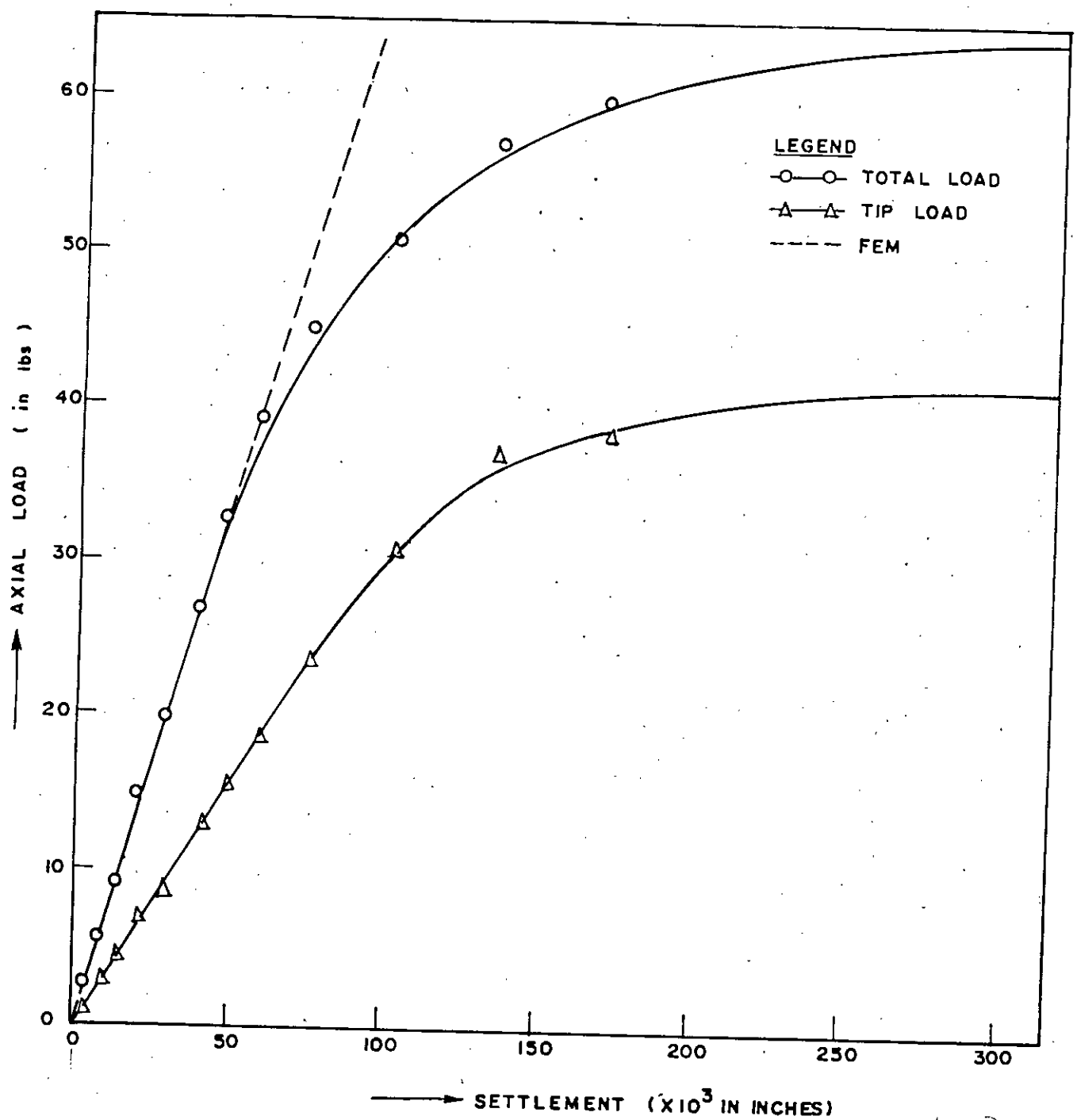


Fig. B-8 Displacement Piles (Single) in Dense Sand (Dia = 0.75")

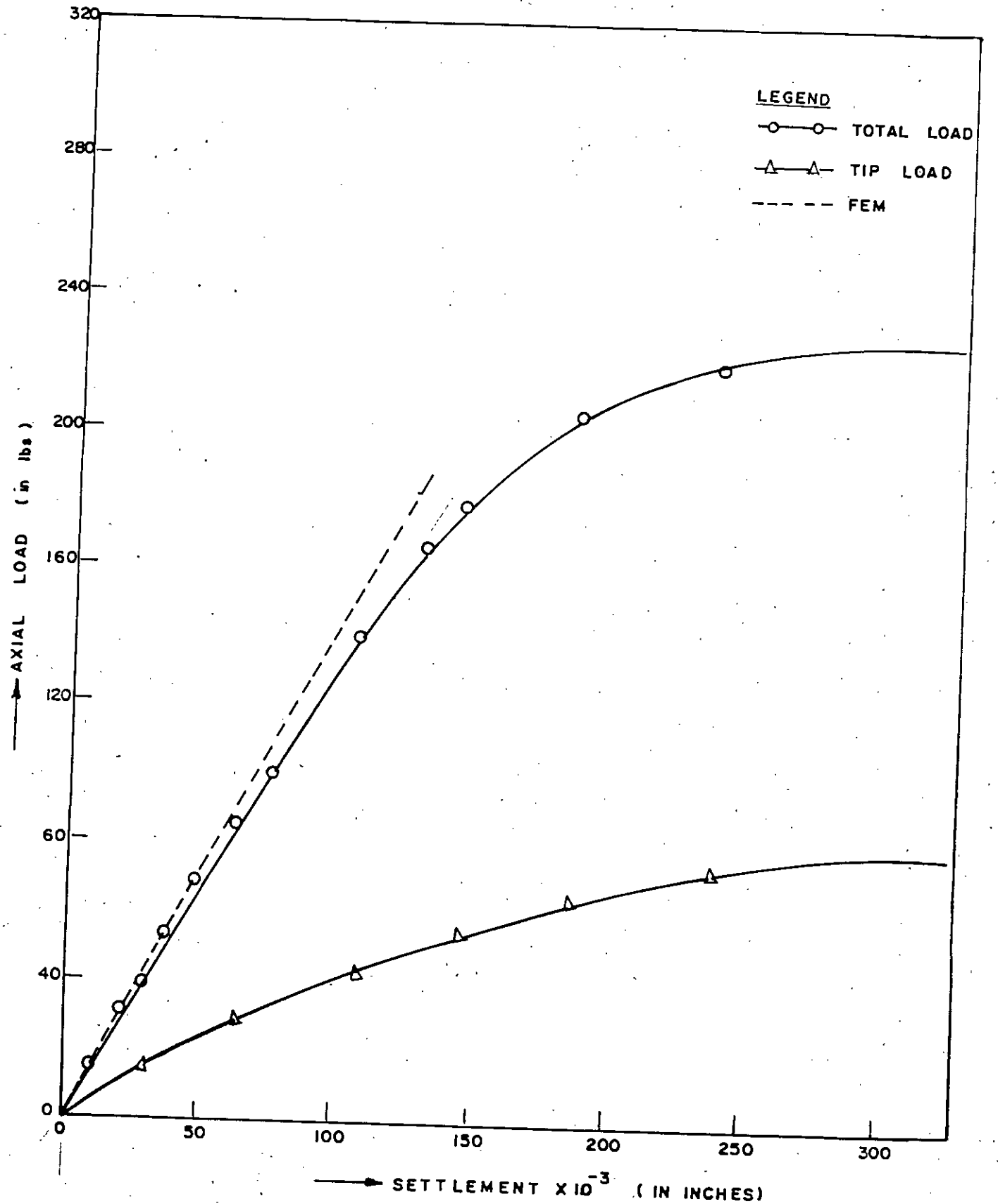


Fig. B.9 Displacement Piles in Dense Sand ( Dia = 2.0")

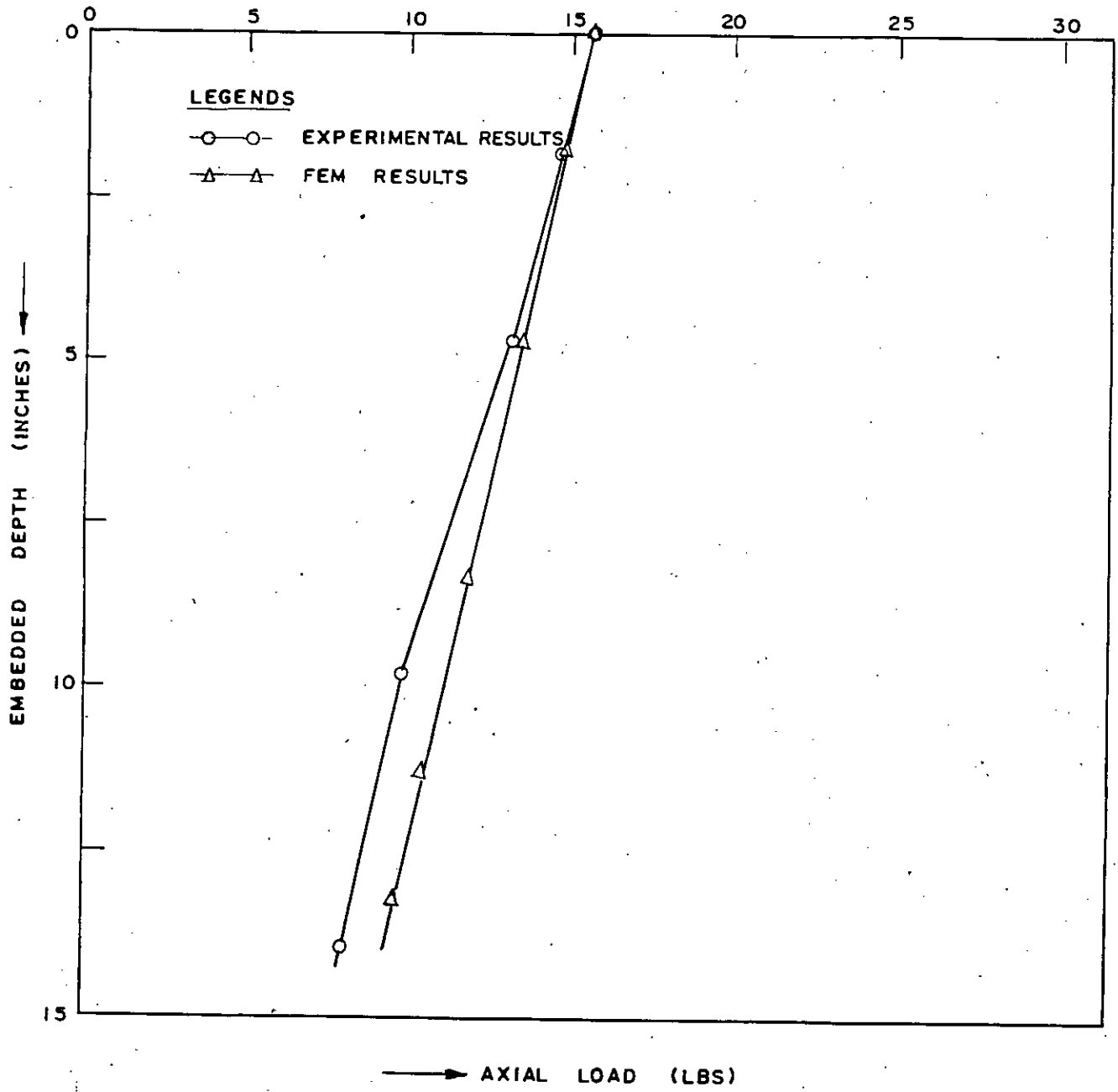


Fig. B.10 Nondisplocement Piles in Loose Sand (Dia = 0.75")

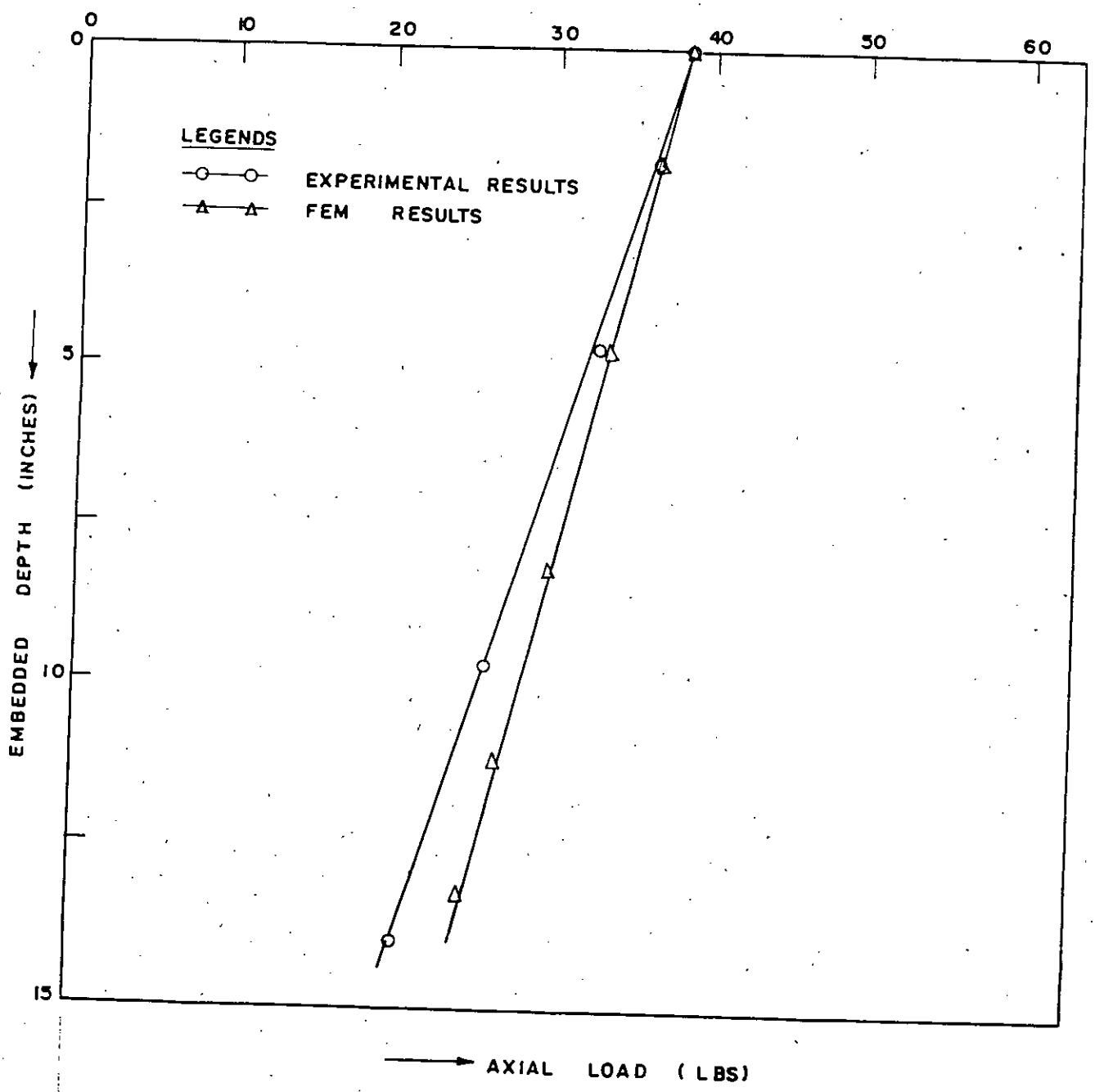


Fig. B.11 / Nondisplacement Piles in Loose Sand ( Dia =1.1875")

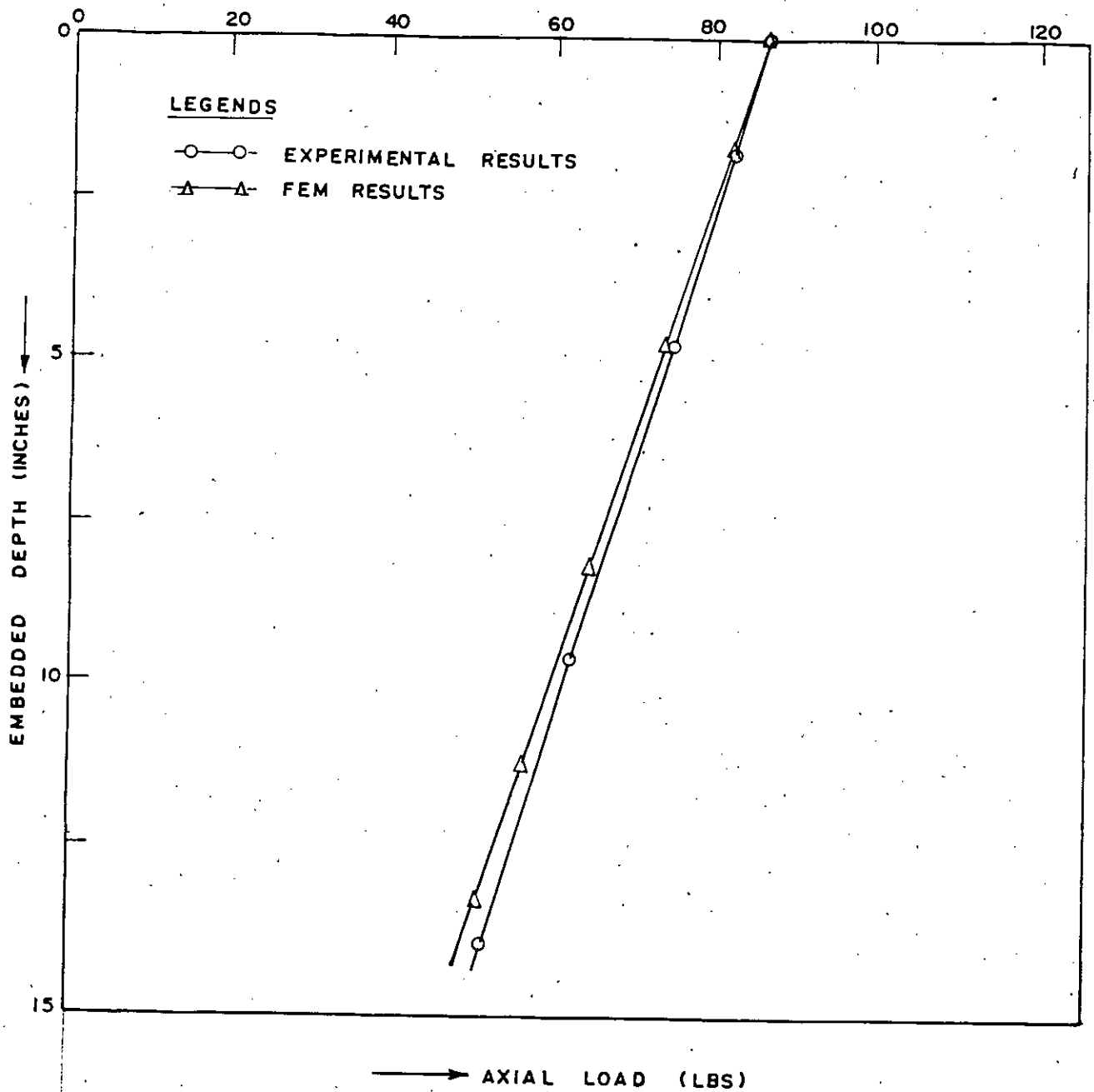


Fig. B.12 Nondisplacement Piles in Loose Sand ( Dia = 2.0" )

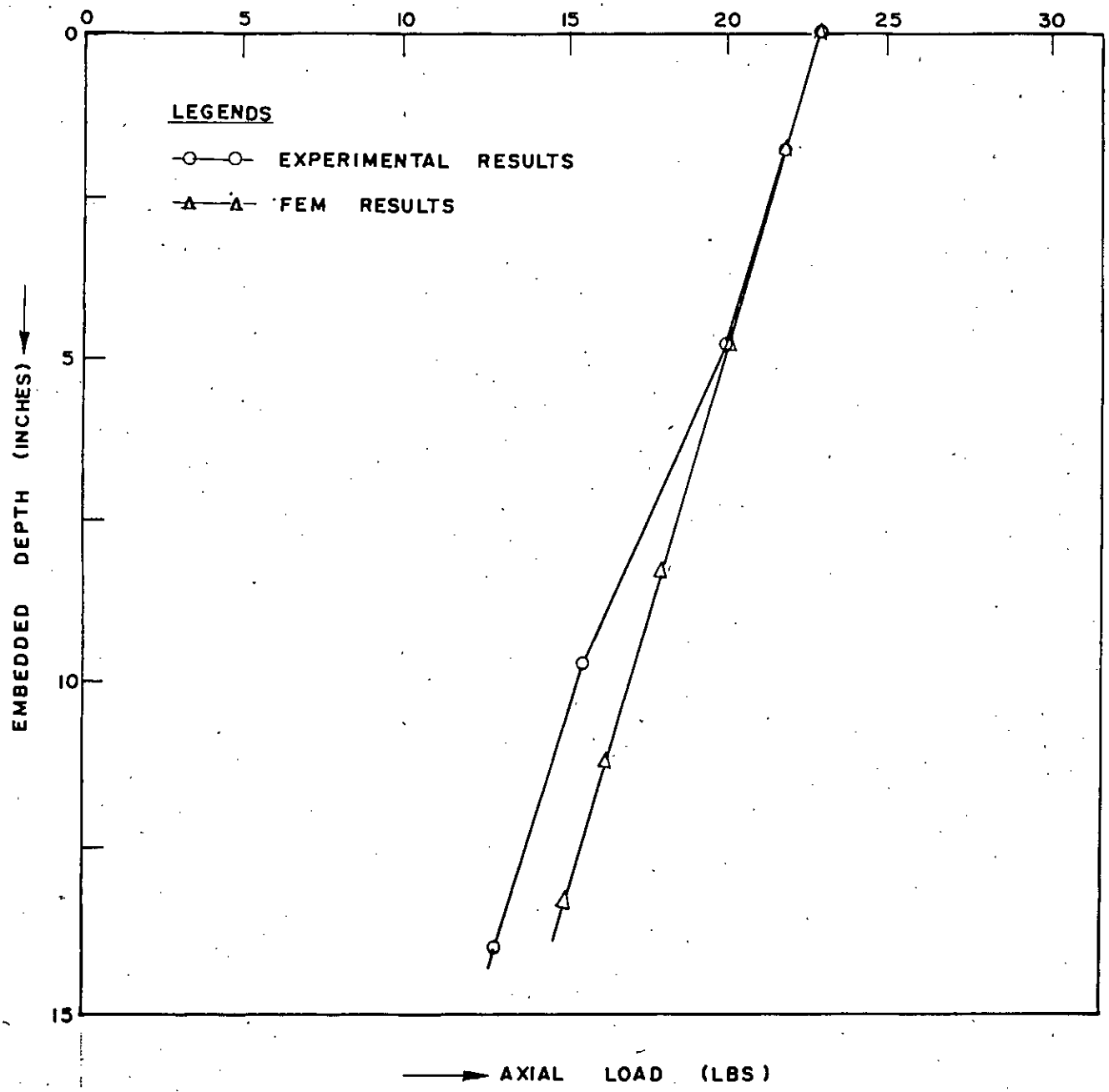


Fig. 8.13 Displacement Piles in Loose Sand (Dia = 0.75")

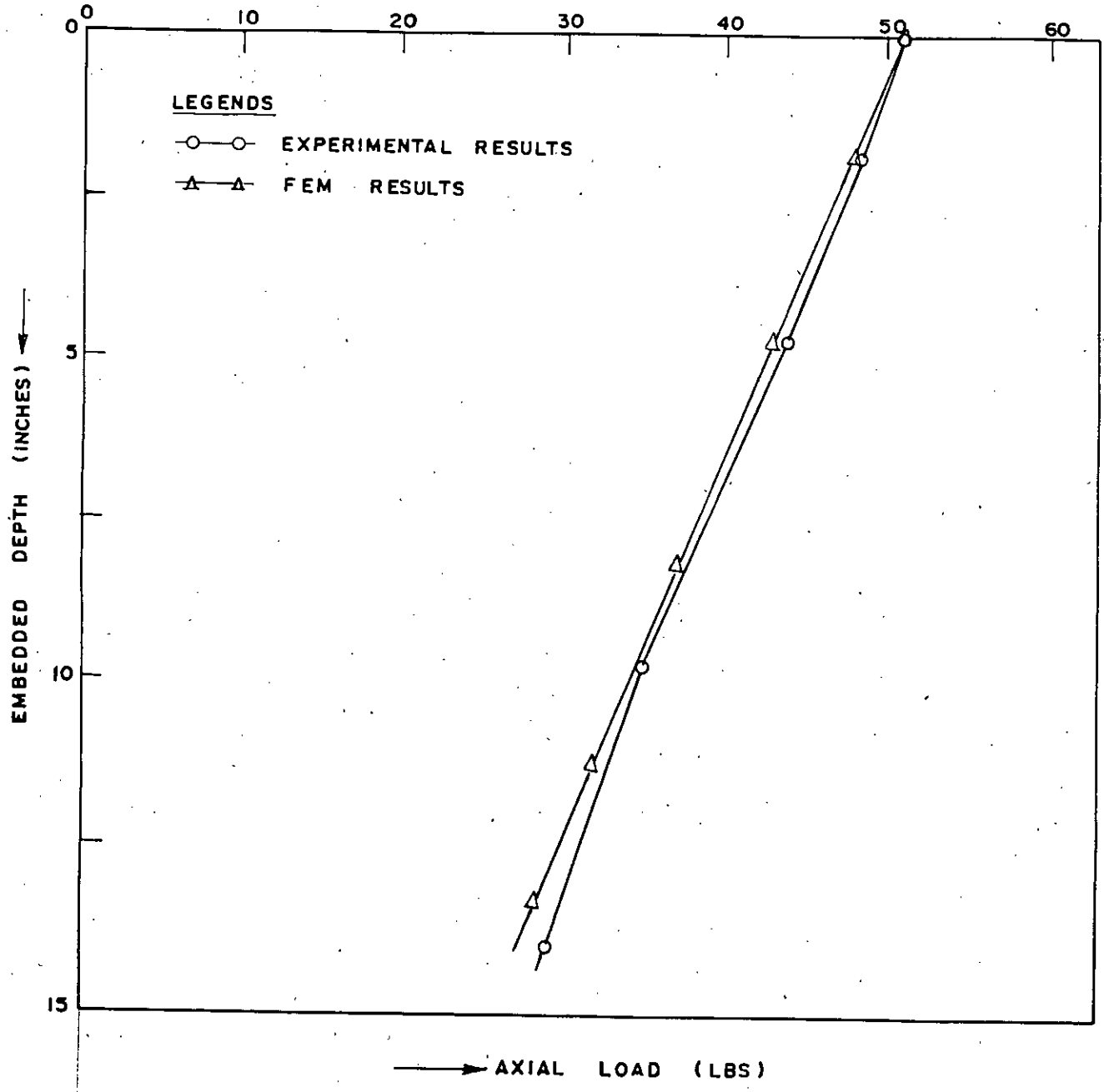


Fig. B.14 Displacement Piles in Loose Sand (Dia = 1.1875")

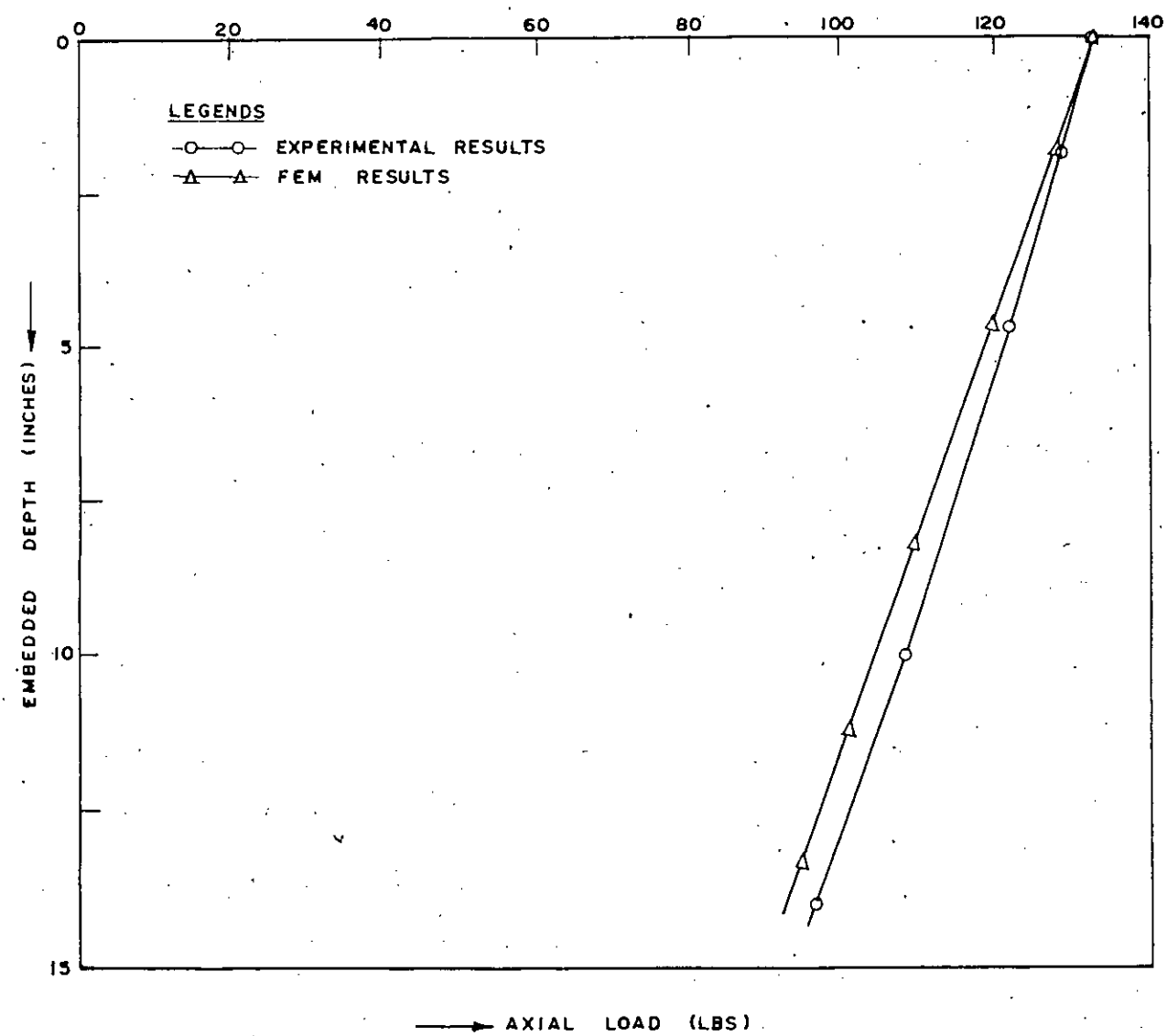


Fig. 8.15 Displacement Piles in Loose Sand (Dia = 2")

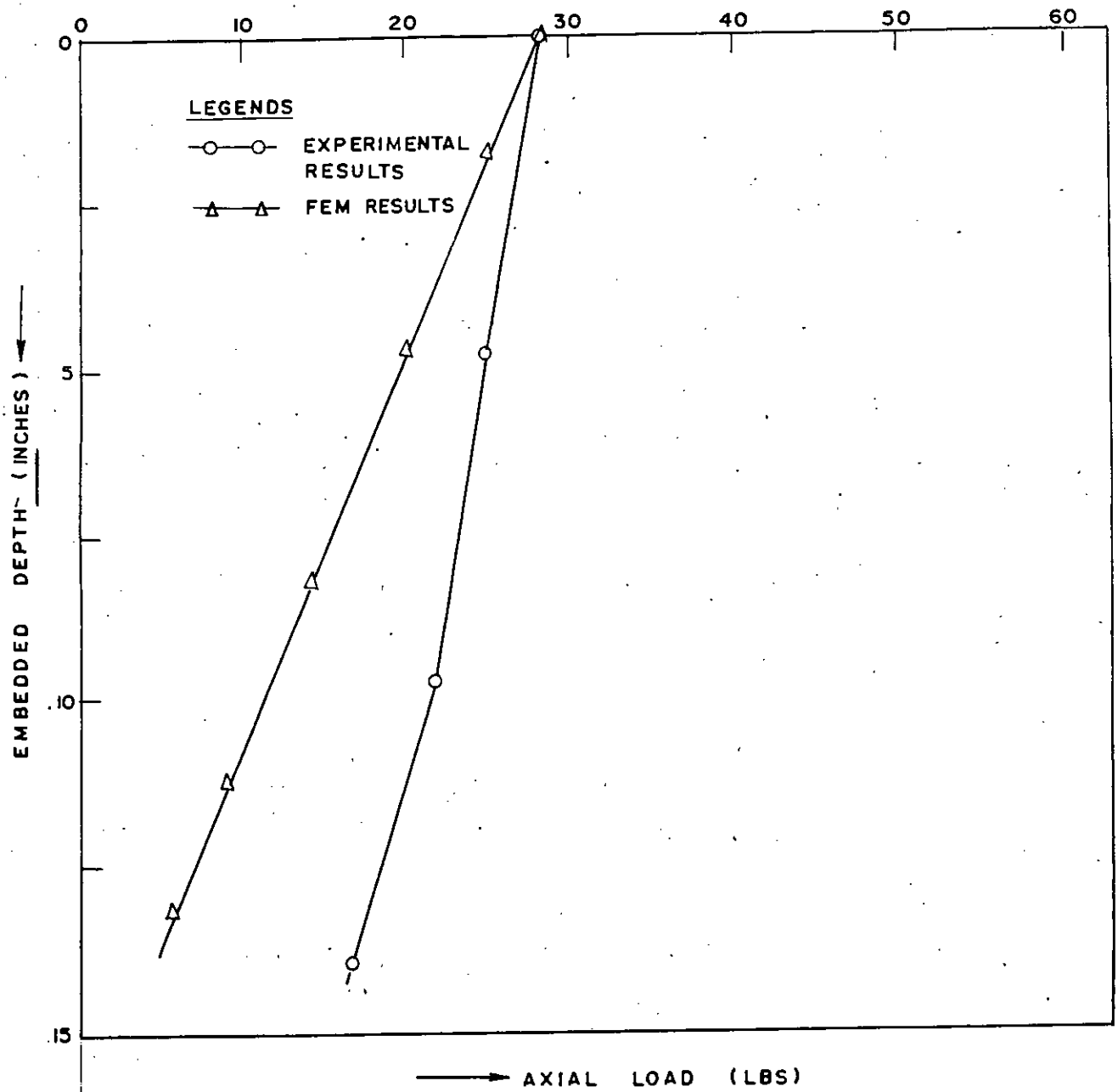


Fig. 8.16 Non displacement Piles in Dense Sand (Dia = 0.75")

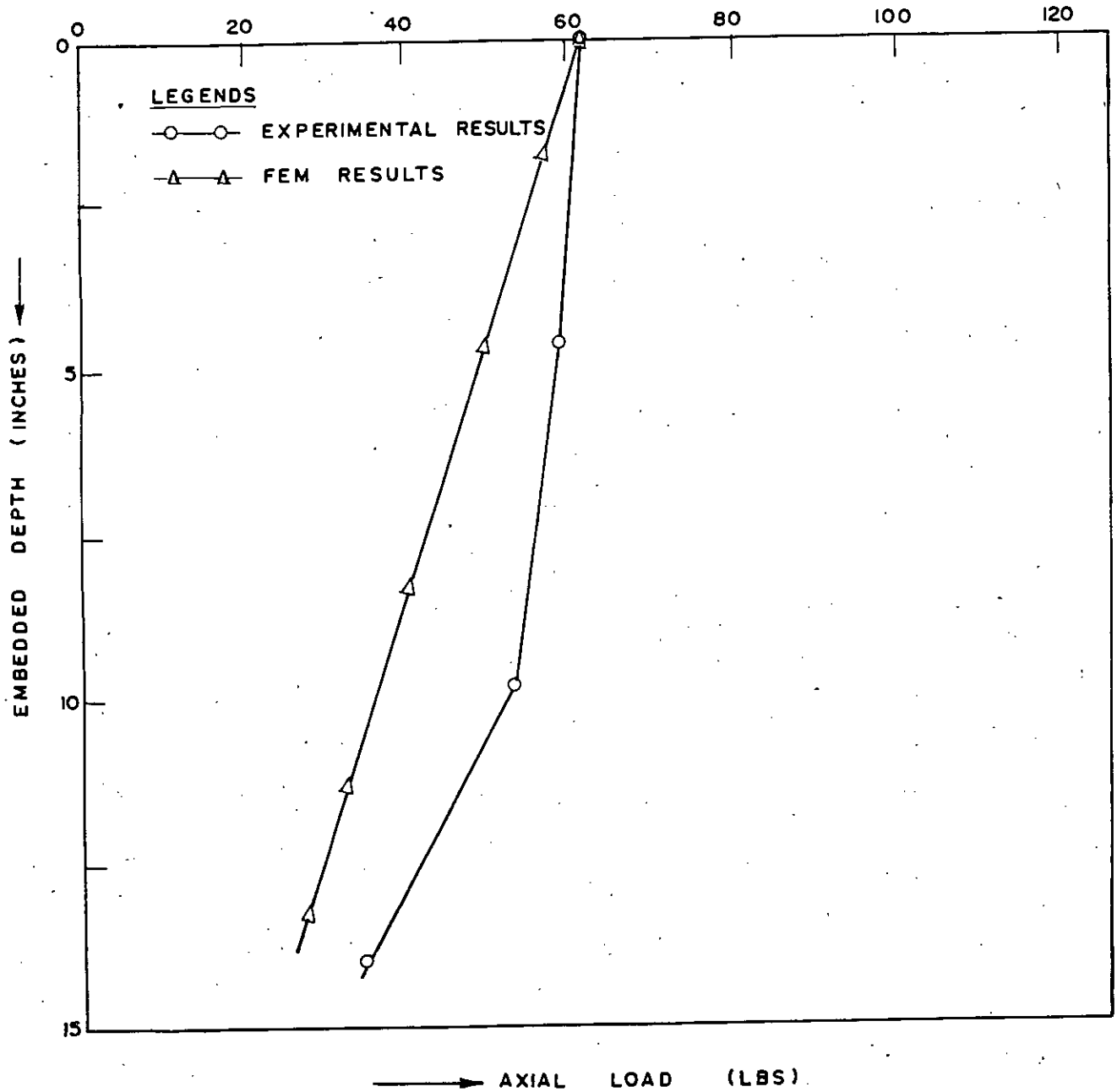


Fig. B.17 Nondisplacement Piles in Dense Sand (Dia = 1.1875")

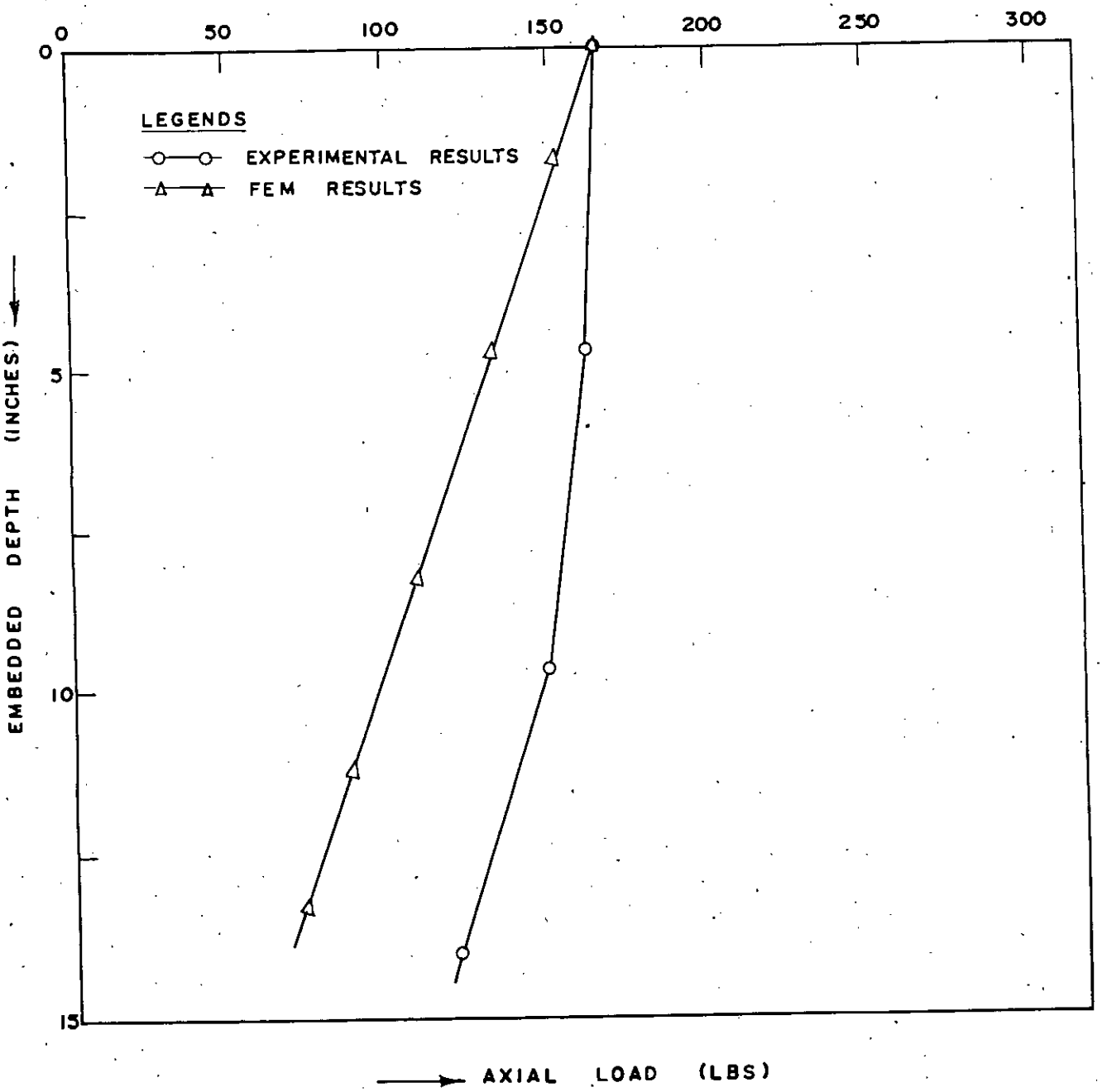


Fig. 8.18 Nondisplacement Piles in Dense Sand ( Dia = 2.0" )

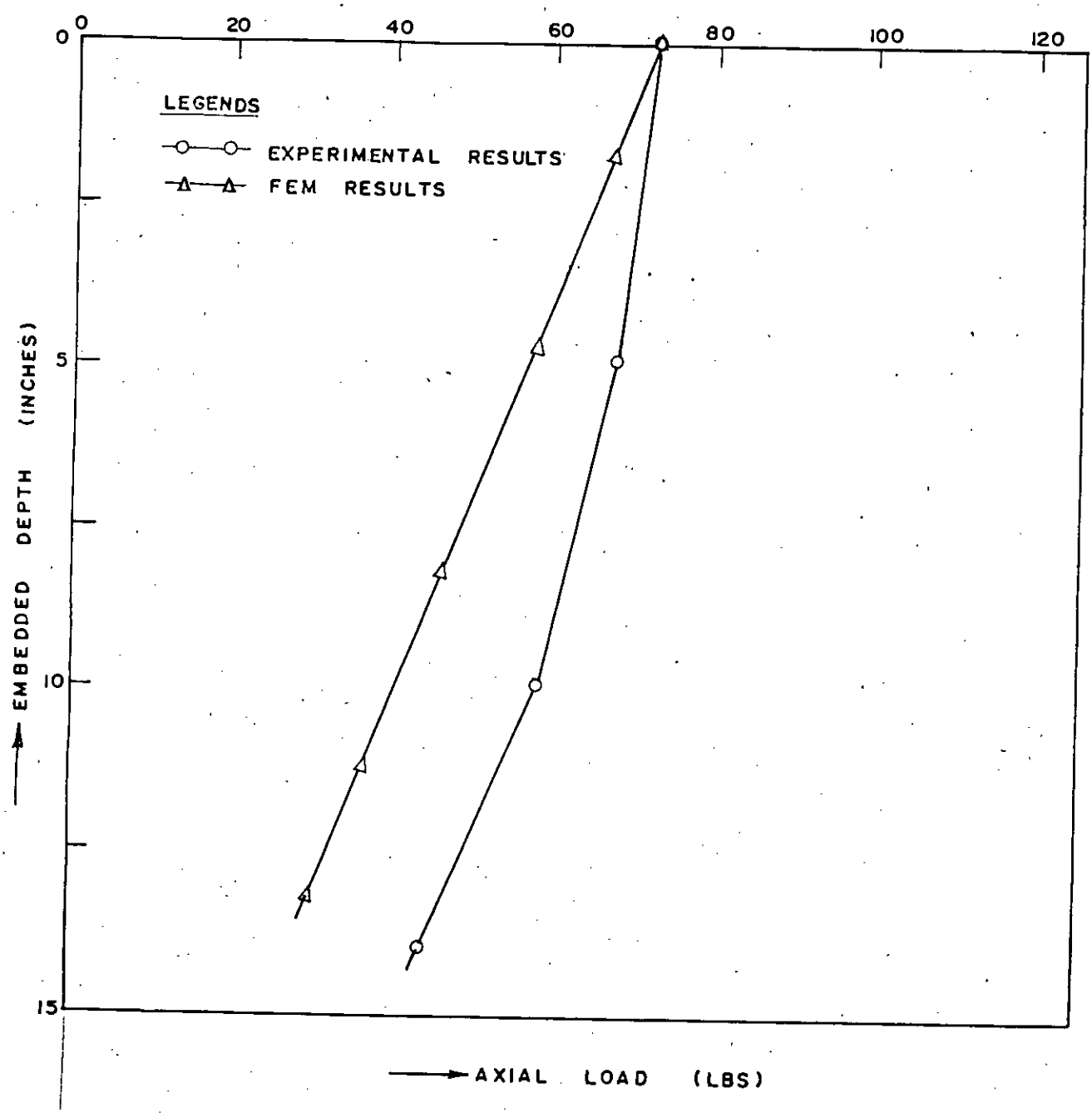


Fig. 8.19 Displacement Piles in Dense Sand (Dia = 1.1875")

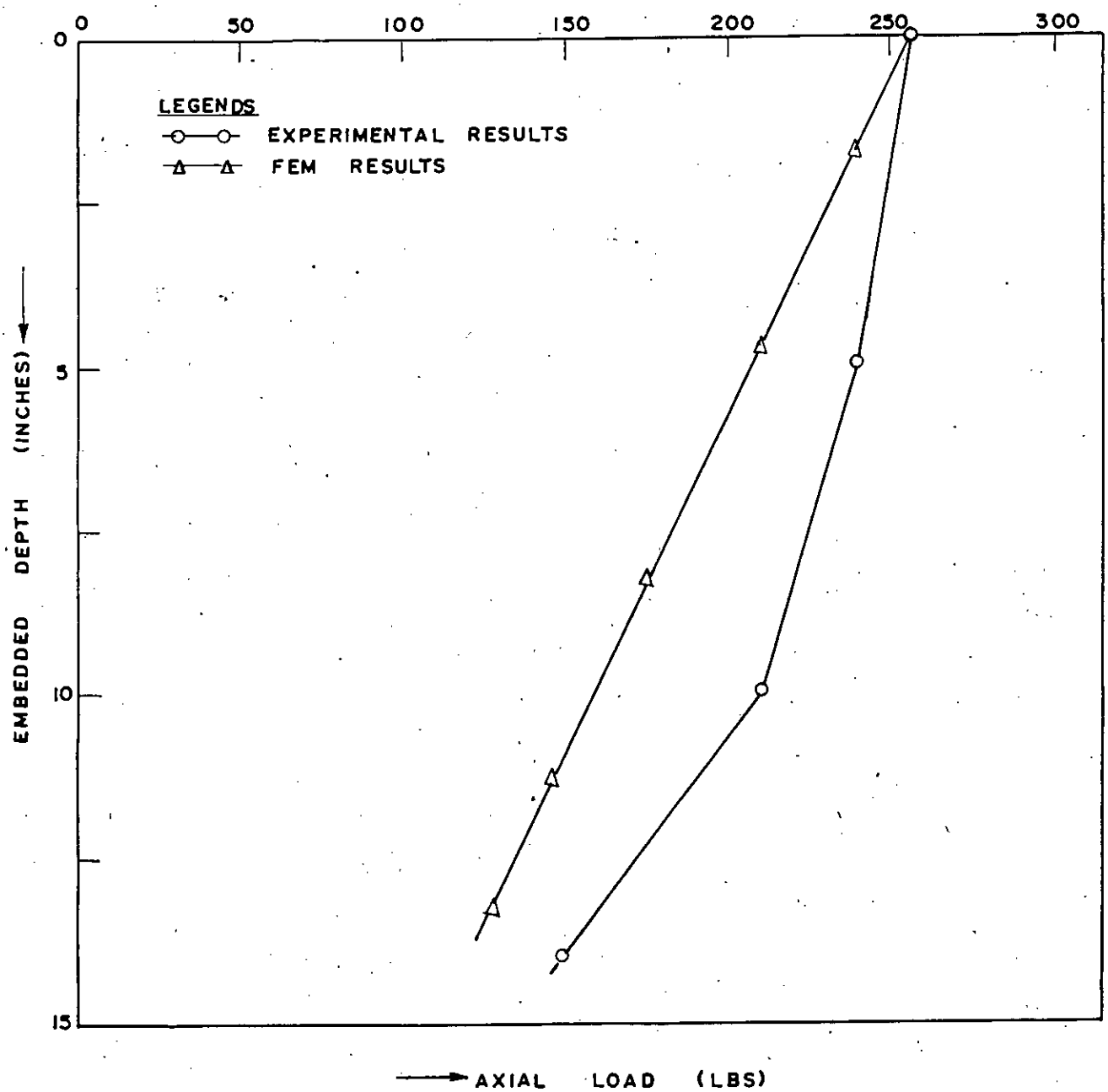


Fig. B.20C Displacement Piles in Dense Sand ( Dia = 2.0")